MICROWAVE PRETREATMENT OF A LOW GRADE COPPER ORE TO ENHANCE MILLING PERFORMANCE AND LIBERATION

by

Grant Scott

Thesis submitted in partial fulfillment
of the requirements for the Degree

of

**MASTER OF SCIENCE IN ENGINEERING
(CHEMICAL ENGINEERING)**

in the Department of Process Engineering
at the University of Stellenbosch

Supervised by

S.M. Bradshaw

J.J. Eksteen

STELLENBOSCH
APRIL 2006

Declaration

I, the undersigned, hereby declare that the work contained in this thesis is my own original work and that I have not previously in its entirety or in part submitted it at any university for a degree.

Signature: _________________________

Date: _________________________

i. SUMMARY

As easy to mine high grade ore bodies are being depleted, many mining industries are experiencing an increasing need to process lower grade ores, and thus the high costs involved in the mineral recovery from these ores (of which comminution energy costs are a large component) are of major concern. It has been estimated that up to 70% of the total energy consumption in mineral processing is used up by comminution processes, which characteristically may have efficiencies of less than 0.1% in terms of the transfer of electrical energy into particle breakage. In many cases, very fine grinding is required to liberate the valuable inclusions in such low grade ores, which also leads to slimes losses of valuable minerals due to the inefficiencies of recovery methods in the ultra-fine size ranges.

For many years the use of thermal pretreatment has been suggested as a way to decrease the costs of size reduction, and improve the liberation of valuable minerals in ores to aid later beneficiation technologies, but it was not until exploration into the use of microwaves to selectively heat only some of the minerals in ores, that this form of treatment became economically viable.

A low grade copper ore from Palabora was subjected to microwave treatment and then tested for ore strength in a laboratory rod mill, using the developing cumulative size distributions of the rod mill products with time to quantitatively determine the effects of microwave treatment on ore strength. It was seen that after microwave treatment the ore responded more readily to milling, producing a finer grind than for untreated ore at every measured time interval of milling. From this data, comminution models were created to describe the grinding of this ore in various flowsheet simulations.

An investigation was also performed to determine the effect of the application of microwave treatment on the liberation of minerals, due to the preferential breakage

induced along grain boundaries during the selective thermal expansion of certain mineral inclusions in ores during microwave treatment. To ensure consistency between results for microwave treated and untreated material, it was decided to use the same grinding time for both when preparing ore for the next stage of testing. A grinding time was chosen which would produce an 80% passing size of 800 μm for the microwave treated ore. This time was determined from the previous grinding tests and was found to be approximately 16 minutes. After particle size classification of the mill products through sieving, a size range suitable for gravity separation processes was chosen for sink-float testing, with the aim of investigating whether microwave treatment had liberated enough gangue material at large particle sizes to offer the possibility of removing this hard gangue material early on in the process, before costly fine grinding is required. XRF analysis of the products showed little difference in recoveries of gangue material to the floats between treated and untreated material, and that while most of the copper reported to the sinks, that some of the copper was always entrained in the floats. These losses of valuable minerals to the gravity tailings will lead to overall losses in copper mineral recovery from the plant.

QEMSCAN® analysis showed that there was a significant increase in mineral liberation in the size ranges associated with flotation as a result of the microwave treatment. An increase in liberation of the copper minerals which are easily recovered by flotation (i.e. chalcopyrite, cubanite, bornite, chalcocite and digenite) of 8.4% over that of the untreated ore was seen. This indicates that significant increases in copper recovery are possible after microwave treatment, and also that less fine grinding is then required to extract the valuable minerals from the ore, which leads to a reduction in loss of these valuable minerals to slimes.

Palabora Mining Company supplied enough data on their plant operations from 1989 to enable models to be built to describe the operation of the mills and classifiers used in their comminution circuit. This data, together with the work performed to compare the performance of microwave treated and untreated Palabora ore in both milling and liberation (which allowed for basic recovery models to be built), allowed flowsheet simulations of the plant operations. Simulations of the plant after the addition of microwave pretreatment of the ore showed that the total energy used in comminuting the ore (including that of the microwave treatment) to the correct size distribution for mineral recovery by flotation were reduced by 19% from that required for untreated ore, and was mainly due to reductions in the circulating loads over the mills. By exploiting the greater milling capacity allowed for by these lower circulating loads, it was shown that it was theoretically possible to obtain increases of up to 46% in maximum throughput after microwave treatment, while retaining the same final grind size in the feed sent to flotation as is required for untreated ore.

The addition of gravity separation processes to remove liberated gangue material from the comminution circuit early on, led to further savings in energy and also grinding media, and also decreased the requirements for flotation reagents and smelter fuel later on in the flowsheet. Unfortunately, the losses of entrained copper to the gravity separation tailings were such that overall economic losses were incurred by the operation. It was concluded that when dealing with low grade ores, only the implementation of very efficient and mineral specific separation technologies could make the removal of gangue material at large particle sizes (i.e. > 1 mm) viable.

Economic analyses based on the simulations of the plant under various operating conditions showed potential increases in plant profitability after the addition of microwave pretreatment of the ore before milling, and were reported using net present value (NPV) calculations for the plant over a 10 year period with monetary values discounted at 20%. When operating under the same conditions and throughput as in the 1989 data provided by Palabora Mining Company, an increase in the NPV of the plant of 23% over that for the reported operation was seen after the addition of microwave pretreatment, and an increase of 72% in NPV given a 10% increase in throughput which is made possible by microwave pretreatment of the ore. In real money terms, after 10 years of operation the increase in NPV of the plant with the addition of microwave pretreatment of the ore was seen to be around R259 million (under the conditions reported for the plant operation in 1989), and around R795 million if the 10% increase in throughput which is only made possible by microwave pretreatment is realized.

Current conditions at Palabora are very different from those supplied by the plant for the operation in 1989, however, as the mining operation has since been moved underground resulting in the throughput of the plant being greatly reduced, with the consequence that the plant is currently operating at a loss. Palabora mining company posted a net loss of R158 million over the 6 months leading up to June 2004, while an economic analysis of the proposed addition of microwave pretreatment of the ore at an increased throughput of 10% made possible by this treatment, indicated that a loss of only R138 million would have been incurred over the same 6 month period had this been implemented. Thus, while benefits from the introduction of microwave pretreatment of the ore before milling can still be seen under the operating conditions of the plant during the time period investigated, these alone would not have be able to bring the plant to profitable operation.

ii. OPSOMMING

As gevolg van die vinnige verbruiking van hoër graadse ertsliggame, is daar ‘n toeneemende aanvraag om lae graadse ertse te verwerk, en dit bring mee dat die hoë koste verbonde om hierdie minerale te herwin (grootliks die groottereduksie-energie komponent) ‘n saak van belang is. Daar is vasgestel dat tot 70% van die totale energieverbruik in ertsverwerking is geassosieër met die groottereduksieprosesse wat ter selfde tyd ‘n swak energiebenutting toon (waar minder as 0.1% van die toegevoerde elektriese energie omgeskakel word na die skep van nuwe oppervlakte deur partikelbreking). In baie gevalle moet daar ook gebruik gemaak word van ‘n fyner gemaalde produk om herwinning van die waardevolle korrels in lae graadse ertse te verkry. Dit lei verder tot ‘n verlies aan selektiwiteit in meeste mineraalskeidingsprosesse, sodat die graad van die konsentraat te laag is.

Vir baie jare is die gebruik van voorverhittingsbehandeling voorgestel as 'n moontlikheid om koste effektief laag te hou tydens die opbreek van die erts in kleiner dele, en ook om die groter korrels van volle vrygestelde waardevolle minerale te behou en dié te benut in latere tegnologieë. Dit was egter eers na die gebruik van mikrogolfverhitting, om selektief net ‘n klein deel van die minerale in erts te verhit, dat hierdie proses ekonomies vatbaar geraak het.

'n Lae graadse kopererts van Phalaborwa is aan mikrogolfbehandeling blootgestel en daarna is die erts-sterkte in 'n laboratorium staafmeul getoets, deur die tyd-afhangklike kumulatiewe partikelgroteverspreidings van erts binne die staafmeul te meet, om kwantitatief die effek van mikrogolfvoorverhitting op die erts sterkte te bepaal. Daar is waargeneem dat na mikrogolf-behandling die erts makliker gemaal kon word, en op elke tydstip waar metings geneem is, is na voorbehandeling 'n veel fyner produk in die staafmeul verkry. Hierdie data is gebruik om ontbindingsmodelle te skep om die maal van die erts in verskeie vloeidiagramme te simuleer.

'n Ondersoek was ook gedoen om vas te stel wat die effek is van die toepassing van mikrogolf behandeling op die vrystelling van minerale gedurende die opbreking van die erts, as gevolg van selektiewe breking van die ert tussen mineraalkorrels veroorsaak deur die veskillende termiese uitsetting van hierdie minerale gedurende voorverhitting. Om te verseker dat vergelykbare resultate verkry word in die eenvolgende stadium van toetsing, was daar besluit om die onbehandelde erts aan dieselfde malingstyd as die behandelde erts bloot te stel. 'n Malingstyd is gekies wat 'n 80% deurganggrote van 800 µm vir die mikrogolf behandelde erts sal bewerkstellig. Hierdie tyd is verkry van vorige maaltoetse en is op ongeveer 16 minute vasgestel. Na klassifikasie van die gemaalde produkte deur siwwing, is 'n grote geskik vir gravitasieskeidingsprosesse gekies vir dryf-sink behandeling met die doel om vas te stel of daar as gevolg van die mikrogolfbehandeling gangsteen vrygestel was met partikelgrotes groot genoeg om die verwydering van die harde gangsteen in 'n vroeë stadium te bewerkstelling, voordat daar met die duur proses van maal begin word. XRF analise van die produkte het gewys dat daar geen verskille in die herwinning van die gangsteen tot die dryfproduk was tussen die behandelde en onbehandelde erts nie, en ook dat terwyl die meeste van die koper in die sinkproduk herwin is, is daar ook koperminerale verloor in die dryfproduk. Die verliese van hierdie waardevolle minerale in die uitskot (dryfproduk) sal lei tot groot verliese van koper op die aanleg.

QEMSCAN® analises het bewys dat daar beslis ‘n vermeedering in mineraal vrystelling is in die partikelgroteklasse wat geassosieër is met flotasie as gevolg van mikrogolfbehandeling, wat lei tot 'n vermeedering van 8.4% in die vrystelling van koperminerale, wat met flotasie maklik herwin kan word, na behandeling van die erts. Dit bewys dat daar ‘n besliste vermeerdering in koperherwinning moontlik is na mikrogolfbehandeling, asook dat daar minder verfyning van die erts nodding is om die waardevolle minerale te herwin na behandeling met mikrogolfverhitting, en dus dié sal lei na 'n afname in die verliese van waardevolle minerale in die slyk.

Palabora Mynmaatskappy het genoeg data van hulle aanlegbedryf vanaf 1989 beskikbaar gestel om toe te laat dat modelle gebou kon word wat die bedryf van die meule en hidrosiklone in hul meulbane beskry. Hierdie data, tesame met die navorsing wat gedoen is om die maal en vrystelling van die behandelde en onbehandelde erts te vergelyk (wat ook die bou van basiese herwinningsmodelle toegelaat het), het vloeidiagram simulasies van die aanleg bedryf teogelaat. Simulasie van die aanleg na die toevoeging van mikrogolf behandeling van die erts het gewys dat die totale energie wat gebruik word (ingesluit dié van die mikrogolf behandeling) in die maling van die erts tot die korrekte grootteverspreiding vir flotasie verminder het tot 19% teenoor die van die onbehandelde erts. Dit is hoofsaaklik tewyte aan die vermindering in die belading van die meule met sirkulerende materiaal. Deur gebruik te maak van die groter kapasiteite van die meule wat moontlik gemaak is deur die kleiner hoeveelheid sikuleerende materiaal, is daar gewys dat na mikrogolf behandeling is dit teoreties moontlik om die vloeitempo met tot 46% te verhoog, en terseldertyd nog dieselfde partikelgrotevesrpeiding na flotasie toe te stuur soos wat benodig word vir onbehandelde erts.

Die gebruik van gravitasieskeidingsprosesse om vrygestelde gangsteen van die proses te verwyder, het tot verdere besparing in energie- en maalmediaverbruik gelei, en het ook gelei tot 'n vermindering in die nodigheid vir flotasiereagente en smeltoondbrandstof later in die vloeidiagram. Ongelukkig is die meesleuring van koper in die uitskot van die gravitasieskeidingsproses van so 'n aard dat dit die proses ekonomies onvatbaar maak. Hiermee is tot die gevolgtrekking gekom dat, waar lae graad erts bewerk word, slegs die implimenteering van hoogs spesifieke skeidings tegnologieë om die verwydering van net die groot (d.w.s. >1 mm) gangsteen partikels te verseker (sonder meesleuring van waardevolle minerale), hierdie proses vatbaar sal maak.

Ekonomieses analises van die aanlegbedryf het daarop gewys dat, na mikrogolf voorbehandeling van die erts, daar potensieël ‘n vermeedering in die winsgewendheid van die aanleg is, en hierdie stelling is gesteun met netto-huidige-waarde (NHW) berekeninge, wat die bedryf van die aanleg oor 10 jaar beskry met die geldwaardes teen 20% gediskonteer. As die aanleg bedryf word onder dieselfde toestande en met dieselfde vloeitempo as gesien is in die 1989 data voorsien deur Phalaborwa Mynmaatskappy, lei die insluiting van mikrogolf voorverhitting na 'n toename van 23% (of R259 miljoen) in die NHW van die aanleg teenoor bedryf sonder mikrogolfvoorverhitting van erts, en tot 'n verhoging van 72% (of R795 miljoen) in die NHW as ‘n 10% verhoging in vloeitempo (wat net deur die mikrogolfbehandeling moontlik gemaak is) ingestel word.

Huidiglik is die toestande by Phalaborwa baie verskillend van dié wat in 1989 deur die aanleg gerapporteer is, as gevolge daarvan dat die mynwerke in 2002 ondergronds geskuif het en wat prosesvloeitempo benadeel het. Huidige omstandighede het gelei tot die situasie waar die aanleg teen 'n verlies bedryf word. Phalaborwa Mynmaatskappy se finansieële state het 'n netto verlies van R158 miljoen getoon oor die ses maande tydperk tot en met Junie 2004, terwyl 'n ekonomiese analise daarop dui dat die voorgestelde byvoeging van mikrogolf voorbehandeling van erts met ‘n 10% verhoging in vloeitempo (wat weerheens as gevolg van die mikrogolfbehandeling moontlik is) tot 'n kleiner verlies van net R138 miljoen oor dieselfde tydperk lei. Dus terwyl daar baat gevind sou word met die byvoeging van mikrogolf voorbehandeling van die erts by Phalaborwa, sou dit nie genoeg invloed hê om die aanleg tot 'n winsgewende vlak te bring nie.

iii. ACKNOWLEDGEMENTS

I would like to especially thank the following people for their advice, insights and help in obtaining difficult to find information during this project:

S.M. Bradshaw
J. Eksteen
S.W. Kingman
K. Jackson
B. Roussouw
R. Rabe
A. Cumbane
E. Louwrens
K. Duarte
E. Spicer
M. McDonald
J. Scholtz
A. Bullock
P. Dicks

I would also like to thank my parents, Julia and Graham, for the love and support that they have always shown me in all my endeavours. I hope they are as proud of me in the completion of this thesis, as I have always been of them.

iv. TABLE OF CONTENTS

v. NOMENCLATURE

A	cross-sectional area of mill (m^2)
A_c	cross-sectional area of mill charge (m^2)
$\widetilde{A}$,**A**	square matrix describing particle breakage
b_{ij}	breakage function (for class j breaking into class i)
B(x;y)	breakage function (y is parent particle size, x is daughter particle size)
BWI	Bond Work Index
c	speed of light (2.998 x 10^8 m/s in a vacuum)
c_v	coefficient for variation of transport velocity with particle size
C_{EQ}	cost of equipment
C_{FC}	fixed capital cost
$\widetilde{C}$,**C**	column vector describing breakage of largest particle size class
CC	concentration criterion
d_p	particle size
d_{pl}	largest particle size
D	electric flux density
D_m	mill diameter inside shell liners (m)
D_p	power penetration depth
E	electric field intensity
E_a	amplitude of electric field strength
E_b	bulk material electric field
$\|E_z\|$	magnitude of the electrical field
E_0	electrical field strength at the surface of the absorbing material
E_2	guest material electric field
E^*	time dependant electric field strength
f	frequency (Hz)
f_L	Lang factor

F_e	experimentally determined size distribution
F_p	predicted size distribution
$\widetilde{F}$,**F**	cumulative size distribution
$\widetilde{F}_0$,$\mathbf{F_0}$	initial cumulative size distribution
g	acceleration due to gravity (m/s^2)
h	depth of charge (m)
H	magnetic flux intensity
H_{charge}	vertical distance between the mill roof and the charge surface
H_m	mass hold up of material in the mill
i	daughter size class
j	parent size class
J	current density
k_i	selection function value for particle size i
k_i^E	specific breakage rate function value for particle size i
k_j	selection function (rate of breakage of size class j)
$k(d_p)$	specific rate of breakage of a particle of size d_p
K	factor used to determine current density from unified approach
m_i	mass of material in size class i
m_j	mass of material in size class j
m_k	mass fraction of balls of size k
nt	number of grinding times required to accurately estimate S and B parameters
N_p	number of phases
N	number of size classes
NPV	Net Present Value
p_i^F	fraction of feed in size class i
p_i^P	fraction of product in size class i
p_j^P	fraction of material in size class j
P	power density
P_{net}	net mill power
P_v	time average power dissipated per unit volume in a material
P_0	power density at surface of material

r, r_{mill}	radius of mill inside liners (m)
r_{cp}	radius from the mill centre to the particle centre of gravity (m)
$r_{particle}$	radius of particle
rpm	revolutions per minute
S	chord length (m)
S_f	split function
S_i	selection function value at particle size i
$S_i(k)$	value of S_i for ball size k
$\overline{S_i}$	average value of S_i
S_1	selection function at 1 mm
SSQ	sum of squares
t	time
$\tilde{u}$,**u**	eigenvectors of **A**
$v(d_p)$	velocity of particle with size d_p
v_w	average velocity of water through mill
v_1	volume fraction of material comprising the matrix
v_2	volume fraction of material comprising the spheres
V	estimate of mill filling (%)
V_i	velocity of particles of size class i
$\tilde{v}$,**v**	eigenvectors of $\mathbf{A}^T$
x	size of the progeny particle
y	parent particle size (in mm)
y_0	reference parent size (usually 5 mm)
z	depth below surface of material

α	constant in Austin selection function
α_{chord}	angle that chord subtends at mill centre (degrees)
α_z	parameter used in determining electric field skin depth
β	parameter in Austin breakage function
γ	parameter in Austin breakage function

δ	constant
δ_z	skin depth / electrical field penetration depth
ε	absolute permittivity
ε_0	permittivity of free space
ε_r	relative permittivity
$\varepsilon', \varepsilon_r'$	dielectric constant
$\varepsilon'', \varepsilon_r''$	dielectric loss factor
ε_b	bulk dielectric property
ε_i^*	permittivity of phase i (can be either solvent or dispersed phases)
ε_m^*	permittivity of the medium
ε_1	dielectric property relating to the material comprising the matrix
ε_1^*	permittivity for the solvent (or continuous) phase
ε_2	dielectric property relating to the material comprising the spheres
ε_2^*	permittivity of the dissolved phase
λ	constant in Austin selection function
λ_c	wavelength (m)
λ_i	i^{th} eigenvalue of **A**
μ	fixes the particle size at which the selection function attains its maximum value
μ_m	magnetic susceptibility
ρ_f	density of suspending fluid (kg/l)
ρ_h	density of heavy mineral (kg/dm^3)
ρ_l	density of light mineral (kg/dm^3)
σ	conductivity
σ_d	conductivity of dielectric
σ_m	conductivity of metal
τ	residence time in mill
ϕ	weighting factor
ϕ_5	value of ϕ at the reference parent size (usually 5 mm)

Φ volume fraction of the dissolved phase

Φ_i volume fraction of phase i

ω angular frequency of electromagnetic wave

ω_p angular velocity of particle in rad/s

1. INTRODUCTION

It is a necessity of many mining industries to look to processing lower grade ores, and thus the associated requirement of finer grinding, to liberate minerals from such ores, means that the high energy requirements of comminution processes are of major concern. It has been estimated that, on average, around 30-50% (and as high as 70% for very hard ores) of the total energy consumption in a mineral concentrator can be attributed to comminution processes (Napier-Munn et al., 1996), and it is reported that as much as 1.5% of the total electrical energy consumption in the USA is attributable to comminution alone (Charles and Gallagher, 1982).

Traditional comminution processes consume approximately 30 kWh of energy to convert 1 tonne of rock to 100 μm sized particles. Surface energy measurements have shown, however, that if all the energy could be applied directly to the process of breakage, the actual energy input required for this process should be in the order of 0.01 kWh per tonne (Kanellopoulos and Ball, 1975). While these values should only be taken as order of magnitude estimates, the calculated productive energy use of < 0.1% clearly shows the inefficiency of such processes.

Added to the enormous energy consumption of comminution processes, the loss of grinding media through wear is also a significant cost in any minerals beneficiation process. Mintek, 1991, reports that often the cost of grinding media is of the same order as that of energy usage during comminution. Thus any reduction in ore strength (leading to shorter grinding times, or a reduction of milled tonnage in recycle) will result in significant cost savings from energy and grinding media conservation.

Another important concern faced by the minerals processing industry is that where very fine grinding is required to liberate valuable mineral inclusions for recovery, which is usually the case for low grade ores, the loss of valuable minerals to slimes escalates due to the inefficiencies of mineral recovery in these size ranges.

One mechanism which was identified as a possible solution to the problem of reducing ore strength before comminution was decrepitation, which is the spontaneous fracturing of ore particles on heating. This effect was investigated for many years, with the traditional means of thermal treatment that of heating followed by rapid quenching, to produce the largest thermal shock possible at the time from conventional heating techniques.

While successes were achieved in many cases in the form of reductions in ore strength after thermal treatment, the common limiting factor in preventing the process of heat treatment being economical was the enormous amounts of energy required to heat the bulk material to suitable temperatures (Prasher, 1987). A possible solution to this was found by Chen et al., 1984, who discovered that when exposed to microwave energy, minerals heated at different rates, with most gangue materials being transparent to microwave energy, while most valuable materials were good absorbers of microwave energy. This opened the way for the selective heating of only a small fraction of the bulk ore, and thus an economically viable form of thermal treatment.

Microwaves also have the advantage of heating any susceptible mineral quickly and volumetrically with substantially higher heating rates than are possible from conventional treatments, which then leads to greater stresses and particle fracturing, and consequently greater reductions in ore strength. It was discovered that this stress fracturing tended to occur at grain boundaries as a result of microwave induced differential heating (Fitzgibbon and Veasey, 1990), which could lead to better liberation of valuable minerals. Kingman et al., 2004, showed this to be true, reporting significant increases in the liberation of valuable minerals in ore mined at Palabora (a low grade copper ore) after microwave treatment, as well as 30% reductions in grinding energy, using microwave energy inputs of < 1 kWh/t.

It was thus seen that microwave pretreatment could potentially solve the problems of both reducing ore strength (reducing energy and media consumption) and increasing the liberation of valuable minerals in low grade ores at higher particle sizes (reducing the potential for slimes losses). What was missing from the literature, however, was a rigorous investigation of the significant economic potential of this technology, based on not only savings in grinding media and energy during milling, but also the downstream benefits of the improved liberation of valuable minerals as a result of microwave pretreatment.

It was decided to fill in this knowledge gap by studying the specific case of a single plant, and determining what changes the implementation of microwave pretreatment of the ore before milling could have on the minerals beneficiation flowsheet, and of equal importance, the economic impact on plant profitability shown after the implementation of this technology.

To this end, the work in this thesis forms an investigation into the operation of the minerals processing plant at the Palabora open pit copper mine; starting with quantifying the effects of microwave pretreatment on ore strength and mineral liberation, building on these results to create models to represent the effect of these changes in ore characteristics on the process equipment (of interest to the work in this thesis) at the plant, and then simulating the plant process flowsheet to investigate the existing plant operation after microwave treatment of the rod mill feed, and identify processing alternatives (such as processing higher throughputs or reducing the circulating loads over the mills) which better use the advantages offered by microwave pretreatment.

Apart from the direct benefits obtained from milling softer ores and the liberation of valuable minerals, what is also of considerable interest to the minerals processing industry is the concept of removing liberated gangue early on in the process flowsheet at large particle sizes. If possible, this would in many cases remove large quantities of often very hard to grind material from the processing stream before the very fine grinding, which is required to liberate valuable minerals for recovery, takes place. The possibility of implementing such a process into the Palabora flowsheet was investigated through sink/float experiments on Palabora ore, followed by simulations of an alternative process flowsheet which includes a gravity concentration unit after the rod mill (see Figure 6.6).

The ultimate aim of this thesis was then to investigate the economic viability of the implementation of microwave technology into a minerals processing plant, and comment on the best ways to successfully achieve this based on the results obtained from the flowsheet simulations performed in this work. This is done in chapter 7 where, similar to what is done in industry, net present value calculations are used to compare the profitability of the various projects studied in chapter 6 against one another, and thereby determine the viability of implementing microwave pretreatment for ores in the minerals processing industry.

It was proposed to do this in a step-by-step fashion, and this is reflected in the layout of the thesis which is as follows:

Chapter 2 - Presents a literature review of work performed in the field of microwave treatment of ores, and provides the reader with a good overview of the strengths and weaknesses of some of the work performed by researchers to date.

Chapter 3 - Presents essential theory to the reader. It is strongly suggested that the reader acquaint himself or herself with the basic theory which is presented in chapter 3 before reading further into the body of the work, as it will not only help the reader in understanding how microwave-mineral interactions occur and the effects of microwave treatment on an ore, but will also help the reader in understanding many of the topics touched on later during the experimental work and flowsheet simulations performed.

Chapter 4 - Collects the experimental data obtained during the work performed for the thesis and includes: rod milling tests and characterization of the rod mill products through sink/float testing, XRF and QEMSCAN analysis.

Chapter 5 - Provides an interpretation of the experimental results and develops the necessary models for use in the flowsheet simulations to follow.

Chapter 6 - Describes the flowsheet simulations of the existing operation, as well as those of the proposed alternative operations.

Chapter 7 - Analyses the economic viability of each processing option studied, and compares the ensuing plant profitability, after the implementation of such options, against the base case of the existing conventional process flowsheet at Palabora.

While the work in this thesis is based on data concerning the operation of the minerals processing plant at Palabora, it must be kept in mind that this work is first and foremost a comparison of microwave treated and untreated ore processed in the same flowsheet, and with the same economic considerations applied in analyzing the viability of implementing microwave treatment.

2. LITERATURE REVIEW

The thermal treatment of ore to bring about thermal fracturing, and thereby a reduction in ore strength, is by no means a novel idea. The 1st century BC Greek historian, Diodorus Siculus, recorded in his Bibliotheca Historica the ancient practice of fire setting, verifying his work with that of another Greek historian, Agatharcides, who had visited the gold mines in Egypt around the 2nd century BC (Meyer, 1997).

Oldfather, 1967, provides a translation of Diodorus's account of the practice: "The gold-bearing earth which is hardest they first burn with a hot fire, and when they have crumbled it...they continue the working of it by hand; and the soft rock which can yield to moderate effort is crushed with a sledge…".

The practice of fire setting basically consisted of constructing a large fire against the rock face to be mined. As the rock heated unevenly, it would fracture internally, severely weakening the rock. After the fires died down the rock face would be doused with water, though whether this rapid quenching was employed to further weaken the rock or to allow the miners to immediately continue working the rock face is not known (The Tech, 1886).

Using this process, it was possible to weaken the rock face to the depth of approximately a foot at a time, after which the soft ore was mined and when the harder rock face was again encountered, fire setting was again employed (Cowen, 1999).

Archeological evidence supports the notion that the practice of fire-setting was a world-wide phenomenon and may indeed be much older than those activities reported in the records of Diodorus Siculus, with ancient mining sites discovered at Rudna Glava in the Balkans suggesting the use of fire setting around 4500 to 4000 BC, at Ai Bunar in southern Bulgaria also dated at several thousand years BC and from which it is estimated that between 20 000 and 30 000 tonnes of ore were mined while employing the method when required (Cowen, 1999), at the ancient mining sites around Isle Royale in the Lake Superior region in North America to mine copper and up until just a few centuries ago in Japan for creating long tunnels (The Tech, 1886)

In fact, it remained a vital part of the mining industry until the first use of gunpowder for blasting in 1613 (The Tech, 1886), after which the use of thermal treatment declined in favour of the quicker processes of drilling and blasting.

It is reported in a review paper by Fitzgibbon and Veasey, 1990, that work on the use of thermal treatment to aid in rock breakage during comminution processes began again early in the 20th century, with practical studies on Cornish tin ores (Yates, 1919) and quartzites (Holman, 1927). Fitzgibbon and Veasey, 1990, report that this early work showed that the thermal pretreatment of ores before comminution resulted not only in a reduction in the strength of the ores studied, but also in fewer fines being produced.

Work by Myer, 1925, and Holman, 1927, also studied the dependence of the susceptibility of ores to heat treatment on particle size and concluded that the effectiveness of the treatment decreased with particle size (Fitzgibbon and Veasey, 1990).

Fitzgibbon and Veasey, 1990, further report in their review paper that there is a general agreement of results between different authors (Holman, 1927, Brown et al., 1958) which show that the degree of weakening of an ore is related to the heating rates applied, and that quicker treatments tend to produce better results.

As early as 1962, it was known that the effect of thermal treatment on ore strength varies with ore mineralogy, and that fluorites and byrites, in particular, are susceptible to this effect, but studies showed that the process of thermal treatment was uneconomical when compared to the use of conventional grinding alone (Prasher, 1987), due to the enormous energy requirements associated with heating the bulk ore to the required temperatures, where Wills et al., 1987, report that other workers have calculated that the cost of heat treatment and subsequent grinding could be as high as 6 times that of conventional grinding alone (Scheding et al., 1981).

Kanellopoulus and Ball, 1975, defined the possible mechanisms associated with thermal fissuring as:

- Differential thermal expansion or contraction due to temperature gradients and differences in properties of the various minerals present.
- Inter-granular stresses generated between individual crystals of the same mineral due to anisotropic thermal expansion (e.g. in quartzite).
- Stresses associated with volume changes during phase transitions (e.g. the α-β transition of quartzite at 573°C).
- Stresses accompanying the dramatic volume changes associated with gaseous evolutions from volatile inclusions (which includes the evaporation of water from fractures and micropores).

Their investigations of the particle size distributions obtained from the milling and crushing of quartzite material showed that heat treatment above 400°C improves the comminution of the ore, but that the best results are obtained after heating the quartzite to temperatures above the α-β phase transition temperature of quartz (i.e. 573°C), at which a sudden volumetric expansion (i.e. a volume increase of 0.86%) of quartz crystals occurs. It was seen that any further heating of the ore above this did not markedly affect the comminution of the ore, and it could be concluded that the rapid volumetric changes occurring during the phase transition caused the most damage to the material. Comparative testing of material which was slow cooled from 680°C to ambient, and material which was shock cooled through water quenching, showed no difference in the product size distribution of the material after milling. Comparisons of results obtained from the same heat treatments after comminution by slow crushing, however, indicate that quenching the ore results in a change in the product particle size distribution, with significantly less material passing at larger sizes with the difference in passing size decreasing with particle size, thus resulting in a finer product without a significant increase in the production of very fine material. This was the first indication that the manner of the post-processing of the material may be as important as the thermal treatment itself.

Pocock et al., 1998, investigated the use of various quenching solutions to ascertain whether any improvement could be seen from using acid, alkali or salt solutions instead of water. It was found that all of these showed improvements in grinding energy reduction over the use of water, and of these, it was found that the use of acid or alkali solutions provided the best results. At the same time, it was seen from UFLC tests that as comminution of the treated particles continued (i.e. as the particles become smaller), the observed effects of the thermal pretreatment are reduced. What this indicates is that as the easily exploited newly formed fractures are used up, the strength of the ore begins to once again approach that of the untreated ore.

Fitzgibbon and Veasey, 1990, report in their review paper one of the early documented observations of increases in mineral liberation after thermal treatment, with the almost ideal liberation occurring in certain high carbonate rocks being attributed to the evolution of carbon dioxide along grain boundaries, which subsequently causes intergranular fracturing (Jones and Fullard, 1966).

Wills et al., 1987, investigated the thermally assisted liberation of cassiterite in an ore mined at South Crofty. Previous work on this ore (Sherring, 1981) had shown a 55% reduction in grinding resistance when the ore was heated to 650°C and then rapidly cooled, however, this was greatly offset by the energy required to heat the material. It was suggested by Manser, 1983, that an increase in tin recovery of 1% would offset this cost in the case of the South Crofty ore, due to the value of the recovered minerals. Employing similar conditions in their work, and heat treated polished sections of the ore which could be photographed before and after the treatment to look for any induced fractures which might indicate that this increase in liberation may be possible. Their results showed that while some intergranular fracturing was observed as a result of their heat treatment, in most of the cases extensive transgranular fracturing occurred, and later separation tests showed no enhanced liberation or recovery of this material with heat treatment.

An important result of their work, however, was the observation that intergranular fracturing was most prevalent between cassiterite and quartz grains which had smooth boundaries, while transgranular fracture occurred mostly across protrusions of cassiterite extending from the host cassiterite grains. It was concluded that, during thermal treatment, regularly shaped grains are more likely to be liberated without breaking than those grains in which complex intergrowths with adjacent minerals are present. Based on the slight disparity between the results of the fracture analysis work (which showed that at least some effect was seen) and experimental separation testing (which showed no effect had taken place), it was also suggested that any improvements in liberation which could have been indicated by the separation tests would have been masked by the indiscriminate process of rod milling used to grind the ore, and that other forms of comminution may have better results, once again indicating that the manner of the post-processing of the material is extremely important.

In all the studies which were performed, the major limiting factor in preventing the process of heat treatment becoming economical was the enormous amounts of energy required to heat the material to suitable temperatures. A possible solution to this problem became known after much research into the field of the microwave treatment of minerals, which has wide applications in the minerals industry, not only in thermally assisted liberation, but also extractive metallurgy, the desulphurization of coal, drying and anhydration of minerals, leaching and waste management to name a few (Kingman and Rowson, 1998, Haque, 1999).

It is reported in a review paper by Xia and Pickles, 1997, that the earliest work on the microwaving of minerals began with a study of the high temperature processing of certain oxides and sulfides using a resonant cavity operating at 2.45 GHz and variable power up to 1.6 kW (Ford and Pei, 1967). The results of this early work were qualitative in nature, concluding that, in general, dark coloured compounds heated rapidly (reaching temperatures of up to 1000°C), while lighter coloured compounds heated slower but were capable of being heated to higher temperatures. This was followed by further work by Wong, 1975, who expanded the knowledge of the field of the dielectric heating with a study of the heating of metal oxides.

Perhaps the most important of the early work was that of Chen et al., 1984, who investigated the reaction of 40 minerals to microwave exposure in a waveguide applicator which allowed the mineral samples to be inserted in an area of known high electric field strength. Though by this time it was already known that microwaves would heat some minerals selectively, this work further showed that microwave heating is dependant on the composition of the mineral, and thus elemental substitutions would affect the behaviour of a mineral in an electric field. An example of this was noted with sphalerite, where high iron sphalerite would eventually heat quite well after a period of slow heating at low temperatures, but that low iron sphalerite did not heat readily. From the large number of minerals tested, it was noted that most silicates, carbonates and sulfates, and some oxides and sulfides are transparent to microwave energy, while most sulfides, arsenides, sulfosalts and sulfarsenides, and some oxides, heat well when subjected to microwave irradiation.

Haque, 1987, investigated the application of microwave treatment to a refractory arsenopyritic gold ore. It was found that the results for microwave treatment of the ore were comparable to those obtained using conventional roasting (in terms of gold and silver recovery), but that the required treatment time for conventional roasting of about 2½ hours per tonne of concentrate could be reduced to around 15 minutes when using microwave treatment. Other advantages offered by using microwave treatment were immediate control over the heating process, material selective heating which reduced treatment energy requirements and independence of the necessity of a critical amount of sulphur in the concentrates. At the same time it was also concluded that particles of 2 mm in size could easily be calcined using microwave treatments.

Fitzgibbon and Veasey, 1990, and Xia and Pickles, 1997, indicate in their review papers on the microwave treatment of minerals that this work was later expanded by Walkiewicz et al., 1988, who also showed that thermal stress fracturing along grain boundaries was induced in some samples after microwave heating, and suggested that this could significantly influence not only the grindability of microwave treated ores, but mineral liberation as well. Walkiewicz et al, 1991, later investigated the former claim with tests on the grindability of several microwave treated ores, and showed reductions of between 1.3% and 23.7% in work index, depending on the manner of microwave treatment and the type of ore tested (Xia and Pickles, 1997).

Work by Tinga, 1988, in the field of microwave sintering suggested that preferential heating of grain boundaries occurs. This should be the case for any high loss dielectric grain of reasonable diameter embedded in a relatively low loss host material. Effects such as conduction losses and the rate of heating do play a role, however, and care should be taken before assuming this is true for any particular situation. Tinga, 1988, also stated that the single most important factor when considering microwave heating was the design of the applicator, where choosing the wrong applicator for a task will mostly likely result in very few of the expected benefits of microwave processing being seen, and therefore very little improvement in results from the treatment versus those of conventional practices.

Standish et al., 1991 performed drying experiments on particulate Al_2O_3 and Fe_3O_4 to investigate particle size effects on microwave absorption. It was found that fine Al_2O_3 heated faster than coarse Al_2O_3, while coarse Fe_3O_4 heated faster than fine Fe_3O_4. It was noted that the heating of the Al_2O_3 was influenced by the initial water content of the samples tested, while for the Fe_3O_4 the effect of moisture content was negligible due to the high loss factor of this material. It can be expected that, in general, high loss minerals will behave similarly to what was observed for Fe_3O_4, with samples consisting of coarser particles heating better than those made up of fine particles. This holds great advantages for the minerals processing industry as microwave treatment of lossy materials at larger sizes would reduce comminution costs.

Experiments by Tavares and King, 1995, compared conventional heating methods with low power microwave heating in a multimode cavity. It was found that where sufficient lossy material (i.e. material with a high susceptibility to microwave energy) was present, microwave treatment showed larger decreases in particle strength than conventional heating, but in the cases of a low grade ore, there was not enough lossy material and little benefit from microwave treatment could be seen. At the same time, it was seen that after either conventional or microwave thermal treatment of multiphase materials, small changes in the fragmentation pattern of these ores were observed, and it was suggested that this was attributable to differential thermal expansion of mineral grains resulting in grain boundary fracture.

Tavares and King, March 1996, investigating samples of specific iron, taconite and titanium ores in a multimode cavity using a low power input of between 0 and 1.2 kW, compared the strengths of untreated ore with that of ores treated both conventionally and with microwaves. It was observed that in all cases the thermal treatments affected the ore favourably in terms of both reductions in fracture energy and increased damage, however, there was very little difference between the results for the conventional and microwave treatments, with the exception of a greater reduction in fracture energy of the iron ore and greater damage to the titanium ore from microwave treatment. From examinations of the single particle breakage functions, it was further seen that the thermal pretreatments resulted in a shift in the top of the breakage function to smaller sizes without an increase in the production of very fine material, and also that the microwave treated ores tended to produce a greater shift in the top of the breakage function than conventionally treated ores. It was concluded that this change in fragmentation pattern, together with observations from image analysis of a 50% increase in grain boundary fracture in the microwaved iron ore, may result in improved liberation. Later tests by the same authors (Tavares and King, August 1996) on a copper ore showed no difference between the fracture energies of microwave pretreated and untreated material, though it was noted that there was a slight indication of grain boundary fracture around the sulfide grains. It is not stated what kind of microwave treatment was used, however, and thus these results are not comparable to those of other workers.

Walkiewicz et al., 1993, investigating the effect of power level on Bond work index, found that the larger temperature gradients associated with the more rapid development of heat within the particle grains as a result of higher microwave powers, led to a larger decrease in ore strength than for exposure to lower microwave powers.

Salsman et al., 1996, used a finite element numerical model of a single pyrite particle in a calcite matrix to further investigated the phenomenon of thermally assisted liberation using microwave energy. Using power densities which are likely to be possible within the pyrite grains, it was seen that large tensile stresses, exceeding the tensile strengths of most common rock material, were generated along the pyrite-calcite interface. It was discovered that a decrease in either particle size or in the grain size of the microwave susceptible mineral inclusions, led to a decrease in the intergranular stresses developed within the particles. The influence of power density on the absorption of microwave energy by minerals was also investigated, and it was found that by using short concentrated microwave pulses to increase the power density within the material, substantially higher stresses could be generated within the particles at the same power inputs.

While studying the effect of microwave processing on Palabora open pit ore, Kingman, 1998, determined that significant increases in recovery from magnetic separation could be achieved by microwaving, however, longer exposure times brought about the opposite effect due to partial melting and oxidation of the magnetite present, thus showing that over treating material was possible. After an initial small increase in recovery of the copper, during flotation, after short exposure times, a drastic decline in recovery in this process was also noted. This was explained as being due to the oxidation of the sulfide minerals.

Later work by Kingman et al., 2000, encompassing tests on several commercially exploited ores to investigate the influence of ore mineralogy on microwave assisted grinding showed that the most responsive ores were those with a consistent mineralogy, containing good absorbers in a transparent gangue, while those with small lossy particles that are finely disseminated in discrete elements were shown to have the worst response in terms of reduction in required grinding energy. One extremely important result from this paper was the suggestion that purpose built microwave cavities may be important in making the treatment of ores more economically viable.

Work on the grindability of coal by Marland et al., 2000, indicated that reductions in work index of up to 50% occur after microwave pretreatment. The greatest strength reductions were obtained from lower ranked coals, and it was suggested that this was most likely due to the higher inherent moisture content of such coals, with gaseous evolutions of water and volatile matter the main causes of damage to the coal particles. It was also found that microwave radiation affected the calorific value to the same extant as would be expected from conventional drying procedure, and it was concluded that the application of microwave treatment did not alter the fuel potential of coal.

Wang and Forssberg, 2000, performed tests on three ores (i.e. limestone, dolomite and quartz) to investigate their microwave heating behaviour and subsequent grindability during dry ball milling, after pretreatment. Each ore was crushed and sized into three fractions for testing, these being -9.75+5.75 mm, -4.7+1.6 mm and -1.6 mm. It was noted that the particle size of the material undergoing thermal pretreatment had a significant effect on the heating behaviour and subsequent grindability of two of the ores, with tests on the quartz and limestone material showing that the microwave pretreatment was only effective for the -9.5+4.75 mm material, which then subsequently showed improved grindability. Below 4.75 mm, little or no effect was seen, and it was suggested that this was due to conductive heat transfer which plays a more important role in heat loss from smaller particles. It was also found that increasing the exposure time led to a further increase in the grindability of these two ores. Dolomite showed little reaction to microwave pretreatment during subsequent dry milling experiments. Tests were also performed to determine the degree of liberation of sulfide minerals in a low grade copper ore (0.22-0.4% Cu) from Aitik after crushing. SEM photomicrographs showed that thermal stress cracks occurred readily along the sulfide-gangue mineral grain boundaries, and image analysis software showed a substantial increase in the liberation of sulfide minerals in the ore matrix with microwave pretreatment prior to crushing.

Vorster et al, 2001, performed several tests on a massive copper ore and a massive copper-zinc ore, both from Neves Corvo in southern Portugal, using a 2.6 kW multimode cavity operating at 2.45 GHz. Quenching after 90 seconds of microwave exposure led to a 70% reduction in the work index of the massive copper ore. The effect of quenching was also illustrated with tests on the massive copper-zinc ore, where after 90 seconds of microwave exposure with no quenching, a reduction of 50% in the strength of the ore was obtained, while the addition of quenching directly after microwave treatment led to a further 15% reduction in work index. Copper flotation trials showed that no benefit in terms of improved copper recovery was seen after microwave treatment, and it was concluded that the improved liberation after microwave treatment which was noted from SEM analysis, was most likely offset by some surface oxidation of the recoverable sulfide minerals.

Whittles et al., 2003, investigated the effect of power density on the microwave treatment of ores, using finite difference techniques to model microwave heating, thermal conduction, thermal expansion, thermally induced fracturing and strain softening of a particle containing dispersion of 2 mm square pyrite grains in a 15 mm by 30 mm calcite host matrix. Simulations were also performed to determine any change in the uniaxial compressive strength of the particle after microwave heating. It was shown that power density is an important factor in microwave treatment of ores, with the application of high power densities resulting in much greater damage to the particle. It was concluded that utilizing high power densities for shorter times could also drastically reduce the microwave treatment energy required to below 1 kWh/t.

Kingman et al., 2004, investigated the treatment of a copper carbonatite ore from a mine in South Africa using a single mode, high power applicator (i.e. a variable power input of up to 15 kW). Their results showed that a sort of threshold value existed for the power input into the system, which once passed, caused serious damage to the particle in a very short treatment time (< 0.5 seconds). The importance of this discovery is best seen when the values are turned into values of power densities within the valuable minerals, in which case these values are no longer specific to a certain microwave system, allowing the design of any system with the goal of obtaining these power densities. It was shown that reductions of up to 30% in grinding energy could be achieved with microwave energy inputs of less than 1 kWh/t. QEMSCAN analysis of the product of drop weight tests also showed a decrease in the amount of locked and middling copper sulfides in the +500 µm size class.

Jones et al., 2004, also investigated the effect of microwave treatment through numerical simulations of a system of microwave absorbing pyrite grains in a microwave transparent calcite host. An important result of this work was the verification and explanation of the observations of Wills et al., 1987, who determined that regularly shaped mineral inclusions with smooth boundaries were much more likely to result in thermally induced intergranular fracture than irregular grains which tend to be damaged by transgranular fracturing as a direct result of thermal treatment. It was determined that for spherical absorbing grains the occurrence of transgranular fracture is highly unlikely as the symmetry of the grain ensures that the compressive stresses generated inside the microwave absorber are equal in all directions, thus reducing the likelihood of shear stresses developing within the grain. As grain shape deviates from spherical, the likelihood of transgranular fracture rises. It was also seen that as the grain size of the microwave absorber decreased, conduction losses resulted in lower temperatures being reached within the absorbing grain at the end of the same exposure time. This resulted in lower stresses being generated around the absorbing grain, with less damage to the host particle as a result.

The use of microwave treatment to enhance the liberation of gold for subsequent recovery by gravity separation techniques has also been investigated. Amankwah et al., 2005, performed tests on samples of a gold ore containing quartz, silicates and iron oxides with a head grade of 6.4 g/t of gold, using 2 kW of power in a multimode cavity. It was seen that the microwave treatment resulted in a maximum reduction of 31.2% in crushing strength and a reduction of 18.5% in work index. SEM analysis clearly showed that microwave induced fractures were occurring in the ore, and an improvement of 12% in gold recovery from gravity separation tests showed that this resulted in the liberation of the gold at coarser particles sizes during comminution.

Al-Harahsheh et al., 2005, have investigated the leaching kinetics of chalcopyrite under the influence of microwave treatment. Comparison of the amount of copper recovered from chalcopyrite under conventional and microwave heat treatment show marginal, but consistent, improvements in copper recovery when using microwave treatment as opposed to conventional treatment. It was suggested that the increase in copper recovery with microwave leaching was due to localized higher temperatures around the outer shell of the leaching solution as a result of the high dielectric loss factor (and thus low penetration depth) of the solution, and also selective heating of the outer skin of the chalcopyrite particles due to the high conductivity of this material.

From the previous research in this field, it is thus seen that when correctly applied thermal treatment can provide benefits to the minerals processing industry, and that the use of microwave treatment is not only more cost effective than conventional treatments, but can influence mineral liberation as well as ore strength, and can in certain cases even be employed during recovery processes to ensure heightened reaction kinetics and better recoveries.

3. ESSENTIAL AND APPLICABLE THEORY

3.1. ELECTROMAGNETIC THEORY

3.1.1. INTRODUCTION TO ELECTROMAGNETIC WAVES

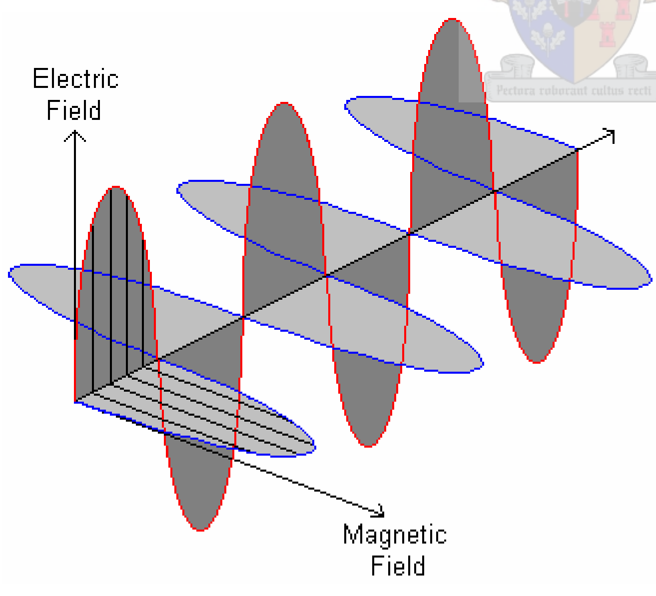

Figure 3.1 - Electric and Magnetic Fields in an EM Wave

Electromagnetic (EM) radiation may be characterized as a stream of photons travelling in a wave-like pattern at the speed of light. The electromagnetic spectrum is the group name for all waves that propagate by means of electric and magnetic field interactions at right angles to one another (Figure 3.1).

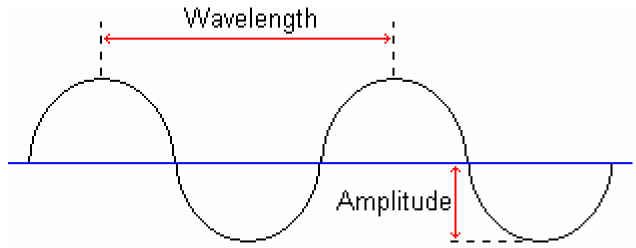

Figure 3.2 - Simplified Representation of an EM Wave

The frequency and wave length (see Figure 3.2) of electromagnetic waves are related to the speed of light in a vacuum through the following equation

$$c = f \cdot \lambda \qquad \textbf{3.1}$$

where c speed of light (2.998×10^{8} m/s in a vacuum)
f frequency (Hz)
λ_c wavelength (m)

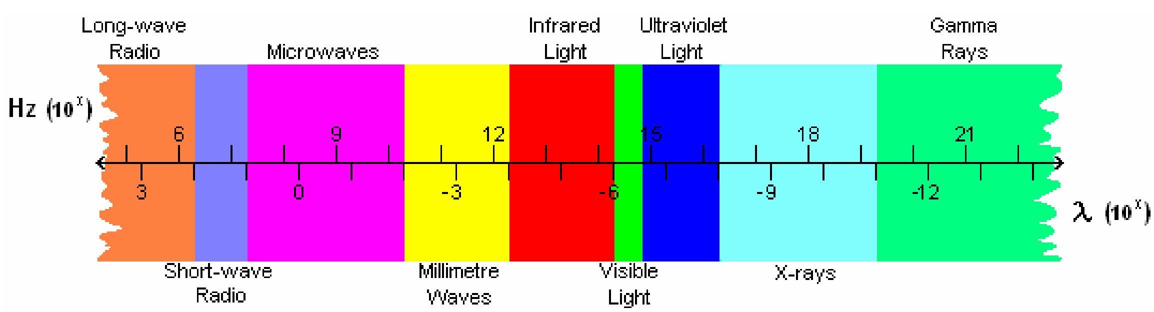

Figure 3.3 - Representation of the Electromagnetic Spectrum

Microwaves form part of the electromagnetic spectrum and occupy a bandwidth between around 10^7 and 10^{10} Hz, with associated wavelengths in free space then ranging from $3x10^1$ to $3x10^{-2}$ metres.

The amount of energy carried by these waves increases with increasing frequency, so that when ranked from lowest to highest energy we have: long-wave radio waves, short-wave radio waves, microwaves, millimeter waves, infrared light, visible light, ultraviolet light, X-rays and gamma rays.

As such, microwaves carry less energy than many other wave types in the spectrum, however, other factors such as their relatively large penetration depth into bodies coupled with their relatively high power dissipation in certain materials makes them a prime candidate for use in heating applications.

3.1.2. CONDUCTIVE AND DISPLACEMENT CURRENT DENSITY

The classical approach to electromagnetic theory applies Ampere's law to determine the current density developed in a material through the following equation

$$\nabla \times H = \sigma E + \frac{\partial D}{\partial t} \qquad \textbf{3.2}$$

with

with	H	magnetic flux intensity
	σ	conductivity
	E	electric field intensity
	D	electric flux density

Where D is defined by the relation

$$D = \varepsilon E \qquad \textbf{3.3}$$

and ε is the absolute permittivity of the material given by

$$\varepsilon = \varepsilon_0 \varepsilon_r \qquad \textbf{3.4}$$

with ε_0 permittivity of free space

ε_r relative permittivity

Since an electromagnetic wave consists of time harmonic electrical and magnetic fields (see Figure 3.1), the electric field strength, and thus the heating effect produced by the wave-material interactions, must therefore also be time dependent. The variation in electric field strength with time is based on the angular frequency of the EM wave and can be expressed through

$$E = E_a e^{j\omega t} \qquad \textbf{3.5}$$

with E_a amplitude of electric field strength

t time

By combining equations 3.3 to 3.5 with equation 3.2, and differentiating the appropriate term in equation 3.2, we arrive at

$$\nabla \times H = \sigma E + j\omega\varepsilon_0\varepsilon_r E \qquad \textbf{3.6}$$

The current density established within the medium, as a result of the applied electrical field, is represented by the first term on the right hand side of equation 3.6. The second term on the right hand side is known as the displacement current density, and is the main form of electrical conduction within the material.

When dealing with conductive materials such as metals or dielectrics, however, the classical approach will not suffice and it becomes necessary to introduce a complex permittivity to represent ε in the material under the influence of a time harmonic electromagnetic field, thus

$$\varepsilon = \varepsilon_0 \left(\varepsilon' - j\varepsilon''\right) \qquad \textbf{3.7}$$

with ε' relative dielectric constant

ε" relative dielectric loss factor

Similar to the derivation of equation 3.6, by inserting equation 3.7 into equation 3.2 and differentiating the appropriate term in that equation, we arrive at

$$J_t = \sigma_d E + \varepsilon_0 \left(\varepsilon' - \varepsilon''\right) j\omega E \qquad \textbf{3.8}$$

with σ_d being the conductivity of the dielectric, and

$$J_t = \nabla \times H \qquad \textbf{3.9}$$

simply being a single term to represent the current density. By rearranging equation 3.8 and grouping like terms we arrive at

$$J_t = \left(\sigma_d + \varepsilon_0 \omega \varepsilon''\right) E + j\omega\varepsilon_0 \varepsilon' E = \sigma_e E + j\omega\varepsilon_0 \varepsilon' E \qquad \textbf{3.10}$$

where σ_e is the effective conductivity of the dielectric. If we now let $\sigma_e = \sigma$ and $\varepsilon' = \varepsilon_r$, then equations 3.6 and 3.10 are the same. What we see then is that the conductivity, as expressed from the classical point of view, is actually a combination of different mechanisms, specifically here, dipolar rotation ($\omega\varepsilon_0\varepsilon''$) and dielectric conductivity (σ_d).

Metaxas, 1996, has created a unified approach governing the principles of electromagnetic heating, applicable to direct resistance and induction heating for metallic materials as well as radio frequency and microwave heating for dielectrics, based on the mechanism of electrical conductivity, and this approach proceeds as follows.

Based on the similarities between the two equations 3.6 and 3.10 above, it is possible to apply equation 3.10 to any material. This is done by introducing a factor K into a generalized version of this equation where σ applies to either dielectric or metallic conductivity, such that

$$J_t = (\sigma + \varepsilon_0\omega\varepsilon'')E + j\omega\varepsilon_0\varepsilon' E = j\omega\varepsilon_0 KE \qquad \textbf{3.11}$$

and thus

$$K = \frac{[\varepsilon - j(\sigma/\omega)]}{\varepsilon_0} = \varepsilon'\left[1 - j\left(\frac{\sigma}{\omega\varepsilon_0\varepsilon'} + \frac{\varepsilon''}{\varepsilon'}\right)\right] = \varepsilon' - j\varepsilon_e'' \qquad \textbf{3.12}$$

where the latter terms are obtained having made use of equation 3.7. K can now be adapted for each case:

- for a metallic material: the major loss mechanism for induction (direct resistance / ohmic) heating is due to metallic conductivity, while the displacement current density is negligible.

$$\sigma = \sigma_m \qquad \textbf{3.13}$$

$$\frac{\sigma_m}{\omega\varepsilon_0\varepsilon'} >> 1 \quad \textbf{3.14}$$

$$\varepsilon'' = 0 \quad \textbf{3.15}$$

thus $$K_{metal} = \frac{-j\sigma_m}{\varepsilon_0\omega} \quad \textbf{3.16}$$

- for a dielectric with no ionic loss mechanism: the major loss mechanism is then the displacement current density and no conductive losses are present.

$$\sigma = \sigma_d = 0 \quad \textbf{3.17}$$

thus $$K_{dielectric} = \varepsilon' - j\varepsilon'' \quad \textbf{3.18}$$

- for a dielectric with ionic and relaxation type loss mechanisms: the combined loss mechanisms are due to dielectric conductivity and the part of the displacement current that is in phase with the applied dielectric field.

$$\varepsilon_e'' = \frac{\sigma_d}{\omega\varepsilon_0} + \varepsilon'' \quad \textbf{3.19}$$

thus $$K_{dielectric} = \varepsilon' - j\left(\frac{\sigma_d}{\omega\varepsilon_0} + \varepsilon''\right) \quad \textbf{3.20}$$

It is then possible to use K factors to determine the current density developed in a material when dealing with any form of electromagnetic heating (Metaxas, 1996).

3.1.3. TRANSMISSION OF MICROWAVE ENERGY

Similar to light shining on a glass pane, when microwave energy ($E_{incident}$) is applied to a load, the energy can be reflected ($E_{reflected}$) off the surface, or transmitted ($E_{transmitted}$) into the interior of the load (see Figure 3.4).

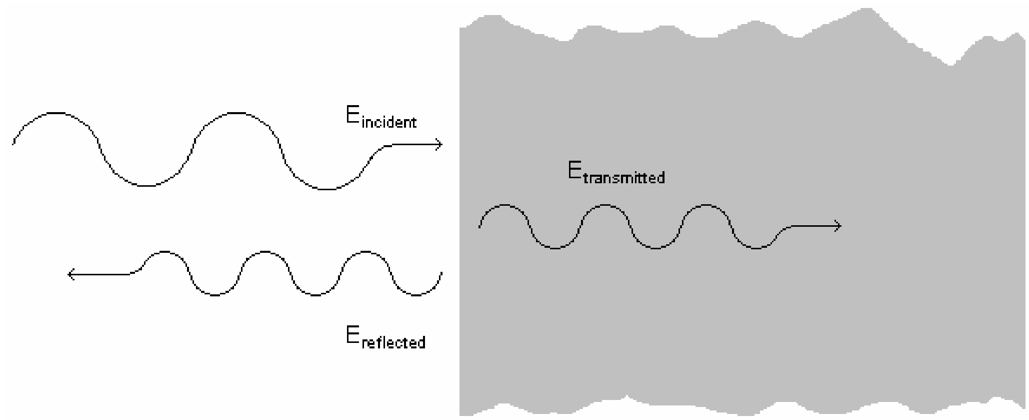

Figure 3.4 - Transmission of Microwaves Through a Material

The concept of impedance matching can be utilized to attempt to reduce the amount of reflected energy. For dynamic systems, this is usually done by attaching a tuner to the microwave source, before it enters the cavity, which will feed the microwaves into the load more efficiently.

3.1.4. PENETRATION DEPTH

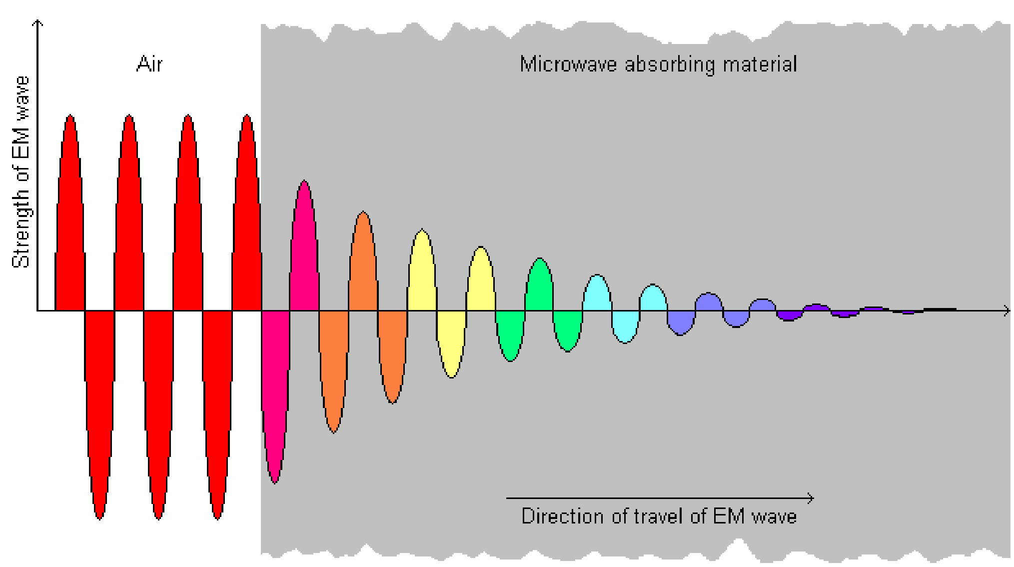

Figure 3.5 - Attenuation of microwave energy as load absorbs power

Figure 3.5 shows how the electrical field decreases in strength when a microwave penetrates a lossy (absorbing) material. As the field penetrates further into the material, its amplitude decreases due to the energy lost in heating the material it passes through.

The skin depth, or electrical field penetration depth, (δ_z) of an electrical field is defined as the distance the wave travels through the material until its magnitude reduces to 1/e of its value at the surface of the absorbing material.

Metaxas, 1996, derives a formula for calculating the penetration depth to give

$$\delta_z = 1/\alpha_z \qquad \mathbf{3.21}$$

with the value of α_z obtained by

$$\alpha_z = \omega\sqrt{\frac{\mu_m \varepsilon_0 \varepsilon'}{2}}\left[\sqrt{\sqrt{1+\left(\frac{\sigma_e}{\omega\varepsilon_0\varepsilon'}\right)^2}-1}\right] \qquad \mathbf{3.22}$$

The penetration depth can then be used to quantify the reduction in electrical field strength of microwaves passing through lossy dielectric materials mathematically as follows

$$\left|E_z\right| = E_0 e^{-z/\delta_z} \qquad \mathbf{3.23}$$

where	$\lvert E_z \rvert$	magnitude of the electrical field
	E_0	electrical field strength at the surface of the absorbing material
	z	depth below surface of material

For a metallic material, it is the penetration depth of the magnetic field which is important. Similar to the case for dielectrics, the skin depth is defined as the value at which the magnetic field decreases to 1/e of its surface value. We then use

$$\delta_z = \sqrt{\frac{2}{\sigma_m \omega \mu_m}} \qquad \textbf{3.24}$$

3.1.5. POWER ABSORPTION INTO A LOAD

The power dissipation in a load is proportional to the square of the applied electric field density (Metaxas, 1996), and thus the time average power dissipated per unit volume in a dielectric material, under the influence of a time dependent electric field, can be calculated from

$$P_v = \frac{1}{2}\sigma_e \int_v E \cdot E^* dV \qquad \textbf{3.25}$$

If the material is subjected to a constant electric field, then this can be simplified to

$$P_v = \frac{1}{2}\sigma_e \,|\, E \,|^2 \qquad \textbf{3.26}$$

with $\sigma_e = \sigma + \omega\varepsilon_0\varepsilon''$ and |E| the magnitude of E (the electric field strength). It is also possible to define a power penetration depth, D_p, where the value of the power density falls to 1/e of its surface value.

The reliance of power density on the square of the electrical field strength means that it is important to differentiate between the power penetration depth and the electric field depth. This relationship is obtained from

$$D_p = 1/2\alpha_z = \delta_z/2 \qquad \textbf{3.27}$$

and can then be used to determine the power density at any depth beneath the surface of an absorbing material through

$$P = P_0 e^{-z/D_p} \qquad \textbf{3.28}$$

where	P	power density
	P_0	power density at surface of material
	z	depth below surface of material

In general, the penetration depths of microwaves at frequencies allocated to industrial use are small, and thus the size of any material to be treated must be taken into account. If the width of the material is several times larger than D_p, non-uniform heating of the sample will occur.

It is noted that for metals, however, the power dissipation is related more to the magnetic field than the electrical field of the electromagnetic wave and must be calculated using the following equation

$$p_v = |J|^2 / 2\sigma_m \qquad \textbf{3.29}$$

where $J = \sigma_m E$ and $\sigma_e = \sigma_m$.

3.1.6. MIXING RULES

When dealing with heterogeneous materials, that is those which consist of several components with an identifiable boundary (be it distinct or indistinct) between each component, then the differences in the dielectric properties of each component will add to the bulk properties of the material.

Several equations exist for determining the bulk dielectric properties of heterogeneous materials theoretically (Roussy and Thiebaut, 1994, Roussy and Pearce, 1995). These include the formulas by Rayleigh and Böttcher, the Bruggeman-Hanaï formula and the Looyenga equation.

Probably the most useful formula for dealing with multi-component systems is the Lichtnecker formula. For a single component suspended in a host material, the following form can be used.

$$\varepsilon_m^* = \left(\varepsilon_1^*\right)^{(1-\Phi)}\left(\varepsilon_2^*\right)^{\Phi} \qquad \textbf{3.30}$$

where ε_1^* permittivity for the solvent (or continuous) phase

ε_2^* permittivity of the dissolved phase

ε_m^* permittivity of the medium

Φ volume fraction of the dissolved phase

For multiple components, the equation can be extended as follows:

$$\varepsilon_m^* = \prod_{i=2}^{N_p}\left(\varepsilon_i^*\right)^{\Phi_i} \qquad \textbf{3.31}$$

where ε_i^* permittivity of phase i (can be either solvent or dispersed phases)

ε_m^* permittivity of the medium

Φ_i volume fraction of phase i

It should be clear that $\sum \Phi_i = 1$ must apply to equation 3.31.

It is cautioned, however, that none of the above formulas have strong theoretical bases, and that the underlying assumption in all of them is that the particulate phases consist of relatively small particles dispersed in large volumes of a solvent dielectric.

Tinga, 1988, suggests an interesting formula which provides a bounded region for multiphase mixtures which is claimed to be of more use when predicting high temperature dielectric properties and field strengths. His solution for a two phase mixture of spheres in a continuous matrix is as follows:

$$\frac{\varepsilon_b - \varepsilon_1}{\varepsilon_1} = \left(\frac{v_2}{v_1}\right) \cdot \frac{3(\varepsilon_2 - \varepsilon_1)}{(2\varepsilon_1 + \varepsilon_2) - \left(\frac{v_2}{v_1}\right)^3 (\varepsilon_2 - \varepsilon_1)} \qquad \textbf{3.32}$$

where ε_b bulk dielectric property

ε_1 dielectric property relating to the material comprising the matrix

ε_2 dielectric property relating to the material comprising the spheres

v_1 volume fraction of material comprising the matrix

v_2 volume fraction of material comprising the spheres

This formula then gives the dielectric loss factor for the material under consideration (structured as either a guest phase of spheres in a continuous phase of host material, or vice versa).

The electric field in a specific phase can also be determined using Tinga's equations.

$$\frac{E_2}{E_b} = \frac{3\varepsilon_1}{(2\varepsilon_1 + \varepsilon_2) - \left(\frac{v_2}{v_1}\right)^3 (\varepsilon_2 - \varepsilon_1)} \qquad \textbf{3.33}$$

where E_b bulk material electric field

E_2 guest material electric field

3.1.7. DIELECTRIC PROPERTIES OF MINERALS

The use of microwaves, as a heat source for the thermal treatment of ores, was not given much recognition until Chen et al., 1984, discovered that microwaves had the characteristic of being able to selectively heat only certain minerals in an ore. His work gave a qualitative overview of the degree of a large number of minerals subjected to microwave radiation (see Table 3.1).

From these results it was seen that most sulfides, arsenides, sulfosalts, sulfarsenides and some oxides heated well subjected to microwaves, while it was also seen that most silicates, carbonates, sulfates and some oxides and some sulfides are transparent to microwave energy. From these observations, it was concluded that ore minerals tended to respond favourably to microwave heating, while the gangue minerals showed little or no heating in response to microwave treatment. A potential application was then suggested for the selective oxidation of gold ores, or other minerals, to enhance subsequent recovery processes such as flotation and magnetic separation.

In 1992, researchers at the U.S. Bureau of Mines attempted to analyze the dielectric properties of over 60 minerals to search for trends in dielectric properties, based upon crystalline structure and mineralogical classification (Holderfield and Salsman, 1992).

Table 3.1 - Qualitative measure of the reaction of various pure minerals to microwave exposure (after Chen et al., 1984)

Mineral	Heating response
Allanite	Does not heat / transparent
Fergusonite	
Monazite	
Sphalerite (low Fe; Zn 67.1, Fe 0.2, S 32.7%)	
Stibnite	
Aragonite	
Calcite	
Dolomite	
Siderite	
Argentojarosite	
Synthetic natrojarosite (zinc plant residue, Kidd Creek Mines Ltd)	
Synthetic plumbojarosite (zinc plant residue, Cominco Ltd)	
Almandine	
Allanite	
Anorthite	
Gadolinite	
Muscovite	
Potassium feldspar	
Quartz	
Titanite	
Zircon	
Barite	
Gypsum	
Nickeline/cobalite (3 vol.%)	Difficult to heat
Covellite/anilite (60% vol.%)	
Columbite (40% vol.%) - pyrochlore in silicates (almandine 40%)	Difficult to heat when cold
Sphalerite (high Fe; Zn 58.9, Fe 7.4, S 33.7%)	
Tennantite (Cu 42.8, Ag 0.1, Fe 4.8, Zn 1.7, As 12.5, Sb 10.6, S 27.5%), (90 vol.% tennantite, 6% chalcopyrite, 4% quartz)	
Bornite	Heats readily
Chalcopyrite	
Tetrahedrite(Cu 24.9, Ag 18.0, Fe 1.9, Zn 4.8, Sb 25.6, As 1.3, S 23.4%), (85 vol.% tetrahedrite, 10% quartz, 5% pyragyrite, galena, chalcopyrite)	
Cassiterite	
Magnetite	
Pitchblende (90 vol.%); contains chlorite, galena, calcite	
Pyrite	
Arsenopyrite	Heats, some sparking
Hematite	Heats rapidly, arcing at high temperatures
Pyrrhotite	
Galena	Heats readily with much arcing

While their investigations into mineralogical classification extended the work of Chen by providing quantitative results in terms of dielectric constants, it was found that dielectric properties could not be predicted accurately based on crystalline structure.

3.1.8. HEATING MECHANISMS

Dielectric heating occurs through two mechanisms (Metaxas, 1996), namely the rotation-like motion of dipolar species in the presence of a high frequency electromagnetic field and the resistive losses associated with the drift of ionic species under the same field. The former loss mechanism is associated with dielectric relaxation, while the latter is associated with the dielectric conductivity.

At radio frequencies, ionic loss dominates, while at microwave frequencies it is the dipolar loss mechanism which is more important.

At low frequencies the dipoles have ample time to follow the variations in the applied external electric field, and the applied energy can be fully stored in the dielectric. As the frequency increases, however, the dipoles are unable to fully restore their positions during the field reversals associated with electromagnetic waves, and thus the dipolar polarization begins to lag the applied external field. A further increase in frequency results in a total failure of this polarization to follow the applied field. This fall of effective polarization manifests itself as a fall in the value of the dielectric constant and a rise in the loss factor. The result of this is that the dipoles can no longer effectively store the energy supplied by the electric field and instead this 'lost' energy is dissipated in the dielectric, resulting in a temperature rise in the material.

3.1.9. CAVITY TYPES

Perhaps the most important choice in microwave processing is which applicator to use (Roussy and Pearce, 1995, Metaxas, 1996, Meredith, 1998). The choice of applicator is limited by the requirements of the process, and often specialized cavities must be constructed to suit a certain purpose.

The most common form of applicator is the multi-mode oven. They are simple in design (essentially just a metal box) and can be used for a wide range of applications. The limitations of this type of cavity lie in its inability to supply high power densities to a load, and the problem of providing uniform heating. To combat the latter, the use of circulators, the rotation of the load within the cavity and more recently frequency sweeping have been developed as effective means of redistributing the heating within the cavity. The multimode applicator is capable of providing low to medium heating rates at average power densities, while treating large volumes of material at a time.

The simplest cavities (and perhaps the most versatile) are those in which the applicator is formed fully, or partially, by the waveguide delivering the energy itself. Examples of the former would be the standing or travelling wave waveguide applicators, where the load is passed through the waveguide perpendicular to the main direction of travel of the microwaves within the waveguide.

With slotted waveguide applicators the material to be processed is placed near a waveguide which is slotted to allow the transmission of microwaves into the material. To ensure personnel safety and to comply with legislation on emissions, the entire heating volume must be shielded within an enclosure. The heating rates within such cavities varies widely, depending on the electric field patterns generated within, from a low to average uniform heating rate generated in travelling waveguide applicators, to the high non-uniform heating rates generated by standing wave or single mode rectangular waveguide cavities.

Single-mode cavities provide the highest heating rates possible. They are characterized by the occurrence of only a single mode (or area of high electric field density). A major drawback of these types of cavity are the non-uniformity of heating caused by the drop-off of this area of high electric field density as it approaches the cavity walls, and the necessity of small load dimensions as a result of the size of the mode (which is generally the same size as one half wavelength of the microwaves at the operating frequency. None the less, by feeding material at a rapid rate through this heating volume, it is possible to maintain high processing capacities while retaining the high heating rates required of some processes.

Any form of continuous microwave treatment will necessarily require that the cavity has openings to the environment to allow the entry and exit of material. This invariably leads to undesired microwave emissions from the process. There are several ways to combat these emissions (Meredith, 1998) such as the use of choke tunnels employing reactive choking, which reflects escaping energy back to the cavity, or active electronic systems which shut down the microwave generator if leakage is detected. In extreme cases, a fully screened room housing all the equipment may have to be used.

3.2. MECHANISMS OF ROCK FRACTURE

3.2.1. TYPICAL BEHAVIOUR OF ORES

Griffith showed that since stress concentrates in regions around the tips of flaws, crack propagation will be initiated at these points. Energy balances on moving crack tips further showed that the overall stress around the tip must reach a critical value, and that once this value has been reached the crack starts to propagate. If the stress is not rapidly relieved at this point, the system becomes unstable and the crack propagation will accelerate to high velocities, with the limit of this velocity being around 40% of the speed of sound in the solid. The strain energy relaxed during this rapid propagation will exceed the energy associated with the new surface produced, and this surplus energy is then available for the initiation of other cracks as well.

Prasher, 1987, summarizes the factors influencing 3-dimensional stress patterns induced in a particle under the influence of applied external forces:

- the number and direction of the forces
- the deformation behaviour (elastic or plastic)
- the rate of deformation
- the particle size and shape

Hoffmann and Schönert, 1971, showed that the number of contact points is important in determining the fracture patterns which will develop in the material. It was found that the breakage probability of a particle assemblage increases with the number of contact points per particle, up to a limited number of around 10, at which point the breakage probability decreases, with a greater tendency for the cracks to run near the surface of the particle.

This would obviously increase the tendency for bed breakage to produce fine material, further negatively affecting the particle breakage. It was suggested that fine material of output size is removed as soon as possible from any particle bed breakage activity to prevent this occurring.

Viljoen et al., 2001, showed that the application of particle bed breakage (using a Loesche air-swept table-mill) could not only produce less fines than is possible in a conventional ball mill, but through flotation studies on a copper ore, showed that a higher degree of liberated valuable material, and thus better flotation recoveries, were achieved. The explanation for the reduction in fines in their studies is through the shielding of primary breakage fragments by a bed of particles of sufficient porosity. Once broken, the particle fragments fill the holes in the bed in such a manner that they experience no compressive forces (see Figure 3.6).

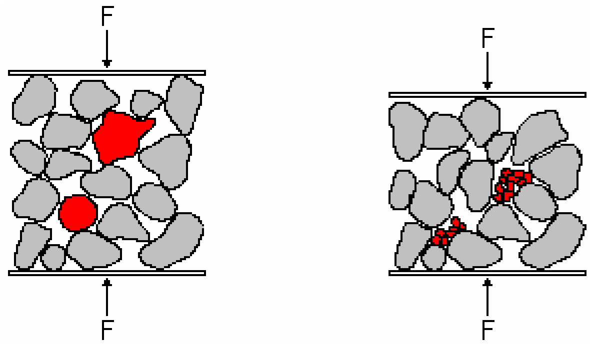

Figure 3.6 - Shielding of particles in particle bed breakage

The porosity of the bed can be increased by ensuring that a narrow size distribution of particles are treated in the bed, and thus that no chance exists for smaller particles to fill these voids before hand. This narrow size range of particles would also limit the number of contact points between particles, thus preventing the surface fracturing observed by Hoffmann and Schönert, 1971.

Studies on the fracture of spheres have showed that for elastic material, the stresses just below the contact area of the applied external force are much greater than anywhere else in the particle. This produces a more intense size reduction in these areas than in the rest of the particle. A bimodal size distribution is therefore produced from the particle breakage, with the fines from the contact zones being described as the complement to the residue from the rest of the particle. The opposite is noted for plastic material, where the areas under the points of contact are driven into the material as a cone shaped volume, pushing the rest of the surrounding material sideways. This cone remains undestroyed, thus producing no fines from this region.

For areas away from the points of contact, the effects are more complex. For elastic material:

- ring and cone cracks develop around the contact circle (because of high longitudinal tensile stresses developed there)

- cracks run around curved surfaces (described in the manner of an onion peel) following surfaces of constant strain
- no meridional cracks appear because of low latitudinal tensile stresses

while for plastic material :

- due to the cone-shaped volume being driven into the material from the contact points, the outer shell is strained as if under internal pressure, and cracks form parallel to meridional planes (producing fragments likened to the segments of an orange)

Much has been said about the differences between impact and compressive breakage, but the mechanisms of each differ only in the rate at which the external forces are applied. Prasher, 1987, determines the practical deformation velocities associated with the varying modes of comminution to be as follows (see Table 3.2):

Table 3.2 - Rate of application of compressive forces in comminution machines (after Prasher, 1987)

Machine	Velocity
	m/s
Crusher, roll mill, ball mill	0.1 - 10
Impact mill	20 - 200

The effects of an increase in deformation rate are two-fold:

- There is a change in the stress field inside an elastic body. Each distortion caused by a contact force is distributed through the body in waves, which on internal reflection meet oncoming waves to change the stress values associate with the wave fronts. Under favourable conditions, cracks can be caused by such waves in spherical particles, however, it is highly improbable that the reflection conditions associated with irregularly shaped particles would ever favour crack formation.

- For visco-elastic bodies, the increase in deformation rate leads to a decrease in the deformation of the body and an increase in the internal stresses, thus material which acts in this manner is better crushed by impact than by slow compression.

Schönert, 1972, determined that energy utilization (measured as a surface area increase per unit of energy applied) is significantly greater under slow compressive loading than has been measured in single point impact loading, and that this energy utilization in slow compression increases as the applied energy decreases.

It is also known that the internal stress patterns of small particles differ from those observed in larger ones. Three reasons exist for this:

- Flaw size must decrease with particle size. This leads to an increase in particle strength with a decrease in particle size.
- The elastic energy stored within a particle at the moment of crack release decreases proportionally with particle volume, while the energy required for crack propagation decreases proportionally with the cross-section. Thus as particle size decreases, it can happen that less energy is stored in the particle than is required for crack propagation and the crack will stop unless more energy is added to the particle (this phenomenon is especially notable in plastic materials where several impacts may be required to ensure breakage)
- Lastly, plastic deformation effects become increasingly more important as particle size is reduced. As particle size decreases, the number of radial cracks increase due to increased plastic deformation in the middle of the particle. Below a certain size, however, the plastic deformation spreads out to such an extent that there is no increase in the number of cracks formed, and as size decreases even further, eventually a point is reached where the entire particle exhibits plastic behaviour (i.e. unfractured deformation occurs).

In general, most ores display non-linearity in the relation between strains and stresses during loading, even in the range of initial, small loads in both compression and tension. Kidybinski, 1966, found that the type of the load and the time of it's interaction with consolidated sedimentary rocks also had an effect on the resulting complex, non-linear deformations.

Tests by Gorbatsevich, 1996, on a large number of hard crystalline rocks, at low temperatures, showed that they deformed elastically and non-linearly up to around 77 to 98 percent of the breaking load, after which plastic deformation began to occur. It was found that in most cases, failure of the rocks follows progressive opening of microcracks in the direction of the least principal stress, with the occurrence of the failure itself being an avalanche-like connection of microcracks and the intergrowth of main cracks in the direction of the largest stress. He further observed that for each of the rock types in his study, a limiting value of the lateral strain factor could be found, and it was suggested that this could be a useful failure criterion.

Experiments on calcareous rock types by Rutter, 1971, showed that the oven-dry uniaxial strength of this rock type decreased by 30% when the specimens were impregnated with water. It was also noted that a decrease in both yield strength and ultimate strength came about as the strain-rate was decreased, while ductility was found to increase. At low strain rates the rock can accommodate less permanent deformation before macroscopic fractures develop, while at higher strain rates dilatancy hardening occurs.

3.2.2. FRACTURE PATTERNS ASSOCIATED WITH THERMAL TREATMENT

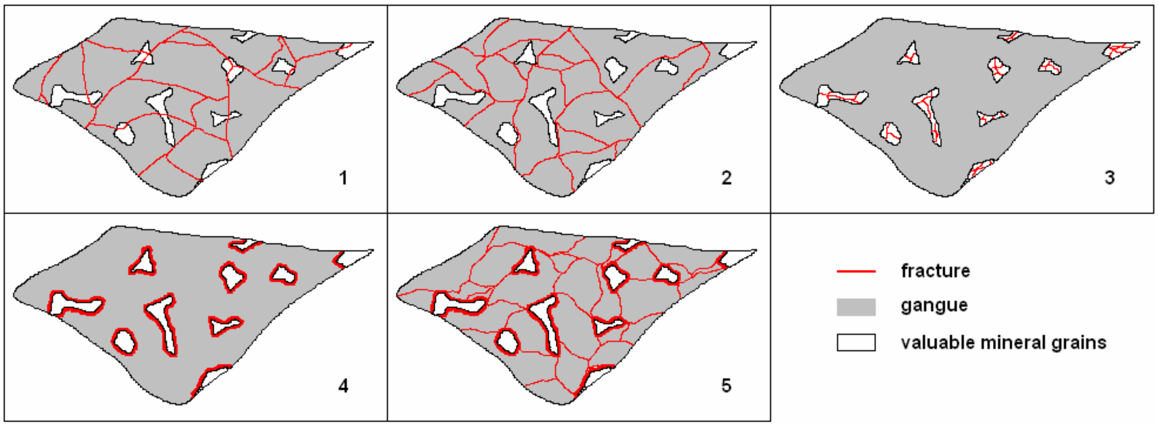

Figure 3.7 - Possible fracture patterns in ores resulting from microwave treatment

It is a reasonable assumption that the type of fracture induced in the ore from microwave treatment, or any other form of treatment, will be the key factor in determining the process flowsheet required for further treatment of the ore. There are only 5 types of fracture which may occur given any form of microwave treatment, the extreme cases of which are shown in Figure 3.7.

1) Fracture from microwave treatment is random, crossing both valuable mineral grains and gangue material with no preference for either (which is the assumed type of breakage for conventional treatment). This would mean that the microwave treatment was enhancing existing breakage patterns and not inducing any benefit to liberation. The result would most likely be a reduction in BWI on a macroscale in the ore (that is that a reduction in strength would be visible until the newly formed fractures had all been exploited, after which the ore would respond in the same manner which it would have if no microwave treatment had been performed). The most benefit would therefore be expected in the crushing section of the plant, with smaller benefits being visible in the milling section (as the last of the cracks are exploited). Treatment would then most likely not change the flowsheet structure considerably, but allow for higher throughputs and lower

comminution costs and residence times in mills. The crushers could perhaps be set to finer closed side settings, because the ore is easier to crush, thus sending a smaller feed to the milling section. Lower recycle could result in the mill section due to lower BWI (as described above).

2) Fracture is limited to the gangue material, but does not occur around grains in a manner which would induce intergranular fracture, and thus no enhanced liberation of valuable material could be expected. However, changes to the flowsheet could be made to allow for early removal of liberated gangue at large particle sizes, before further costly downstream processes. Most likely a combination of size and gravity separation could be used.

3) Fracture occurs in the valuable grains only. This has been observed before in a limited number of cases, and would most certainly affect the process flowsheet. Initially, one would expect the ore to behave in the same manner as for untreated material. At smaller sizes, however, the breakage might result in a full liberation between gangue and mineral, though there is a possibility that the valuable minerals would be liberated at sizes normally classified as fines and thus be unrecoverable.

4) Only intergranular fracture occurs. At larger sizes it would be expected that the ore remains similar in performance to the untreated ore. At sizes similar to the grain size of the ore, and slightly larger, however, one would expect full liberation to begin occurring in the ore. Changes to the flowsheet might be minimal upstream of the milling section, but milling itself would be to larger product sizes as fine grinding would not be necessary. A special case of this type of fracture is the phase region fracture mentioned by King, 2001, where fracturing occurs in the region of the phase boundary, but not necessarily purely intergranular fracture. This leads to the creation of very small particles which still contain multiple phases and it thus not a desired state. It appears that this may be more prevalent around irregularly shaped grains, which display complex intergrowths with the

surrounding minerals, than around regularly shaped grains with smooth boundaries (Wills et al., 1987).

5) Intergranular fracture, as well as selective fracturing of the gangue occur (most importantly, fracture of the gangue between grain particles, thus forming a linked fracture network). This would most likely have large effects on the type of flowsheet used. It could now be expected that liberation of valuable mineral would begin even at the crushing stage (as the interlinking fracture network causes new particles to be formed along existing fractures, thus exposing valuable mineral which would simply detach from the host rock. The difficult problem of preventing fines losses in crushing (which would now contain greater amounts of valuable mineral than usual) would need to be overcome. It could also be that tertiary or even quaternary crushing (perhaps between high-pressure rollers or from centrifugal spinning plate crushers) could provide full liberation, thus totally eliminating the need for grinding under these circumstances.

At present, the classification of the fracture pattern would have to be determined from SEM images of the particles in question, though the possibility of using a non-destructive measurement technique, such as X-ray tomography of sufficient resolution, would provide scope for measuring fracture patterns before and after microwave treatment. This would allow a much greater understanding of the type of patterns induced by differing ore mineralogies.

3.3. COMMINUTION EQUIPMENT

3.3.1. MILL ROTATION SPEED

The mill rotation speed is usually expressed as a percentage of the critical rotation speed, which can be defined as the speed at which the centrifugal and gravitational forces exerted on a particle at its topmost position in the mill, just balance one another. It can also be interpreted as the speed at which a single particle is just held against the wall for a full cycle of the mill. This angular velocity is determined by a force balance on a particle in rotation (King, 2001), which after simplification yields

$$\omega_p = \sqrt{\frac{g}{r_{cp}}} \qquad \textbf{3.34}$$

where ω_p angular velocity of particle in rad/s

g acceleration due to gravity (m/s^2)

r_{cp} radius from the mill centre to the particle centre of gravity (m)

The critical speed is often reported in revolutions per minute, however, so the above equation can be converted by multiplying by $60/2\pi$, giving

$$rpm = \frac{60}{2\pi}\sqrt{\frac{g}{r_{cp}}} = \frac{29{,}9}{\sqrt{r_{cp}}} \qquad \textbf{3.35}$$

Where the size of the mill is large in comparison to the size of the particle, as with industrial mills, the radius of the particle becomes negligible in comparison to the radius of the mill and the centre of gravity of the particle may be assumed to be flush with the mill liner walls, thus

$$r_{cp} = r_{mill} \qquad \textbf{3.36}$$

In laboratory scale equipment this may not be the case however as the mill radius is usually small, thus it is more suitable to use

$$r_{cp} = r_{mill} - r_{particle} \qquad \textbf{3.37}$$

At the critical speed, the outer layer of charge will begin centrifuging and therefore no relative motion of shell to charge will occur. As the speed increases past the critical speed, the inner layers of charge will also begin to centrifuge, eventually arriving at a situation where the entire mill contents are centrifuging and no comminution is taking place. In general, the various mill types are therefore run at speeds lower than the critical speed, most often between the ranges of 65 to 82 percent (Hayes, 1993) of the critical speed to produce the desired tumbling effect.

The correct choice of mill speed, based on the knowledge of the critical speed of the mill being used, is then of prime importance in ensuring that a mill operates correctly. The previous discussion was thus considered when choosing the mill speed to be used during the experimental phase of this work.

3.3.2. MILL LOADING

The mill loading (or charge level of grinding media in the mill) is expressed as the fraction of the mill cross sectional area occupied by grinding media after a specific grind out period.

This grind out period is required to settle out the mixture of mill media and ore charge so that measurements of the mill filling are not skewed by either the presence of large voids between the media, or by an uneven upper surface of the charge which might occur as a result of the initial packing of the mill. In laboratory mills, this period is usually around 10 to 15 minutes, while for industrial size mills 30 minutes is preferred.

Several geometric relationships are available from which the mill loading can be determined (JKMRC, 1999). Given a mill of known geometry (see Figure 3.8), the following relationships exist:

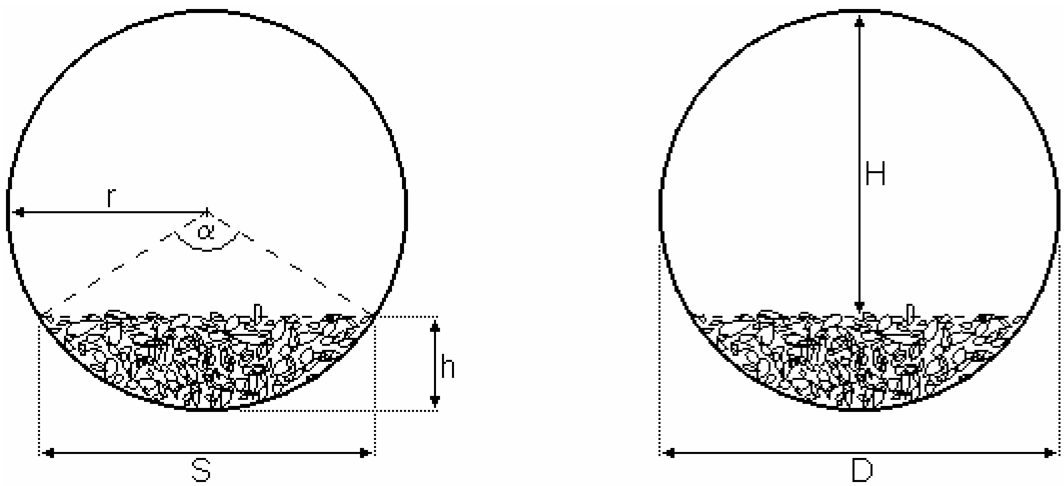

Figure 3.8 - Parameters used in determining mill load

$$S = 2r \cdot \sin\left(\frac{\alpha_{chord}}{2}\right) \qquad \textbf{3.38}$$

$$h = r\left(1 - \cos\left(\frac{\alpha_{chord}}{2}\right)\right) \qquad \textbf{3.39}$$

$$r = \frac{h}{2} + \frac{S^2}{8h} \qquad \textbf{3.40}$$

$$A_c = \frac{h}{6S}\left(3h^2 + 4S^2\right) \qquad \textbf{3.41}$$

$$V = \frac{A_c}{A} \times 100 \qquad \textbf{3.42}$$

$$A = \pi r^2 \qquad \textbf{3.43}$$

where S chord length (m)

r mill radius inside liners (m)

h depth of charge (m)

α_{chord} angle that chord subtends at mill centre (degrees)

A_c cross-sectional area of mill charge (m^2)

A cross-sectional area of mill (m^2)

V estimate of mill filling (%)

A quicker estimate of mill filling may be achieved by using the Allis Chalmers mill filling approximation formula, which requires only the measurement of the vertical distance between the mill roof and the charge surface and the known mill diameter inside the liners. This is then

$$V = 113 - 126\left(\frac{H_{charge}}{D_m}\right) \qquad \textbf{3.44}$$

where H_{charge} vertical distance between the mill roof (inside the liners) and the charge surface

D_m mill diameter inside the liners

It has been shown by Morrell (JKMRC, 1999), however, that this equation is not suitable for situations of low mill filling (i.e. in the region of less than 20%).

In general, mills are operated with a mill charge (grinding media and particles) of between 30% and 50% (Hayes, 1993), and it was thus decided to use a mill loading of approximately 45% during the experimental phase of this work.

3.3.3. BREAKAGE AND SELECTION FUNCTIONS

Several forms exist for expressing the breakage and selection functions which are used to describe the performance of an ore with time in a mill. The most popular selection function is the standard Austin function, which incorporates a maximum that defines the decrease of the breakage rate as the particle size gets large.

$$k(d_p) = \frac{S_1 \cdot d_p^{\alpha}}{1 + \left(\frac{d_p}{\mu}\right)^{\lambda}} \qquad \textbf{3.45}$$

where k(d_p) is the specific rate of breakage of a particle of size d_p

μ fixes the particle size at which the selection function attains it's maximum value

(μ has a value slightly larger than this size)

S_1 is the selection function at 1 mm

α,λ constants

It should be noted that the overall selection function for a mixture of ball sizes (which would be the experimentally determined value of S_i), is in fact made up by the separate contributions of each ball size to this value, for each particle size.

$$\overline{S_i} = \sum_k m_k S_i(k) \qquad \textbf{3.46}$$

where $\overline{S_i}$ average value of S_i

m_k mass fraction of balls of size k

$S_i(k)$ value of S_i for ball size k

This fact is important when dealing with the scale-up of the selection function.

The breakage function used for calculations spanning the work presented in this thesis is of the standard Austin form. Here the progeny population is made up of a mixture of two separate populations, one composed of large particles produced by tensile stresses and the other of smaller particles produced by intense compressive stresses at the points of application. The products of these populations are described by the exponents γ and β respectively in the formula below.

$$B(x;y) = \phi\left(\frac{x}{y}\right)^{\gamma} + (1-\phi)\left(\frac{x}{y}\right)^{\beta} \qquad \textbf{3.47}$$

where B(x;y) breakage function

ϕ weighting factor

x size of the progeny particle

y size of the parent particle

γ,β parameters determined from experimental data

This breakage function is independent of the size of the parent particle and depends only on the ratio x/y. The same function can thus be used for all parent sizes and the function is said to be normalized with respect to parent size. If experimental data shows that this is not the case, then the value of ϕ must be determined as a function of parent size. This is done by using the formula below.

$$\phi = \phi_5\left(\frac{y_0}{y}\right)^{\delta} \qquad \textbf{3.48}$$

where ϕ_5 value of ϕ at the reference parent size (usually 5 mm)

y_0 reference parent size (usually 5 mm)

y parent particle size (in mm)

δ constant

If $\delta = 0$, the breakage function is then independent of parent particle size and is said to be normalized.

3.3.4. GRINDING MODELS

The simulator MODSIM, used in this work, incorporates a plug flow model for the rod mill, where the longitudinal transport velocity of the solids varies with particle size, meaning that the larger particles move slower than the smaller particles, while all the solids move slower than the water (except for entrained particles in the smallest size class which are assumed to move with the water).

The form of this dependence of material transport in a rod mill on particle size was investigated by Rogovin et al., 1986. The velocity distribution of particles in the mill can be modelled by

$$v(d_p) = v_w \cdot e^{-c_v \cdot (d_p / d_{pl})} \qquad \textbf{3.49}$$

where $v(d_p)$ velocity of particle with size d_p

d_p particle size

d_{pl} largest particle size

v_w average velocity of water through mill (lowest velocity is 1/10th the water velocity)

c_v coefficient for variation of transport velocity with particle size

The model structure used by MODSIM in modelling the breakage in a rod mill is defined by

$$V_i \frac{dm_i}{dx} + k_i m_i = \sum b_{ij} k_j m_j \qquad \textbf{3.50}$$

where V_i velocity of particles of size class i

m_i mass of material in size class i

b_{ij} breakage function (for class j breaking into class i)

k_j selection function (rate of breakage of size class j)

The selection function and breakage function used are both of the standard Austin form. The model does not incorporate any scale-up relationships for these selection functions and does not incorporate any details of the mill geometry. The only other parameter required is the mean residence time of the solids.

The simplest ball mill model used by MODSIM is based upon the assumption of a single perfectly-mixed region in the mill with no post-classification. More complex models (Whiten, 1973) using several perfectly mixed regions in series are also available. The size distribution of the product is calculated recursively, starting at the largest class and working through to the smallest or 'sinks' class. The population balance employed is described by King, 2001

$$p_i^P = \frac{p_i^F + \sum_{j=1}^{i-1} b_{ij} k_j \tau p_j^P}{1 + k_i \tau} \qquad \textbf{3.51}$$

where p_i^F fraction of feed in size class i

p_i^P fraction of product in size class i

p_j^P fraction of material in size class j

τ residence time (mass of material in the mill / mass flow rate through the mill)

b_{ij} breakage function (for class j breaking into class i)

k_j rate of breakage of size class j

3.3.5. BACK CALCULATION OF BREAKAGE AND SELECTION PARAMETERS

In order to model rod milling during the flowsheet simulations in this work, it was first necessary to be able to describe the breakage characteristics of Palabora ore in a rod mill (see section 5.4).

Austin and Weller, 1982, describe the three general approaches to the construction of simulation models of steady-state continuous ball milling circuits. The first approach uses data from the milling plant itself to back-calculate the grinding parameters. The second uses data collected from a small-scale reproduction of the large plant, run under steady-state conditions, and the results are used to predict the behaviour in the large-scale plant. The third approach determines the grinding parameters directly from tests on a laboratory mill under batch conditions, and these parameters are then scaled up to estimate those in the large-scale mill. This last approach is also especially useful if only a limited amount of material is available for testing.

Klimpel and Austin, 1977, defined a procedure for the back-calculation of specific rates of breakage and breakage distribution parameters from batch grinding data. They found that using functional forms for the breakage and selection functions was necessary to ensure continuity of these functions between size intervals.

The matrix form of the discretized differential equation describing solid attrition in cumulative form is

$$\frac{d\widetilde{F}}{dt} = \widetilde{A}\widetilde{F} + \widetilde{C} \qquad \mathbf{3.52}$$

where **F** is the cumulative size distribution. The elements of the square matrix **A** are given by

$$A_{ij} = \begin{cases} S_j B_{i,j} - S_{j+1} B_{i,j+1} & i < j \\ -S_{j+1} B_{i,j+1} & i = j \\ 0 & i > j \end{cases} \qquad \textbf{3.53}$$

and those of the column vector **C** are

$$C_{i,1} = S_N B_{i,N} \qquad \textbf{3.54}$$

where the vector **S** and the matrix **B** are derived from the chosen forms of the selection and breakage functions respectively, and the Nth grid corresponds to the largest size class.

The analytical solution to the cumulative batch grinding equation for first order breakage kinetics was proposed by Das et al., 1995, and takes the form

$$\tilde{F}(t) = \sum_{i=1}^{N-1} \left[\exp(\lambda_i t) \frac{\langle \tilde{F}_0, \tilde{v}^i \rangle}{\langle \tilde{u}^i, \tilde{v}^i \rangle} - \{1 - \exp(\lambda_i t)\} \frac{\langle \tilde{C}, \tilde{v}^i \rangle}{\lambda_i \langle \tilde{u}^i, \tilde{v}^i \rangle} \right] \times \tilde{u}^i \qquad \textbf{3.55}$$

Where λ_i is the ith eigenvalue of **A**, and where the components of the eigenvectors **u** of **A**, and the eigenvectors **v** of $\mathbf{A}^T$, are given by

$$u_i^r = \begin{cases} 1 & i = r = 1,2,\ldots,N-1 \\ \left(A_{r,r} - A_{i,i}\right)^{-1} \sum_{j=1}^{r-i} A_{i,r-j+1} u_{r-j+1}^r & i = 1,2,\ldots,r-1 \\ & r = 2,3,\ldots,N-1 \\ 0 & i = r+1, r+2,\ldots,N-1 \\ & r = 1,2,\ldots,N-2 \end{cases} \qquad \textbf{3.56}$$

$$
v_i^r = \begin{cases} 1 & i = r = 1,2,\ldots,N-1 \\ \left(A_{r,r} - A_{i,i}\right)^{-1} \sum_{j=1}^{i-r} A_{r+j-1,i} v_{r+j-1}^r & i = r+1, r+2,\ldots,N-1 \\ & r = 1,2,\ldots,N-2 \\ 0 & i = 1,2,\ldots,r-1 \\ & r = 1,2,\ldots,N-1 \end{cases} \quad \mathbf{3.57}
$$

The correct parameters for the breakage and selection functions are determined by a constrained minimizing of the sum of squares of the following equation (Das, 2001)

$$
SSQ = \frac{1}{nt-1}\sqrt{\sum_{k=1}^{nt}\sum_{i=1}^{N-1}\left(\frac{F_p(i,k) - F_e(i,k)}{F_e(i,k)}\right)^2} \quad \mathbf{3.58}
$$

where SSQ sum of squares

nt minimum number of grinding times required to accurately estimate S and B parameters

F_e experimentally determined size distribution

F_p predicted size distribution

3.3.6. SCALE-UP OF PARAMETERS

Since it has been found that under normal conditions the breakage function is a property of the material being ground, and is thus invariant with mill size, scale-up of breakage parameters for mills of different size is accomplished by adapting the selection function, which is dependent on mill properties.

Austin and Weller, 1982, determined experimentally that the following relation

$$S_i \propto D^{0.5} \qquad \mathbf{3.59}$$

where S_i selection function value at particle size i

D mill diameter

holds true for mills of diameter < 3.8 m and can be used to convert S_i values measured at given mill conditions to S_i values under the same mill conditions in a mill of different diameter.

It was also found that the specific rate of breakage of large particle sizes, near the position of the maximum in S_i values, also have to be scaled with diameter. This is done by manipulating the μ value in the contributions of each ball size (equation 3.45) to the overall selection function as follows

$$\mu \propto D^{0.2} \qquad \mathbf{3.60}$$

Herbst and Fuerstenau, 1980, developed a different form of the selection function, based upon the specific energy input into the system, which allowed for a very simple scale-up procedure. By defining an independent specific breakage rate function, they were able to scale-up their parameters based on power consumption and hold-up.

$$k_i = k_i^E \left(\frac{P_{net}}{H_m} \right) \qquad \mathbf{3.61}$$

where k_i selection function value for particle size i

k_i^E specific breakage rate function value for particle size i

P_{net} net mill power

H_m mass hold up of material in the mill

Once k_i^E has been determined from tests on a laboratory mill, it can be used to find a selection function to suit the prevailing conditions in any mill.

3.4. GRINDING MEDIA CONSUMPTION

It is estimated by Mintek that the South African mining industry uses between 90 kt and 100 kt of steel grinding media at a cost of approximately R80 million (1991) each year. It was also reported by Radziszewski, 1997, that consumption of media through wear processes in comminution activities in Canada and the USA in 1974 was around 300 000 tons of iron and steel.

According to Mintek reports (Mintek, 1991) grinding media consumption (wear) in ball mills in highly abrasive gold/platinum ore is as high as 1 kg to 2 kg of metal per tonne of ore milled. This was related to a cost of R0.80 to R1.50 (1991) respectively in media consumption per tonne of ore milled. This figure is similar to the cost associated with the electrical energy required to operate an industrial mill and illustrates the importance of media wear in the comminution industry.

The media consumption associated with grinding other 'softer' ores such as mixed sulfide deposits of copper, zinc and lead is often less. Cobar, a copper mine which processes around 915 000 tons per year of ore, shows a ball consumption of 0.6 kg/t of ore milled, though Mount Isa, also a copper mine, reports a ball consumption of 1.4 kg/t of ore milled. Palabora reports a rod consumption of 0.167 kg/t of ore processed in their rod mills, and a ball consumption of 0.075 g/t of ore milled in each of their ball mills.

3.4.1. OTHER EFFECTS OF GRINDING MEDIA WEAR

The cost of grinding media is not the only consideration, however, as it has been seen that in sulfide ore grinding, electrochemical interactions between the grinding medium and the minerals can alter the surface properties of the ground minerals. Rajagopal and Iwasaki provide a review of published literature in this field.

Rao et al., 1976, have suggested that the cause of the reduction in the flotability of ground sulfides was the presence of metallic iron which had abraded during grinding and then deposited on the sulfide mineral particles. They also found that contact between iron and pyrite with sphalerite rendered this mineral floatable in the presence of xanthate (due to the large amounts of sulfur deposited on the mineral surface), thereby reducing flotation selectivity.

The most important factors surrounding this sulfide mineral-grinding media interaction were identified by Yelloji Rao and Natarajan during experiments using electrodes of research grade chalcopyrite and galena and others of various metals (platinum, stainless steel, hyper steel, mild steel and cast iron were used). It was found that a longer duration of contact between sulphide minerals and grinding media, a larger potential difference, the presence of oxygen and lesser electrode distance are favourable for increased anodic dissolution (and thus a deleterious effect on flotation). It was also suggested, and shown, that the relative surface areas of the two electrodes could influence the galvanic behaviour of the coupling.

At present, however, not enough work has been done in this field to accurately quantify the effects of these interactions on industrial scale.

3.5. GRAVITY CONCENTRATION

Gravity concentration is a physical process and can be defined as the separation of minerals, usually of differing specific gravities, by their relative movement in response to gravity and one or more other forces, one of which is generally the resistance to motion caused by a viscous fluid such as water.

The factors which are important in determining this relative movement are the weight, size, shape and density of the each of the particles.

While this concentration method has been used for well over 2000 years with early practices described by Pliny around 70 AD, it none the less remains a vital part of the minerals processing industry (Burt, 1984). As late as 1978, the total mineral tonnage treated by this process in the USA was greater than that produced by flotation, and many plants such as Mount Isa in Australia (which reintroducing gravity separation in the form of a dense medium separation plant in 1982) and Palabora in South Africa (which uses one of the world's largest gravity concentrator plants to recover uranium (PMC, 1990)) still rely on this technology.

The use of gravity preconcentration in the processing of sulfide ores has several advantages (Burt, 1984):

- Recovery of heavy metallics, or oxides contained in the ore
- Decrease in the quantity of ore to be ground and treated by flotation
- Decrease in the proportion of siliceous material through gravity preconcentration often results in lower BWI of ores in downstream processing
- Early recovery results in a decrease in the use, and therefore cost, of flotation reagents per tonne of feed

To ascertain whether or not gravity separation will be useful during the concentration of a particular ore, several pieces of information are required (Burt, 1984):

- Composition
- Mineral proportions

- Grain size
- Mineral properties
- Concentration criterion
- Texture
- Liberation

Each of the above helps to provide a better understanding of which process routes are possible for an ore.

The concentration criterion is an expression used to determine the amenability of an ore to gravity concentration (refer to section 5.5 for the application of this criterion to Palabora ore). The criterion is expressed mathematically as follows

$$CC = \frac{\rho_h - \rho_f}{\rho_l - \rho_f} \qquad \textbf{3.62}$$

where ρ_h density of heavy mineral (kg/dm^3)

ρ_f density of suspending fluid (kg/l)

ρ_l density of light mineral (kg/dm^3)

and is equivalent to the hindered settling ratio under Newtonian conditions when presented in this form.

The percent solids of the slurry fed to any gravity separation device will also affect the efficiency of the separation. As the percent solids in the pulp increases, a phenomenon known as *hindered settling* begins to have an effect. That is, the effect of particle crowding causes the particles of different sizes and densities to interact with one another (hindering each other's fall) and, thus, the falling rates of the particles decreases. The result is that the system begins to act as if it were a heavy liquid of the same density as that of the slurry, i.e.

$$\rho_{slurry} = \frac{mass_{liquid} + mass_{solids}}{volume_{liquid+solids}} \quad \textbf{3.63}$$

Thus, under conditions of high percent solids in the slurry, the fluid density in the concentration criterion should be replaced by the slurry density (it should be noted that this also affects the flow characteristics of the slurry, thus not only will the fluid have a higher density, but a higher viscosity as well).

In order to allow for differences in particle shape, the concentration criterion must be multiplied by a shape ratio factor. This factor is the quotient of the shape settling factors for the heavy mineral and the light mineral. The shape factor is the ratio of the terminal velocities of the particle for which the ratio is required, to that of a sphere of the same mineral and of the same size, in the fluid being used in the separation.

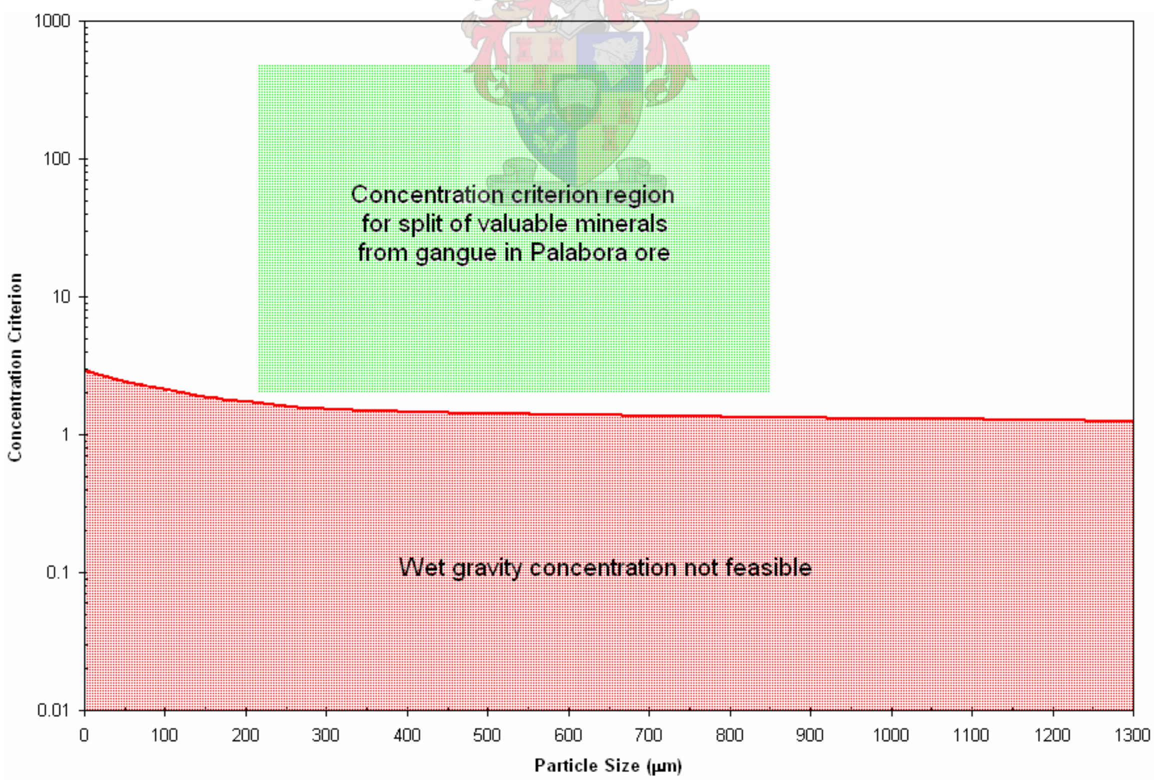

Figure 3.9 - Standard curve for testing of concentration criterion (after Burt, 1984)

The concentration criterion is also dependent on particle size, with successful separation being easier at larger particle sizes.

To establish whether or not the possibility of gravity concentration merits a more in depth study, the calculated concentration criterion is compared against a standard curve such as that presented by Burt, 1984 (see Figure 3.9). If the calculated value falls within the feasible region, then there is a good chance of this process being applied successfully, provided that other requirements, such as good mineral liberation, are also met. From Figure 3.9 it is seen that gravity concentration should be feasible for splitting the most important valuable minerals from the major gangue minerals, for Palabora ore in the size ranges of interest to us (see section 5.5).

Practical testing for amenity to gravity concentration is most easily done through sink-float analysis of a representative sample of the ore, followed by a chemical or modal analysis of the products to determine the composition of each. This analysis involves the use of a heavy liquid, of the same density as the required split density, to separate the test material into two fractions, one which floats (has a density smaller than that of the separating medium) and another which sinks (has a higher density than the separating medium).

By reproducing the sink-float test procedure at different fluid densities, a density curve can be constructed by plotting the cumulative percent weight of sinks or floats versus density of separation. When combined with the actual chemical assays of the sinks and floats at each of the separation densities, the characteristic or elementary assay curve can be constructed to determine the general character of the ore in relation to gravity separation.

In practice, the density of separation deviates within certain limits from the theoretical mean density as determined from the sink-float tests. For jigs, spirals, cones, sluice and other such equipment, this deviation is expected to be about +/- 0.1 to +/- 0.15 kg/dm^3, heavy medium separators deviate by an average of +/- 0.05 kg/dm^3 and heavy medium separators with special controls by +/- 0.01 to +/- 0.02 kg/dm^3 (Burt, 1984).

In terms of ranges of operation, the individual gravity concentration devices available today together cover the largest range of any form of separation technology in the mining industry, with the theoretical top size being the size at which different minerals are sufficiently liberated from one another for there to be a suitable gravity differential. Practically, the top size is limited by the mechanical handling capacity of the device, and though some units are capable of handling particles as coarse as 1 m, the generally accepted top size of separation is 500 mm. Figure 3.10 shows the operating range of various gravity separation devices available today.

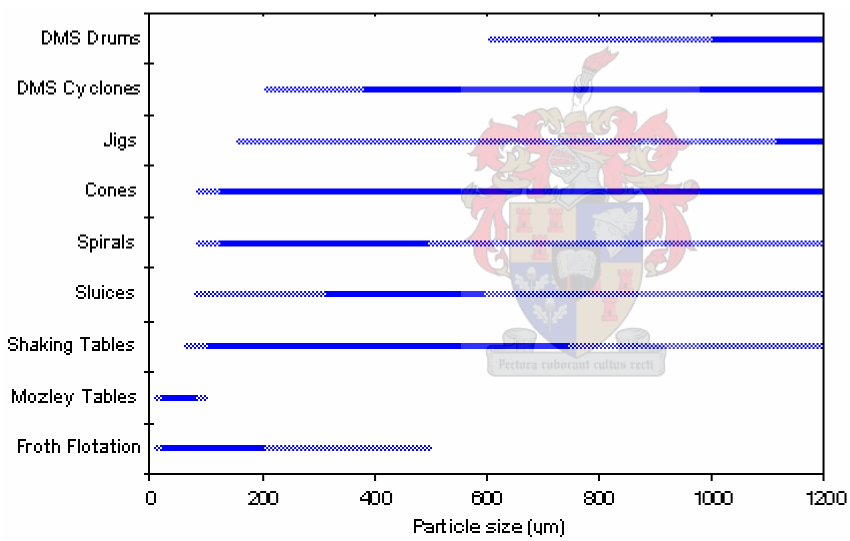

Figure 3.10 - Operating range of several gravity concentration devices (after McCarter, W.A., 1982)

Apart from the shaking table, only the newer devices are capable of separation of particles finer than 0.1 mm. While for many years it was believed that the smallest particles size which could be treated was around 75 μm, the practical bottom size of effective fine gravity concentration is in fact around 6 μm.

The capacity range of gravity concentration equipment is also large, with the highest capacity units being the static heavy medium cones or drums, and jigs, which both can exceed 300 t/h throughput per unit. Lower capacity units such as the Reichert Cone (60-70 t/h), spirals (1-15 t/h per start) or pinched sluices (3-6 t/h per start) require a number of units to successfully treat the required tonnages, and equipment such as shaking tables, Bartles-Mozley separators and crossbelts have lower capacities still.

In general, heavy medium separation is the most efficient gravity concentration process in practice, while the shaking table is perhaps the most versatile.

4. EXPERIMENTAL WORK AND RESULTS

This chapter documents the course of the experimental work done in this thesis. The approach taken is to include the results obtained at each stage of the work so that the reader can better understand, and follow, the reasoning for the guiding decisions which dictated the course of the experimental work. In doing so, it is hoped any future worker in this field could reproduce, and build upon, any of the results in this thesis by a thorough understanding of this chapter alone.

4.1. CHARACTERIZATION OF THE ROD MILL FEED

Palabora Mining Company (South Africa) supplied +/- 70 kg of ore from the rod mill feed of their process. This ore was classified according to size by sieving all the material down to 150 μm. The remaining -150 μm material was then classified by taking a representative sample of this material (obtained by repeated splitting of the ore) and measuring its size distribution. These values were then scaled up to estimate the amount of material in each size fraction in the original ore.

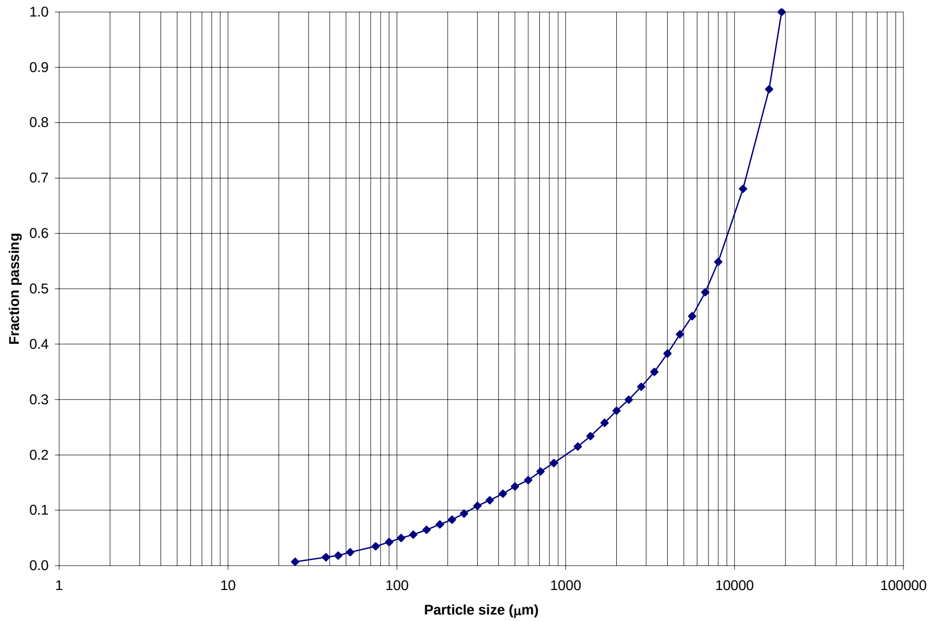

Figure 4.1 - Size distribution of Palabora rod mill feed

Table 4.1 - Major element analysis (mass %) for Palabora rod mill feed

Oxide	Size range (μm)				
	-150	-1180+150	-3350+1180	-6700+3350	-19000+6700
Al_2O_3	1.73	1.95	1.92	3.79	1.30
CaO	28.64	21.72	22.68	19.86	24.41
Cr_2O_3	0.00	0.00	0.001	0.002	0.001
Fe_2O_3	28.21	45.14	42.92	38.84	38.85
K_2O	0.36	0.48	0.37	0.44	0.27
MgO	9.94	8.86	9.69	9.91	10.16
MnO	0.18	0.22	0.22	0.23	0.20
Na_2O	0.84	0.95	1.04	1.53	1.00
NiO	0.04	0.04	0.05	0.05	0.04
P_2O_5	5.99	4.71	4.26	2.25	3.61
SiO_2	8.46	8.22	8.66	14.91	6.85
TiO_2	0.70	0.98	0.97	1.09	0.90
LOI	4.03	3.23	3.54	3.51	3.96
Total	**89.12**	**96.48**	**96.31**	**96.41**	**91.54**

Small samples of each size fraction were kept apart for any future analysis, or experimental work, that might be required. The measured size distribution of the rod mill feed appears in Figure 4.1.

Table 4.2 - Trace element analysis (ppm) for Palabora rod mill feed

Element	Size range (μm)				
	-150	-1180+150	-3350+1180	-6700+3350	-19000+6700
V	229	498	524	552	1482
Cr	114	180	212	367	331
Co	87	167	174	192	381
Ni	74	81	88	94	161
Cu	253	325	325	335	498
Zn	187	172	184	261	324
Ga	12	6	14	22	22
Rb	13	31	26	16	48
Sr	3443	2697	2643	2287	1141
Y	84	69	69	56	56
Zr	839	847	825	656	3657
Nb	18	13	15	16	20
Ba	623	631	612	579	248
La	646	531	503	609	472
Ce	1233	1467	1521	1416	2021
Nd	640	632	630	570	520
Pb	53	57	60	36	52
Th	321	378	355	366	536
U	19	-1	-6	4	8

To ensure that the process could be accurately modelled at a later stage, an XRF analysis was also performed on the rod mill feed. This analysis was performed at the Geology Department attached to the University of Stellenbosch. The major element analysis appears in Table 4.1, while the trace element analysis is shown in Table 4.2.

The low totals appearing in the results for the major element analysis are most likely due to either volatile elements that were not analyzed for (i.e. C, N, S, etc.) in this analysis, or volatiles that did not burn off completely during loss on ignition (LOI) determination. It should also be noted that every analysis above 2000 ppm (in the trace element analysis) is extrapolated from the calibration, and is thus only an approximation of the true value. This was due to a lack of standards in that region at the laboratory which performed this analysis. The negative values reported are noise values within the accuracy of the analysis.

4.2. SAMPLE PREPARATION

To ensure that all of the batches used for testing in our work were as consistent as possible, any splits which were required were performed by first splitting the bulk material into various size fractions. By splitting each of these size fractions individually before recombining the material into however many batches were required, a high degree of consistency between batches was retained (see Figure 4.2 for a graphical representation of this process).

In this case, the rod mill feed was split into 3 samples, one to be kept separate for characterization of the feed, and two others which would serve in the milling experiments of untreated and microwave treated ore.

From previous experiments, it appeared that the effect of microwave treatment (in terms of the reduction in grinding energy) on Palabora ore was greatest in particle sizes above 3350 μm. It was decided that only material greater than this cut-off size would be microwave processed (and subsequently rod milled) in these experiments.

Both S1 and S2 were split into 16 fractions of nearly equal mass, representing approximately 1 kg each of the rod mill feed and closely following the truncated rod mill feed size distribution (i.e. in the range -19000+3350 μm). The average batch size of

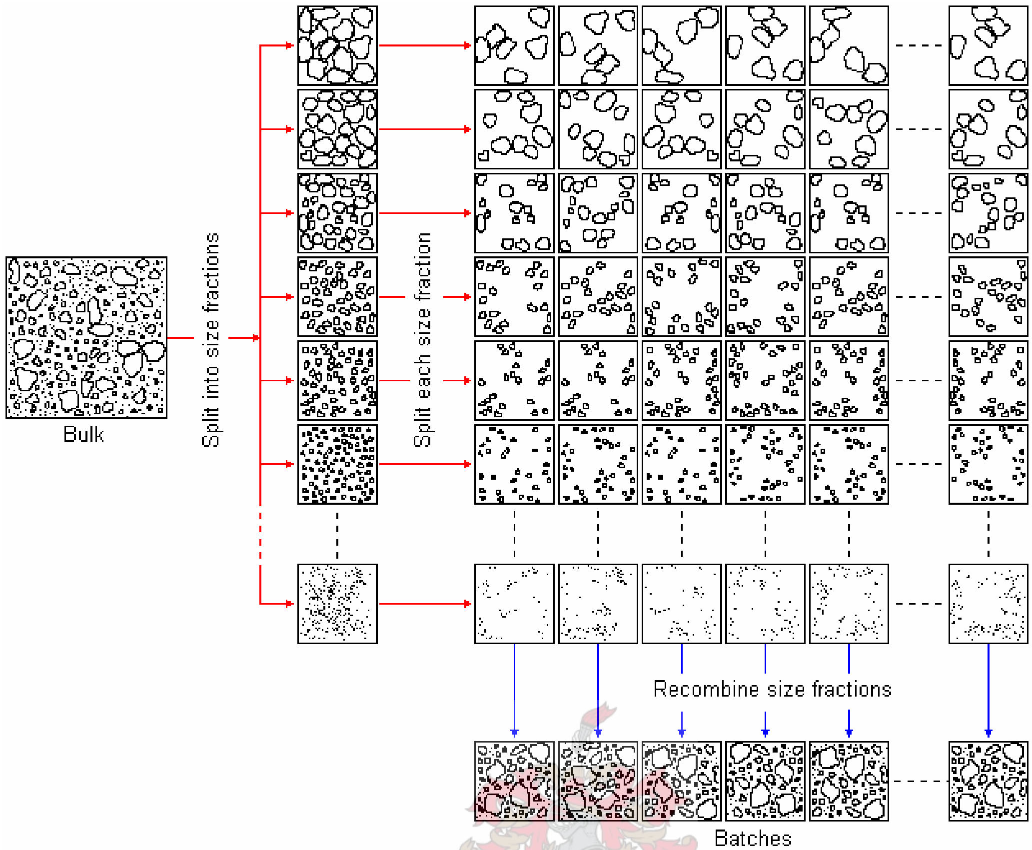

Figure 4.2 - Method for splitting the ore into batches

Table 4.3 - Size distribution of samples for testing

Sieve size	Reserve sample	Untreated (S1)	Treated (S2)
µm	g	g	g
19000	0	0	0
16000	2474	3612	3614
11200	3166	4656	4658
8000	2339	3416	3415
6700	967	1427	1427
5600	756	1123	1123
4750	583	849	849
4000	606	895	895
3350	590	861	860
Total	11481	16839	16841

sample S1 was then 1052 g, while that of sample S2 was 1053 g. The -3350 µm material was reserved in case it later be decided to investigate the processing of smaller particles.

The course of the experimental work performed is shown graphically in Figure 4.3.

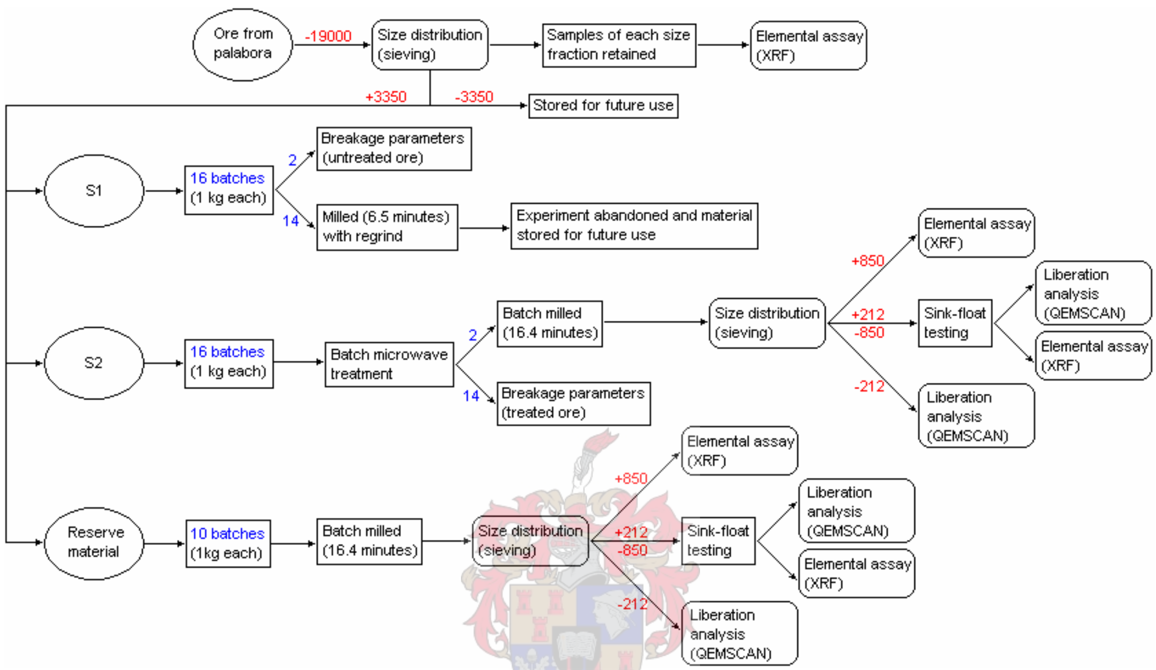

Figure 4.3 - Course of experimental work

4.3. MICROWAVE TREATMENT

The material destined for microwave treatment (S2) was packed securely to prevent damage during transport, and sent to the University of Nottingham. The material was batch processed in the same 1 kg sample sizes that had previously been prepared. The microwave treatment was performed in a single mode microwave applicator using a treatment time of 0.5 seconds at 10 kW (with associated reflected powers during treatment of between 1 and 1.7 kW).

Originally, it was planned to treat the material at 15 kW, but due to rapid heating of some of the particles, the glass tube in which the material is held for treatment also heated and began acting as a receptor. This affected the tuning to such an extent that a massive amount of power was reflected and the system could not get beyond 10.5 kW as a reflected power of 5 kW was detected. By packing the ore with a buffer material, treatment at 15 kW with a reflected power of only 0.8/0.9 kW was possible. It was decided, however, to rather treat the material as is, without adding any material to buffer the reflected power (which would be impossible on large scale) and only treat the material at 10 kW. The material was then securely packed and returned to South Africa.

The resulting reflected power measurements from the microwave treatment of the various batches showed that a reasonable degree of homogeneity in the treatment of the samples was achieved, with only 3 batches out of the 16 showing large reflections of power. This consistency was most likely due to the splitting method used.

Table 4.4 - Particle size distribution after MW treatment

Sieve Size	Mass on sieve
μm	g
16000	3634
11200	4633
8000	3452
6700	1317
5600	1266
4750	733
4000	865
3350	784
-3350	111
Total	16794

On arrival the material was recombined and then resplit into 1 kg samples for grinding. This was to ensure that differences in the microwave treatment would not influence results in the grinding experiments to follow.

To investigate whether or not any microwave treatment induced size reduction occurs in the material, the size distribution was measured once again after the microwave treatment was completed (see Table 4.4).

4.4. MILL CONDITIONS

All the grinding, required in this work, was performed in a laboratory rod mill with the following specifications:

- mill diameter of 19.8 cm
- mill length of 27.8 cm
- rubber mill liners with no lifters

While the available mill media for rod milling was of the following dimensions:

- average rod length of 26.7 cm
- average rod diameter of 2.3 cm

Based on the above restrictions in terms of processing equipment, the following process conditions were chosen:

- critical speed of 101.1 rpm (calculated by taking rod diameter into account, see section 3.3.1)
- mill speed of 75.6 rpm (74.8% of critical speed, see section 3.3.1)
- charge of approximately 45% of the mill volume (see section 3.3.2)
- media load of 17 rods, total mass of 16.8 kg (based on required mill charge)

4.5. ROD MILLING

Two batches from both samples S1 and S2 were selected to be milled to various times in order to determine the breakage and selection functions particular to the treated and untreated Palabora ore. The ore was batch ground, and the particle size distribution in the mill was recorded at the following times:

- 0 minutes (initial particle size distribution of each batch)
- 0.5 minutes
- 1 minute
- 2 minutes
- 3 minutes
- 4.5 minutes
- 6 minutes
- 10.5 minutes
- 15 minutes
- 22.5 minutes

After each of the above grinding times was reached, the mill was stopped and all the material was removed and classed according to size. This size classification took place by mechanical sieving for 20 minutes in a sieve shaker, followed by hand sieving which was continued until the amount of material still falling through each sieve became negligible (i.e. less than 0.1 g after 1 minute of hand sieving). The mass in each size fraction was then recorded and the individual size fractions recombined and reinserted into the mill for grinding until the next time was reached.

Initially, it had been decided to duplicate each test at a smaller number of grinding times to ensure the accuracy of the results, however, comparison of the size distributions for the duplicate test batches after 30 seconds of milling showed a high degree of correlation ($r > 0.99$), and thus later grinding tests times were staggered between the two test batches to increase the number of grinding times investigated. Since the grinding tests showed a high degree of reproducibility, it was considered that this method of obtaining data over a wider test range would still ensure accuracy in the subsequent back-calculations of the grinding parameters, which would still be based on two independent sets of data for both treated and untreated material.

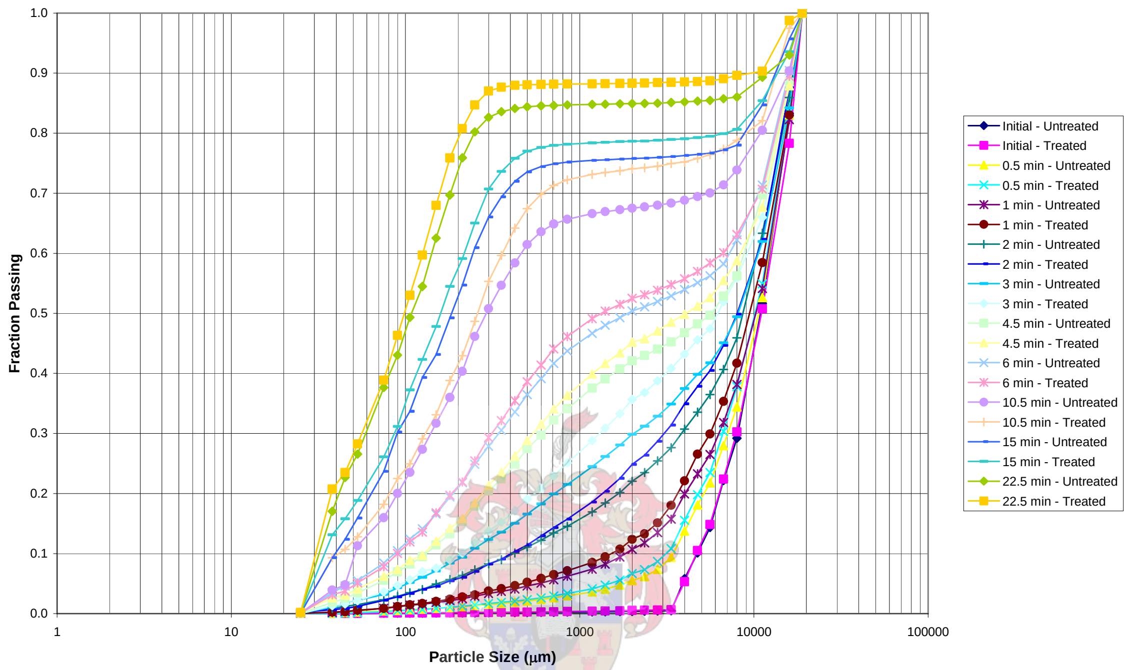

Figure 4.4 - Comparison of rod mill product size for microwave treated and untreated ore

A comparison of the resulting time-dependent size distributions for the treated and untreated material can be seen in Figure 4.4, and show that the microwave treated material produced a finer grind than the untreated material at every grinding time tested. These results were then used to back calculate the breakage and selection parameters for both the treated and untreated material using the MATLAB code found in APPENDIX A.

At this stage it was decided to process the remaining 14 batches of the untreated material with the aim of obtaining the most material possible in the size range -1700+75 μm. This size range was chosen due to it being suitable for a range of different gravity separation methods. Each batch was milled once for 6.5 minutes and the products in each size fraction were combined. All material in the +1700 μm class was then split into batches of more or less 1 kg and remilled, with the products being added to their respective size classes from the first grind. This process was then repeated, once again

regrinding the +1700 μm material. The resulting combined size distribution can be seen in Figure 4.5.

During the grinding, it was noted that the colour of the product material became progressively darker with each grind. This might indicate that the weaker carbonate materials (which are lighter in colour) tend to be ground first, with the darker magnetite

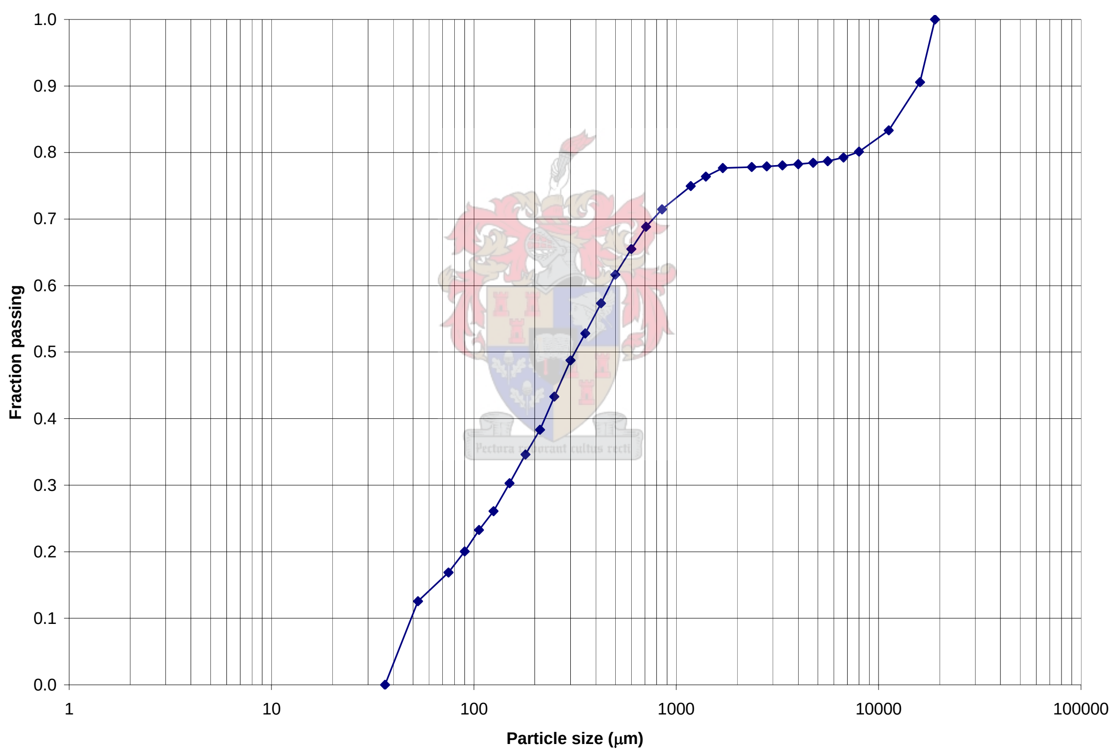

Figure 4.5 - Size distribution of rod mill product after regrind of oversize material

and other materials of similar strength only being comminuted later in the grinding process. While this observation is not of use in continuous rod milling (which has, to some extent, an in-built system of classification), it does indicate that in other processes it might be possible to withdraw the unbroken large particles of hard minerals before they are comminuted further, thus recovering these minerals at larger particle sizes.

Since it was noted that the comminution of the ore proceeded in this manner, there were worries as to the validity of using any material which had been obtained in this manner for further experimentation, as it was thought that any results would not reflect what would happen in a large-scale mill. At this stage it was decided that to achieve better results in the simulations to follow, the ore should only be ground once. To this end, a large portion of the reserve (microwave untreated) ore was used, and sample S1 was stored for later use if needed.

The reserve material was divided into 10 batches (following the same splitting procedure as for samples S1 and S2), each as close to 1 kg in mass as possible (an average batch size of 1036 g was achieved).

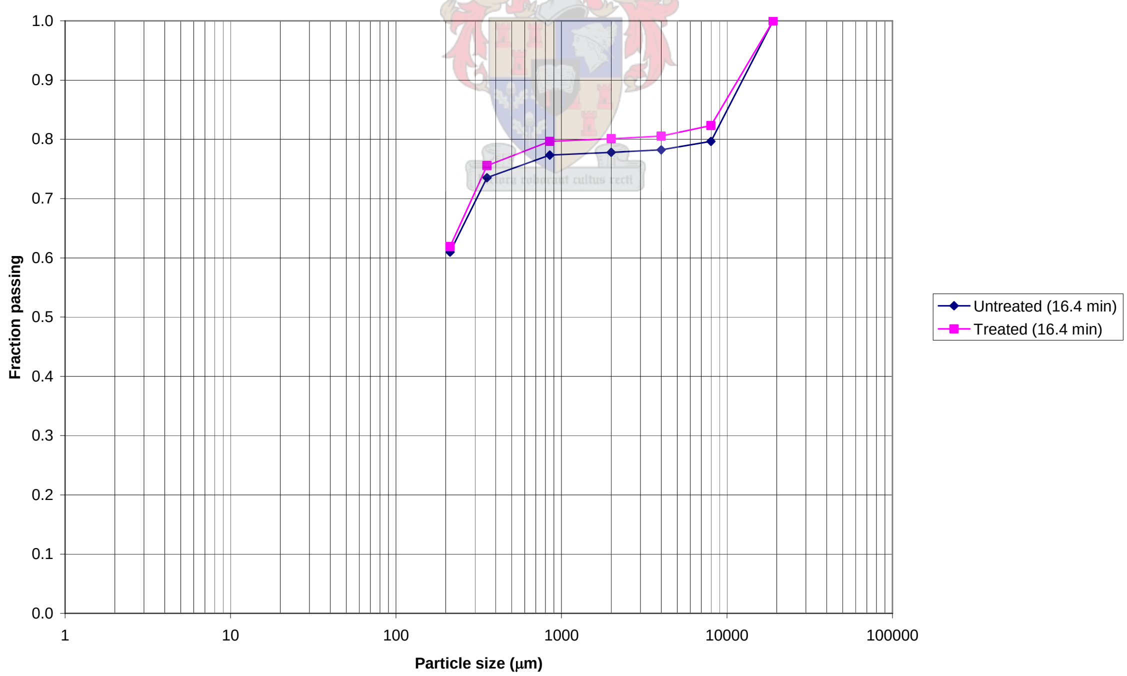

Figure 4.6 - Rod mill product size for treated and untreated material after 16.4 minutes

From the data used to construct Figure 4.4, a milling time was chosen which allowed for an 80% passing 800 µm size for the microwave treated ore. This was determined to be 16.4 minutes and the same grinding time was used for each batch of the untreated reserve material as well, allowing for an accurate comparison of all the results to follow from the experiments to be performed on these ores. The size distributions obtained from combining the mill products of each batch, for the treated and untreated material, appear in Figure 4.6. It can be seen that the combined results from the 24 separate tests which make up Figure 4.6 support the results of the data which was to be used to determine the grinding parameters for the microwave treated and untreated material (which appears in Figure 4.4), and that once again the microwave treated ore produced a finer grind than the untreated material after the same grinding time.

4.6. OBSERVATIONS ON LARGE PARTICLES REMAINING IN PRODUCT

At this time it was decided to investigate the treated rod mill product which had not undergone significant comminution (i.e. in the -19000+8000 µm size range). As had been noted from the grinding time experiments, more large material from the treated ore had been broken than from the untreated ore. This indicated that while some of the large particles had been susceptible to microwave induced fracturing, the remaining lumps in this size fraction had not. Around 20 rocks from this size range were chosen for study. Investigations using density measurements and observations of reactions to the presence of magnets, allowed the unbroken rocks to be roughly classified into three groups:

- a dirty-white, non-magnetic material of low density (average 2886 kg/m^3) suspected to be mainly calcite/dolomite
- a dark, gray-black speckled, non-magnetic material of low density (average 3145 kg/m^3) suspected to be orthopyroxene
- a dark, strongly magnetic material of relatively high density (average density of 4590 kg/m^3) suspected to be composed mainly of magnetite

The high proportions of the magnetite observed among these materials placed in doubt the information that we had originally received about the ore composition, which had suggested that the ore was comprised of mainly calcite.

4.7. GRAVITY SEPARATION

It was decided to subject the mill product in the size range of -850+212 μm to sink/float gravity separation, since this is the region in which gravity separation is most commonly performed. From data on the composition of Palabora ore (supplied by the mine at the beginning of the project), and the known densities of these minerals, an ore

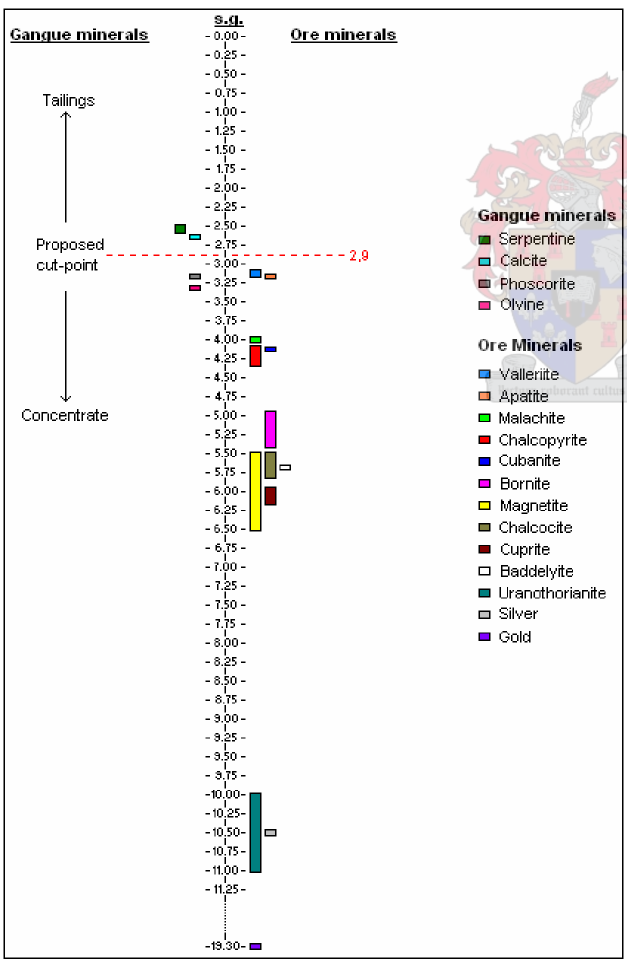

Figure 4.7 - Densities of minerals and cut-size for sink/float tests

density profile was constructed to aid in deciding the best place to split the ore (see Figure 4.7). From this data, it was decided to split the material at a specific gravity of 2.9. This cut-size would then remove a large proportion of the gangue in the material, and if improved liberation of the copper minerals had occurred, then very little of the copper was expected to be lost from the treated ore in this process.

A suitable heavy liquid was found in the form of tetrabromoethane which has a specific gravity of 2.967 @ 20°C/4°C. Due to the hazardous nature of working with this chemical compound, the separation was performed in a fume cupboard, while wearing heavy neoprene gloves, safety glasses and a respirator.

The material was separated using two 250 ml separation funnels. The funnels were filled with TBE, and between 50 g and 100 g of ore was added, stirred to bring any material which had settled out immediately back into suspension. The mixture was left to settle for several minutes, at which time the heavy material was brought back into suspension by gently agitating the bottom part of the funnel. This was to allow any light material which was dragged down with the heavy minerals another chance to float. The mixture was then allowed to stand again, with a minimum settling time of 20 minutes being used for each separation.

At the end of this time period, the material which had settled out was removed as sinks, while the suspended solids and the material floating at the top of the funnel were removed in a single product as floats.

The first separation was performed on the untreated ore and all the material which had been produced in the chosen size range was split using this separation method. Before the splitting of the treated ore began, certain worries were raised as to the accuracy of the procedure employed in our separation. A small amount of material was split out from the treated gravity separation feed to form a test sample which would undergo a very careful splitting so that a benchmark for the splitting of the bulk of the ore could be set. This would allow the efficiency of the separation of the bulk material, which was performed with larger batches being split at a time, as well as slightly shorter settling times, to be determined.

Due to the large amount of treated ore which had been produced in this size range, only half the ore was used in the gravity separation tests, and the splitting proceeded in the same manner as it had for the untreated ore.

All the results from the gravity separation of the treated and untreated material appear in Table 4.5.

Table 4.5 - Results of sink/float tests for Palabora ore

Description	Untreated	Treated	
	Bulk material	Test sample	Bulk material
Total mass (g)	1563	67	1192
Mass of split fraction (g)			
Floats	424	18	316
Sinks	1138	49	876
Percentage of total sample			
Floats	27.2	26.5	26.5
Sinks	72.8	73.5	73.5

A good comparison between the results of the test sample and bulk material separations of the treated ore was noted, and was taken as an indication of the consistency and accuracy of the separation method used.

4.8. ANALYSIS OF PRODUCTS

4.8.1. XRF ANALYSIS

Table 4.6 - Major element analysis (mass %) for feed and products of sink/float testing

Oxide	Untreated (size ranges in μm)					Treated (size ranges in μm)				
	Feed sub-class		-850+212 μm			Feed sub-class		-850+212 μm		
	-355 +212	-850 +355	Feed	Sinks	Floats	-355 +212	-850 +355	Feed	Sinks	Floats
SiO_2	7.29	10.85	8.14	5.23	17.96	7.62	11.09	8.44	4.87	17.94
Al_2O_3	1.73	2.89	2.05	1.51	4.2	1.9	3.04	2.21	1.38	4.05
TiO_2	1.44	1.53	1.48	1.91	0.14	1.43	1.52	1.45	1.93	0.15
Fe_2O_3	57.47	58.79	57.89	77.59	3.29	57.44	59.31	57.54	77.36	3.58
MnO	0.19	0.19	0.2	0.23	0.09	0.2	0.2	0.19	0.23	0.1
MgO	8.21	9.77	8.63	6.08	15.06	8.09	9.59	8.42	6.2	15.53
CaO	12.64	7.73	11.58	5.18	27.98	12.68	7.91	11.51	5.51	28.1
Na_2O	0.16	0.25	0.16	0.18	0.15	0.23	0.23	0.17	0.09	0.14
K2O	0.25	1	0.37	0.08	1.59	0.33	0.96	0.52	0.08	1.57
P_2O_5	2.79	1.5	2.48	2.95	0.41	2.68	1.27	2.36	3.3	0.44
SO_3	0.48	0.32	0.44	0.21	0.25	0.48	0.3	0.42	0.27	0.25
Cr_2O_3	0.02	0.02	0.01	0.02	0.01	0.02	0.02	0.02	0.02	0.01
NiO	0.04	0.04	0.04	0.04	0.01	0.04	0.03	0.04	0.05	0.01
H_2O-	0.19	0.13	0.16	0.07	0.16	0.16	0.22	0.25	0.05	0.19
LOI	6.98	4.39	6.39	-0.98	27.81	7.02	4.67	6.44	-1.09	27.81
Total	**99.88**	**99.4**	**100.03**	**100.3**	**99.1**	**100.32**	**100.37**	**99.98**	**100.24**	**99.88**

Several samples (of between 40 g and 70 g each) of the feed to the gravity separation, as well as the products of the gravity separation, were prepared and sent for XRF analysis. To obtain these samples, all the ore in the respective size range was used and the splitting was performed using a Rap-Hex sample splitter, with the combination of material from two cups on opposite sides of the splitter being combined and used in the next stage of the splitting.

Three samples each for both the treated and untreated material were prepared from the feed to the gravity separation: one covering the entire range of -850+212 μm, and two samples covering different portions of this size range, these being 212 μm to 355 μm and 355 μm to 850 μm. The aim of testing portions of the entire size range was to investigate what sort of variance occurs in the composition of the feed to the sink/float separation with particle size.

The sinks and floats for both the treated and untreated material were analyzed as one sample each, covering the entire size range from 212 μm to 850 μm.

The XRF results for these samples (provided by Scientific Services in Cape Town) are presented separately as a major element analysis (Table 4.6), and a trace element analysis (Table 4.7) for both treated and untreated ore. The major oxides present are shown in weight percent, and the quantities of the trace metals Zn, Cu and Ni are shown in parts per million (which is equivalent to g/ton).

Table 4.7 - Trace element analysis (ppm) for feed and products of sink/float testing

Element	Untreated (size ranges in μm)					Treated (size ranges in μm)				
	Feed sub-class		-850+212 μm			Feed sub-class		-850+212 μm		
	-355 +212	-850 +355	Feed	Sinks	Floats	-355 +212	-850 +355	Feed	Sinks	Floats
Zn	108	115	110	134	25	107	117	107	134	24
Cu	2074	1459	1857	2453	854	2030	1280	1918	2588	895
Ni	203	207	207	263	52	208	214	210	262	54

From these results, as well as some of the QEMSCAN results which had been sent to us at this time (PUG1 and PTG2), it was decided that to make more accurate assumptions about the effects of microwave treatment (especially with respect to the distribution of copper), it would be necessary to fully analyze the composition of the entire rod mill product. It was decided to do this by performing several more XRF analyses on the remaining +850 μm material (results for the -212 μm size class were expected to come from other QEMSEM analysis which were still to be performed).

Table 4.8 - Major element analysis (mass %) for rod mill product in the size range -8000+850 μm

Element	Untreated (size ranges in μm)			Treated (size ranges in μm)		
	-2000 +850	-4000 +2000	-8000 +4000	-2000 +850	-4000 +2000	-8000 +4000
Al_2O_3	4.09	4.66	3.27	3.78	3.83	2.97
CaO	9.07	8.76	10.48	8.82	7.92	9.71
Cr_2O_3	0.001	0.002	0.000	0.000	0.002	0.000
Fe_2O_3	51.67	47.73	56.90	52.62	53.88	54.88
K_2O	1.57	0.60	0.67	1.41	0.36	0.54
MgO	12.37	11.45	10.23	12.52	11.64	12.09
MnO	0.23	0.23	0.24	0.25	0.26	0.25
Na_2O	1.04	1.27	1.28	0.83	0.91	1.01
NiO	0.05	0.05	0.04	0.04	0.05	0.05
P_2O_5	0.86	1.30	0.92	1.27	0.81	1.16
SiO_2	15.18	20.42	12.58	14.88	17.03	13.58
TiO_2	1.35	1.62	1.47	1.50	1.44	1.63
LOI	2.59	2.21	2.57	2.30	2.14	2.50
Sum	**100.05**	**100.29**	**100.65**	**100.24**	**100.26**	**100.37**

As some of the material in the size ranges greater than 8000 μm had been used in density experiments and not been returned from the University of Nottingham, it was decided that the composition of the -19000+8000 μm material would be inferred from the results of the largest particle size range analyzed. The results of this analysis appear in Table 4.8 and Table 4.9.

Table 4.9 - Trace element analysis (ppm) for rod mill product in the size range -8000+850 μm

Element	Untreated (size ranges in μm)			Treated (size ranges in μm)		
	-2000 +850	-4000 +2000	-8000 +4000	-2000 +850	-4000 +2000	-8000 +4000
V	671	816	885	743	906	971
Cr	172	145	515	191	137	660
Co	217	273	247	231	270	297
Ni	95	98	107	103	104	123
Cu	356	382	335	347	384	372
Zn	196	213	291	201	247	275
Ga	20	20	8	29	14	21
Rb	151	48	27	111	42	9
Sr	1364	1423	1133	1279	1246	1064
Y	45	49	55	46	44	49
Zr	698	411	601	733	615	822
Nb	15	19	13	11	16	13
Ba	2378	733	802	2229	669	243
La	258	403	339	339	319	246
Ce	1006	1414	1257	1254	1349	1404
Nd	250	412	324	370	355	304
Pb	46	50	55	35	56	47
Th	357	413	346	347	375	389
U	-1	9	-1	-2	-1	-1

4.8.2. QEMSCAN ANALYSIS

Due to the budgetary constraints of the project and the high cost associated with QEMSCAN (roughly R5000 per sample), only 4 samples were prepared and sent for analysis in this manner, being two for the treated, and two for the untreated ore. The first of the two samples for both the treated and untreated ore fell in the size ranges most suitable for gravity separation, that is the range of -850+212 μm and were designated PUG1 (Palabora Untreated Gravity 1) and PTG2 (Palabora Treated Gravity 2). The last two samples for each were prepared in the size ranges most commonly associated with flotation, this being the range of -212+25 µm, and were designated PUF3 (Palabora Untreated Flotation 3) and PTF4 (Palabora Treated Flotation 4). In order to help reduce the costs associated with the analysis, each of these samples was sieved into 3 size ranges before being sent to Mintek (see Table 4.10 for the split masses of these samples).

Table 4.10 - Split masses of samples sent for QEMSCAN

Sample	Size fraction	Mass	Mass distribution	Sample	Size fraction	Mass	Mass distribution
-	(µm)	g	%	-	(µm)	g	%
PUF3	-53+25	43	38	**PTF4**	-53+25	50	38
	-106+53	31	27		-106+53	36	27
	-212+106	39	35		-212+106	47	35
PUG1	-300+212	163	64	**PTG2**	-300+212	163	64
	-425+300	64	25		-425+300	64	25
	-850+425	29	11		-850+425	29	11

The modal analysis results for the untreated ore appear in Table 4.11, while those for the treated ore are presented in Table 4.12. The 'combined' column is, in each case, the combined results over the entire range covered by the particular analysis, scaled by Mintek with the known size distributions from Table 4.10. No malachite or cuprite was detected in any of the samples, either by optical microscope or scanning electron microscopy.

The calculated copper content of the samples from this analysis were:

- PUF3 (untreated -212+25 µm) = 5300 ppm
- PUG1 (untreated -850+212 µm) = 1900 ppm
- PTF4 (treated -212+25 µm) = 4000 ppm
- PTG2 (treated -850+212 µm) = 2900 ppm

Table 4.11 - Modal composition of PUF3 and PUG1 from QEMSCAN (in weight %)

Mineral phase	PUF3 (size range in μm)				PUG1 (size range in μm)			
	-53 +25	-106 +53	-212 +106	Combined -212+25	-300 +212	-425 +300	-850 +425	Combined -850+212
Bornite	0.39	0.51	0.12	**0.33**	0.06	0.11	0.21	**0.09**
Covellite	-	<0.01	<0.01	**<0.01**	<0.01	<0.01	0.00	**<0.01**
Pyrite/Pyrrhotite	0.03	0.07	0.07	**0.05**	0.08	<0.01	0.01	**0.05**
Chalcocite	0.02	0.16	0.04	**0.07**	0.02	0.01	0.01	**0.02**
NiFe-sulfides	0.01	<0.01	<0.01	**<0.01**	<0.01	<0.01	<0.01	**<0.01**
Chalcopyrite/Cubanite	0.91	0.61	0.41	**0.65**	0.26	0.02	0.04	**0.18**
Valeriite	0.35	0.10	0.10	**0.20**	0.06	0.07	0.10	**0.07**
Magnetite	27	39	49	**38**	60	67	64	**62**
Apatite	13	13	10	**12**	7	3	5	**6**
Calcite/Dolomite	42	32	25	**33**	17	14	11	**16**
Orthopyroxene	6	8	7	**7**	7	6	7	**7**
Amphibole/Clinopyroxene	1	1	1	**1**	2	1	1	**1**
Sphalerite	-	<0.01	<0.01	**<0.01**	0.01	<0.01	<0.01	**<0.01**
Chlorite	0.23	0.14	0.36	**0.25**	0.24	0.5	0.4	**0.3**
Mica	2	1	1	**1**	2	3	6	**2**
Serpentine/Talc	4	3	3	**3**	3	3	3	**3**
Feldspar	2	2	2	**2**	2	3	3	**2**
Gold/Silver	-	0.06	<0.01	**0.02**	<0.01	0.01	<0.01	**<0.01**
Barite	-	<0.01	<0.01	**<0.01**	<0.01	<0.01	<0.01	**<0.01**
Others	0.37	0.20	0.18	**0.26**	0.29	0.26	0.5	**0.3**
Total	**100**	**100**	**100**	**100**	**100**	**100**	**100**	**100**

At this stage it was confirmed that the composition of this ore differed somewhat from the data previously provided by Palabora Mining Company, with the main differences being the large amount of magnetite present in the size ranges analyzed with QEMSCAN (38% in the -212+25 μm fraction and 62% in the -850+212 μm size range, versus around 24% reported in the data provided to us) and the small amount of gangue found (in this analysis consisting mainly of calcite, apatite and orthopyroxene, and totaling around 60% in the -212+25 μm size range and 36% in the -850+212 μm size range, versus approximately 74% in the Palabora Mining Company data). This would obviously impact substantially on the idea of the removal of liberated gangue in a pre-concentration step prior to ball milling, as there was now much less gangue in the ore.

Table 4.12 - Modal composition of PTF4 and PTG2 from QEMSCAN (in weight %)

Mineral phase	PTF4 (size range in μm)				PTG2 (size range in μm)			
	-53 +25	**-106 +53**	**-212 +106**	**Combined -212+25**	**-300 +212**	**-425 +300**	**-850 +425**	**Combined -850+212**
Bornite	0.33	0.26	0.07	**0.22**	0.24	0.10	0.17	**0.20**
Covellite	<0.01	<0.01	<0.01	**0.00**	<0.01	<0.01	<0.01	**<0.01**
Pyrite/Pyrrhotite	0.08	0.24	0.03	**0.11**	0.17	0.01	<0.01	**0.11**
Chalcocite	0.05	0.03	0.01	**0.03**	0.15	0.02	0.13	**0.11**
NiFe-sulfides	<0.01	<0.01	<0.01	**<0.01**	0.02	<0.01	<0.01	**0.01**
Chalcopyrite/Cubanite	0.72	0.72	0.35	**0.59**	0.12	0.33	0.02	**0.16**
Valeriite	0.19	0.11	0.06	**0.12**	0.09	0.11	0.09	**0.10**
Magnetite	32	41	42	**38**	59	65	62	**61**
Apatite	14	12	11	**12**	7	5	5	**6**
Calcite/Dolomite	40	33	30	**35**	18	13	13	**16**
Orthopyroxene	6	6	8	**6**	8	6	8	**7**
Amphibole/Clinopyroxene	1	1	1	**1**	1	1	1	**1**
Sphalerite	0.01	<0.01	<0.01	**0**	<0.01	<0.01	<0.01	**<0.01**
Chlorite	0.21	0.23	0.26	**0.23**	0.24	0.31	0.38	**0.28**
Mica	1	1	2	**1**	1	3	5	**2**
Serpentine/Talc	3	3	4	**3**	3	3	3	**3**
Feldspar	2	1	2	**2**	2	2	3	**2**
Gold/Silver	0.04	<0.01	-	**0.02**	<0.01	-	<0.01	**<0.01**
Barite	-	<0.01	0.01	**<0.01**	<0.01	<0.01	<0.01	**<0.01**
Others	0.38	0.16	0.15	**0.24**	0.28	0.21	0.37	**0.28**
Total	**100**	**100**	**100**	**100**	**100**	**100**	**100**	**100**

In addition to the mineral compositions, the QEMSCAN analysis also provides the liberation, and to some extent the mineral associations, of the various mineral phases.

The liberation statistics of the copper sulfide minerals are presented according to particle morphology, where the particle is classified as either 'liberated' or 'locked', and the mineral associations of the unliberated material is expressed as either 'attached to gangue' or 'attached to other sulfides'. These results appear in Table 4.13 for the untreated ore, and in Table 4.14 for the treated ore.

Table 4.13 - Liberation statistics of copper minerals in untreated ore

Mineral	State of mineral liberation	PUF3				PUG1			
		Avg grain diam	Volume %			Avg grain diam	Volume %		
			-53 +25 µm	-106 +53 µm	-212 +106 µm		-300 +212 µm	-425 +300 µm	-850 +425 µm
Chalcopyrite/ cubanite	Liberated (CLY90 and CLY 100)		76	56	34		15	-	-
	Attached to gangue	10 µm	0.8	5	10	20 µm	84	75	90
	Attached to other sulfides	15 µm	23	39	53		-	1	-
	Locked in gangue (oxides/silicates)	5 µm	-	0.7	3	5 µm	1	24	10
	Total		**100**	**100**	**100**		**100**	**100**	**100**
Bornite	Liberated (CLY90 and CLY 100)		21	66	-		44	-	-
	Attached to gangue	10 µm	78	3	40	20 µm	48	99	100
	Attached to other sulfides	10 µm	0.7	30	60		8	<1	-
	Locked in gangue (oxides/silicates)	5 µm	-	2	0.7	5 µm	<1	-	-
	Total		**100**	**100**	**100**		**100**	**99**	**100**
Valeriite	Liberated (CLY90 and CLY 100)		-	-	-		-	-	-
	Attached to gangue	5 µm	98	43	94	5 µm	80	95	91
	Attached to other sulfides	5 µm	2	50	0.7		9	-	-
	Locked in gangue (oxides/silicates)	5 µm	0.7	7	5	5 µm	11	5	9
	Total		**100**	**100**	**100**		**100**	**100**	**100**
Chalcocite/ Digenite	Liberated (CLY90 and CLY 100)		-	91	-		-	-	-
	Attached to gangue	5 µm	52	3	12	5 µm	89	17	97
	Attached to other sulfides	15 µm	48	5	85		-	83	-
	Locked in gangue (oxides/silicates)	5 µm	-	1	4	5 µm	11	-	3
	Total		**100**	**100**	**100**		**100**	**100**	**100**

Table 4.14 - Liberation statistics of copper minerals in treated ore

Mineral	Mineral state	PTF4				PTG2			
		Avg grain diam	Volume %			Avg grain diam	Volume %		
			-53 +25 µm	-106 +53 µm	-212 +106 µm		-300 +212 µm	-425 +300 µm	-850 +425 µm
Chalcopyrite/ cubanite	Liberated (CLY90 and CLY 100)		56	53	38		-	66	-
	Attached to gangue	15 µm	2	4	24	10 µm	24	19	62
	Attached to other sulfides	10 µm	40	40	36	10 µm	73	-	-
	Locked in gangue (oxides/silicates)	5 µm	2	3	1	5 µm	3	15	38
	Total		**100**	**100**	**100**		**100**	**100**	**100**
Bornite	Liberated (CLY90 and CLY 100)		23	53	43		-	-	-
	Attached to gangue	10 µm	5	12	34	10 µm	59	96	99.8
	Attached to other sulfides	5 µm	73	34	1	15 µm	34	-	
	Locked in gangue (oxides/silicates)	10 µm	-	1	22	5 µm	6	3	0.2
	Total		**100**	**100**	**100**		**100**	**99**	**100**
Valeriite	Liberated (CLY90 and CLY 100)		-	-	-		-	-	-
	Attached to gangue	5 µm	23	6	89	5 µm	88	94	89
	Attached to other sulfides	5 µm	76	22	5	5 µm	0.3	1	-
	Locked in gangue (oxides/silicates)	5 µm	1	73	7	5 µm	12	5	11
	Total		**100**	**100**	**100**		**100**	**100**	**100**
Chalcocite/ Digenite	Liberated (CLY90 and CLY 100)		-	-	-		-	-	-
	Attached to gangue	5 µm	1	29	58	5 µm	11	96	99
	Attached to other sulfides	5 µm	92	71	19		90	-	-
	Locked in gangue (oxides/silicates)	5 µm	7	-	23	10 µm	-	4	1
	Total		**100**	**100**	**100**		**101**	**100**	**100**

From inspection of the particle images used in the analysis and comparison of the results of PUG1/PTG2, and PTF3/PUF4, it was found that often the statistics surrounding the copper bearing minerals (and other trace minerals) are inferred from only a handful of particles containing the particular mineral in the sample. Statistical inferences of trace minerals to the bulk material from these results alone are therefore difficult to perform while retaining any degree of accuracy.

Table 4.15 - Liberation statistics of oxides and silicates in -850+25 μm rod mill product

Mineral	Liberation	Untreated						Treated					
		PUF3 (Volume%)			PUG1 (Volume%)			PTF4 (Volume%)			PTG2 (Volume%)		
		-53 +25 μm	-106 +53 μm	-212 +106 μm	-300 +212 μm	-425 +300 μm	-850 +425 μm	-53 +25 μm	-106 +53 μm	-212 +106 μm	-300 +212 μm	-425 +300 μm	-850 +425 μm
Magnetite	ClY0	100	100	100	100	100	100	100	100	100	100	100	100
	CLY20	98	99	99	100	100	99	97	99	99	99	99	99
	CLY30	98	99	99	99	99	99	96	99	99	99	99	99
	CLY40	97	99	99	99	99	98	95	99	98	99	99	99
	CLY50	97	99	99	99	98	98	94	99	98	99	99	98
	CLY60	97	99	99	98	98	98	93	98	97	98	98	97
	CLY70	96	98	98	97	97	97	91	98	97	98	98	96
	CLY80	93	97	97	97	96	95	88	97	96	96	97	94
	CLY90	89	96	93	92	91	90	75	95	93	93	92	93
Carbonates	CLY0	100	100	100	100	100	100	100	100	100	100	100	100
	CLY20	98	99	98	96	96	93	97	99	97	97	95	96
	CLY30	98	99	97	95	94	93	96	99	96	96	94	94
	CLY40	98	98	97	94	93	90	95	99	95	96	93	91
	CLY50	98	98	96	93	91	90	95	98	95	95	92	90
	CLY60	98	98	96	93	90	86	93	97	93	93	92	90
	CLY70	98	98	96	92	89	85	92	97	92	93	91	88
	CLY80	97	97	95	90	89	78	90	97	90	92	91	87
	CLY90	95	96	94	88	84	75	84	95	84	91	90	87
Apatite	CLY0	100	100	100	100	100	100	99	100	100	99	100	100
	CLY20	99	100	99	98	94	97	97	99	99	97	97	97
	CLY30	99	99	99	97	93	93	97	99	98	97	96	94
	CLY40	99	98	98	95	91	86	96	99	97	96	95	79
	CLY50	99	98	97	95	90	84	94	99	96	95	93	79
	CLY60	99	98	96	95	84	80	93	98	95	94	93	77
	CLY70	99	97	95	93	84	75	92	98	94	92	87	66
	CLY80	98	95	94	90	79	75	86	97	92	86	81	60
	CLY90	92	90	90	84	71	75	76	93	86	83	78	51
Orthopyroxene	CLY0	100	100	100	100	100	100	100	100	100	100	100	100
	CLY20	90	92	91	89	85	86	90	90	90	90	87	88
	CLY30	87	90	87	84	78	81	87	86	86	85	81	85
	CLY40	86	86	82	77	76	71	84	83	82	80	70	75
	CLY50	79	82	78	71	74	66	80	81	80	77	61	64
	CLY60	78	80	72	61	68	57	75	77	75	72	56	57
	CLY70	74	74	67	56	62	50	68	72	67	68	49	51
	CLY80	65	65	56	49	43	41	60	62	60	58	39	29
	CLY90	42	57	44	42	34	22	47	55	49	45	21	16

The degrees of liberation of those materials present in large quantities in the ore (i.e. the oxides and the silicates) are presented according to the cumulative liberation index (see Table 4.15).

4.9. FLOTATION EXPERIMENTS

In an effort to better relate the XRF and QEMSCAN results of these and future analyses, to the outcome of an actual flotation experiment, two samples were prepared and sent for micro-flotation testing to the Department of Chemical Engineering at the University of Cape Town. These samples consisted of -212 μm material from both the treated and untreated material.

Only one flotation test was performed, recovering 25.1 mg of concentrate. Due to the low concentrate recoveries, no reliable assaying of the concentrates would be possible. Since the QEMSCAN results provided insufficient knowledge (especially of the ratio of chalcopyrite to cubanite in the samples) to assist in the assaying of such small quantities of concentrate, the flotation test work was discontinued with no results.

However, work performed by Sahyoun et al., 2004, on Palabora ore showed increased recoveries of up to 7% of the total copper in the ore after microwave treatment at 10 kW of power for 0.5 seconds. As this treatment occurred in the same cavity that was used to microwave treat the material for this work, and on ore from the same mine, these results were considered to be a good substitute for the missing flotation data and were thus used to make up for the lack of our own flotation data.

5. ANALYSIS OF RESULTS

5.1. MINERAL CONTENT OF PALABORA ORE

QEMSCAN analysis revealed that the main constituent of the ore was magnetite, while the primary gangue material was calcite. Table 5.1 shows the minerals detected in the rod mill feed provided by Palabora Mining Company.

An elemental analysis through XRF also determined the presence of trace amounts of Cr, Co, Ga, Rb, Sr, Y, Zr, Nb, La, Ce, Nd, Th and U, none of which are present in the above minerals, and most of which are likely to exist as oxides in the ore.

Palabora reports a copper grade of 0.48% and a magnetite content of 26.9% fed to the rod mill. From the XRF analyses of the ore used in the test work performed for this paper, an average grade of 2687 ppm, or around 0.27%, copper, and a magnetite content of at least 40% was found. It does appear, however, that the ore sent to us by Palabora was mined at a different part of the complex, and this is thus to be expected.

The grade of the ore used in the tests will be used for most of the analysis work. For the flowsheet simulation, however, the results obtained from the analyses will be generalized and, where required, the properties of the ore reported by Palabora will be used.

Table 5.1 - Mineral phases detected in Palabora ore by QEMSCAN

Mineral phase	Formula
Bornite	$CuFeS_4$
Covellite	CuS
Pyrite	FeS_2
Pyrrhotite	$Fe_{0.95}S$
Chalcocite	Cu_2S
NiFe-sulfides	$(Fe,Ni)_9S_8$
Chalcopyrite	$CuFeS$
Cubanite	$CuFe_2S_3$
Valeriite	$(Fe,Cu)_4S.(Mg,Al)_3(OH)_2$
Magnetite	$FeO.Fe_2O_3$
Apatite	$Ca_5(PO_4)_3(OH,F,Cl)$
Calcite	$CaCO_3$
Dolomite	$CaMg(CO_3)_2$
Amphibole	*Group name (Na, Ca, Mg, Al, Si, Fe, O, H)*
Clinopyroxene	*Group name (Li, Na, Ca, Mg, Al, Si, Fe, O)*
Orthopyroxene	*Group name - mainly $MgSiO_3$*
Sphalerite	$(Zn,Fe)S$
Chlorite	$(Fe, Mg, Al)_6(Si, Al)_4O_{10}(OH)_8$
Mica	*Group name (Li, K, Al, Mg, Si, Fe, F, O, H)*
Serpentine	$(Mg,Fe)_3Si_2O_5(OH)_4$
Talc	$Mg_3Si_4O_{10}(OH)_2$
Feldspar	*Group name (Na, K, Ca, Al, Si, O)*
Gold	Au
Silver	Ag
Barite	$BaSO_4$

5.2. MICROWAVE COMMINUTION

It is reported by Kingman et al., IMPC XXII, that some ores respond so violently to the application of microwave energy that they break during the treatment, though this effect is dependant on the type of microwave treatment (i.e. the type of cavity, microwave power and the treatment time employed) as well as the mineralogy of the ore in question.

Where this microwave comminution occurs, it may warrant cost saving changes to the process flowsheet for an ore, possibly even resulting in the removal of a crushing stage from the process. To investigate whether or not the ore used in the work for this thesis reacted in such a manner, the feed and product size distributions from the batch microwave treatment of the Palabora rod mill feed were compared (see Figure 5.1).

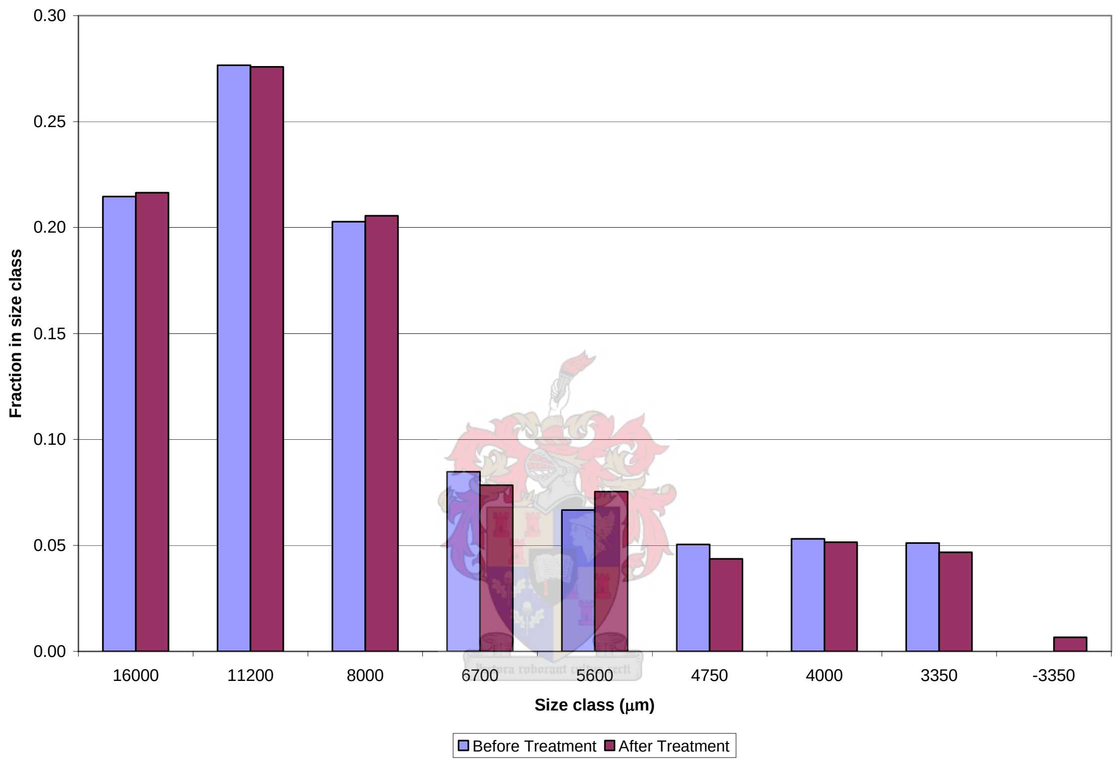

Figure 5.1 - Comparison of the particle size distributions before and after the MW treatment

While there is some slight variation in all the size classes, this is most likely due to the usual inconsistencies associated with sieving large quantities of material (Ruhmer, 1991). The fine material observed in the treated ore is also more likely to be as a result of mechanical damage during handling, and especially sieving where the vibratory motion of the mechanical sieves does lead to some attrition of the material being classed, than from any damage caused by the microwave treatment.

It also would be expected that any daughter particles formed as a direct result of internal stresses from microwave treatment would be quite large, however, the little breakage into the -3350 μm size range which was observed was mostly extremely fine material.

Thus there is not enough evidence to support any claim of microwave comminution taking place in this ore at the treatment conditions used, and from this it was concluded that the microwave treatment of the ore in a single mode cavity, at 10.5 kW of microwave power for 0.5 seconds, was not enough to obtain any direct size reduction from the treatment, given the specific mineralogy of Palabora ore.

5.3. ANALYSIS OF THE FEED AND PRODUCT DISTRIBUTIONS FROM ROD MILLING

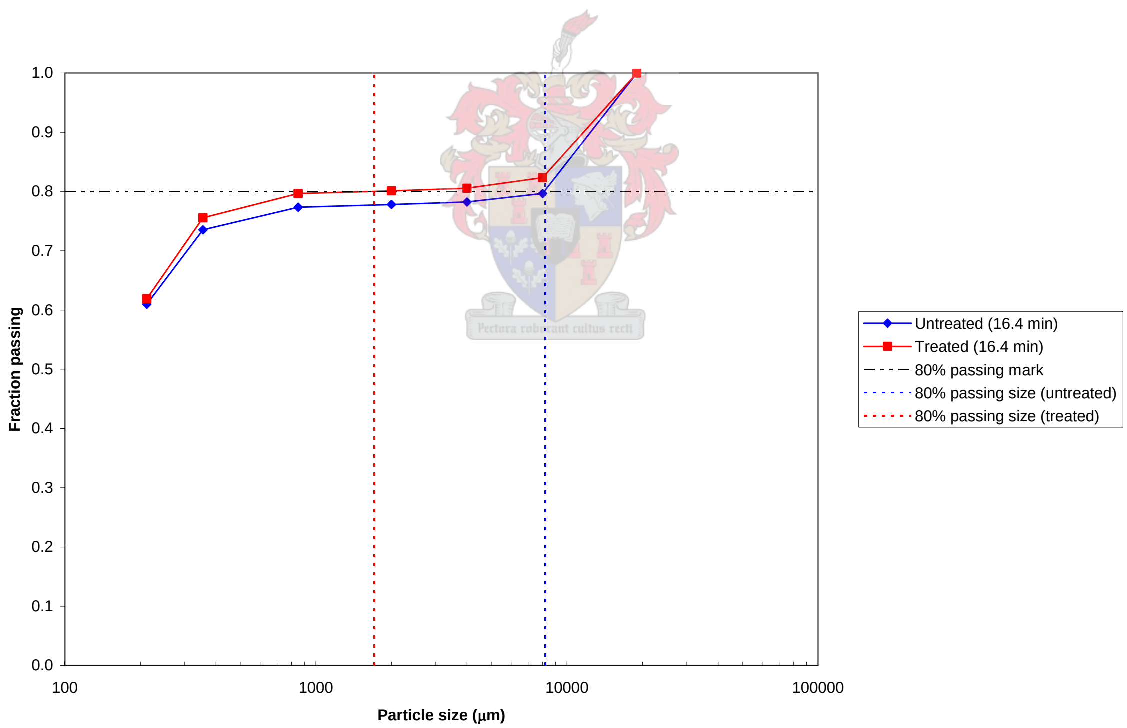

Figure 5.2 - Measured size distributions of rod mill product

Figure 5.2 shows the measured product size distributions of the rod mill for both the treated and untreated ore after each had been milled for 16.4 minutes. It can be seen that the 80% passing size of the Palabora ore is reduced significantly from around 8200 μm for untreated ore, to just 1700 μm for microwave treated ore.

The distribution of minerals with size after comminution in the rod mill will vary between treated and untreated ores, depending on what selective damage the microwave treatment has caused in the ore. A thorough understanding of this phenomenon is required in order to make accurate assessments of possible flowsheet changes that can be brought about in the downstream processing of the ore after milling.

The resulting grade and mass distributions for the two most important valuable ore elements; copper (Figure 5.3) and iron (Figure 5.4), as well as for the three major gangue elements; calcium (Figure 5.5), magnesium (Figure 5.6) and silicon (Figure 5.7) were compared for treated and untreated material.

The error bars on the reported grade values are, in the case of each element, the maximum deviation observed from the plotted mean grade of 4 sets of overlapping data (i.e. 1 set of QEMSCAN data and 3 independent sets of XRF data) in the -850+212 μm size range, this being the size range for which the most information regarding the composition of the microwave treated and untreated ores was available.

The reported mass fraction passing a certain particle size is obtained by combining the data on the grade of the mineral in a certain size class with the measured quantity of ore in the same size class. Hypothesis tests on the data obtained for both the microwave treated and untreated ores in the -850+212 μm size range, reveal that, for each of the elements investigated, the null hypothesis that there is no difference between the mass of the element in this size range for microwave treated and untreated material can be rejected at a significance level of 0.01, in favour of the alternate hypothesis that microwave treatment has indeed changed the distribution of minerals in this size range.

From Figure 5.3 it can be seen that after milling, around 95% of the copper exists in particles smaller than 300 μm for both microwave treated and untreated ore. Due to the high degree of uncertainty present in the analysis of small amounts of material of extremely low grade (i.e. < 0.5% for copper in this case), it can be seen that the error bars for the elemental grade of copper overlap between treated and untreated material. While this brings into doubt the reliability of the analysis, it must also be taken into account the fact that the reported copper mass fraction passing a certain particle size is always higher for the untreated material than for the treated material, as well as the hypothesis testing which shows the significance of this difference, all of which would indicate that the results are not quite as random as one might first be led to believe.

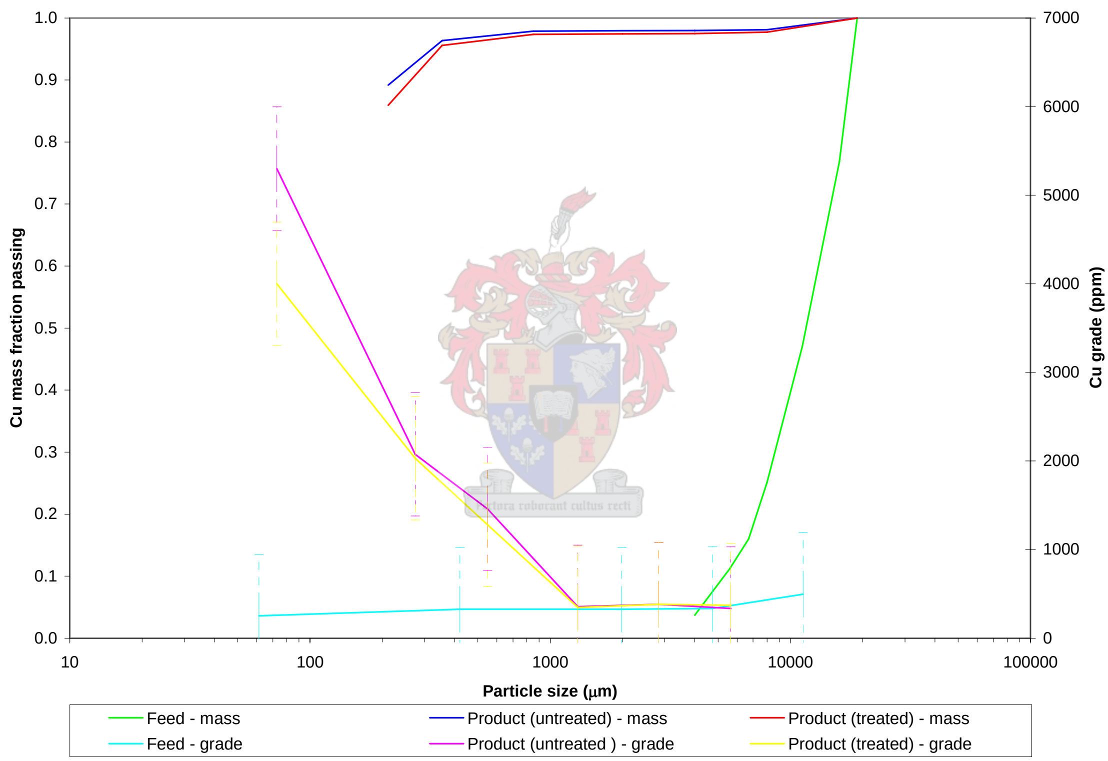

Figure 5.3 - Grade and mass distribution of copper

The implication of this result is that more copper reports to the larger size ranges after milling for microwave treated material, which can only be as a results of the formation of a different fracture pattern in the ore, in this case one which causes the ore to selectively break in a manner which creates less fine particles containing copper minerals (i.e. producing intergranular, rather than transgranular, fracturing between different minerals).

Extending this result further, it would seem likely that this would also mean that the valuable minerals which do report to the finer size classes should be more liberated after microwave treatment (a conclusion which is supported by later analysis in section 5.6).

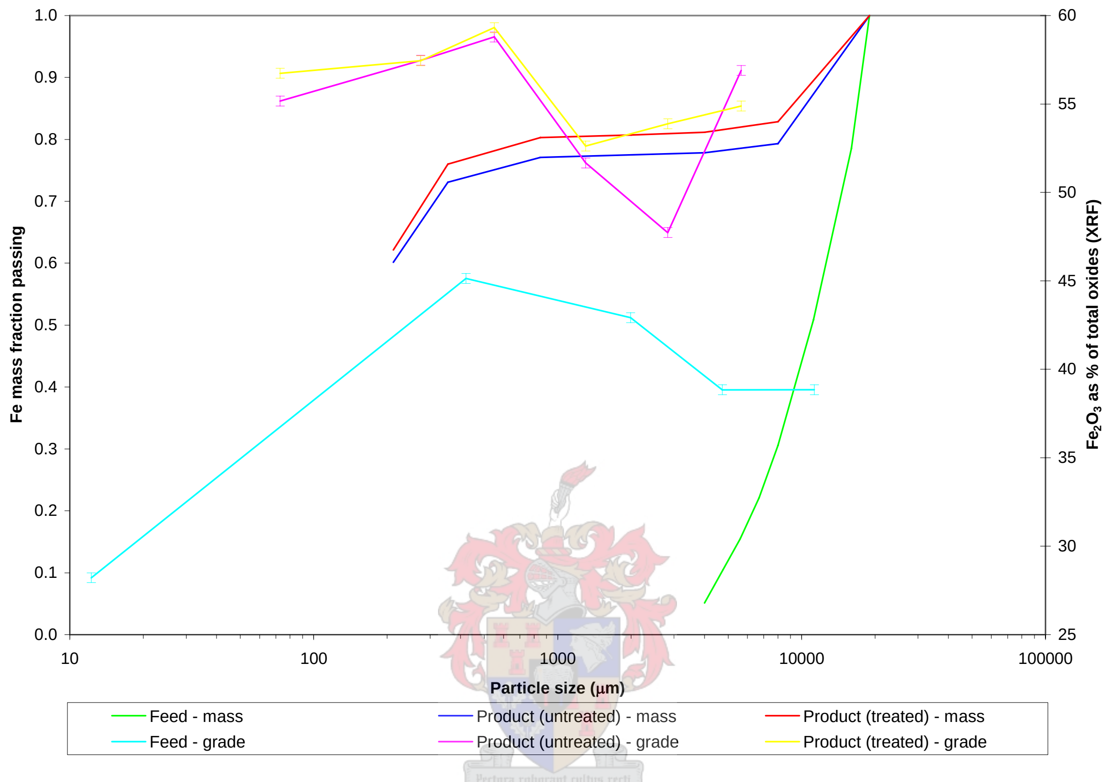

Figure 5.4 - Grade and mass distribution of iron

The iron content of the truncated rod mill feed is in the region of 27%, and most of this exists in the form of magnetite. It was noted that the reliability of the grade analysis of this element was much higher than that of the trace element copper, as can be seen by the much smaller error bars associated with the reported grades in Figure 5.4.

From Figure 5.4 it can be seen that in the rod mil product more of the iron in the treated material exists in smaller sizes than for the untreated material, with 80% of the iron being found in particles less that 8000 µm in size for untreated material, and in particles less than 850 µm in size for treated material. This is due to the weakening, and subsequent breakage, of more large ore particles after microwave treatment, which would otherwise not be broken in a mill of the size used (refer to the observations made in section 4.6 and also the discussion on the effect of rod size on the breakage characteristics of a mill in section 5.4). This difference declines at smaller sizes, as a result of the induced fractures being fully exploited and used up, with the rate of breakage once again approaching that of the untreated ore (an effect which the author has noted in several other microwave treated ores of vastly different mineralogies he has worked with). This analysis then supports the claim that microwave treatment induces thermal fracturing of ore minerals (in this case magnetite), ensuring that a finer product is produced after milling than would be the case for untreated material.

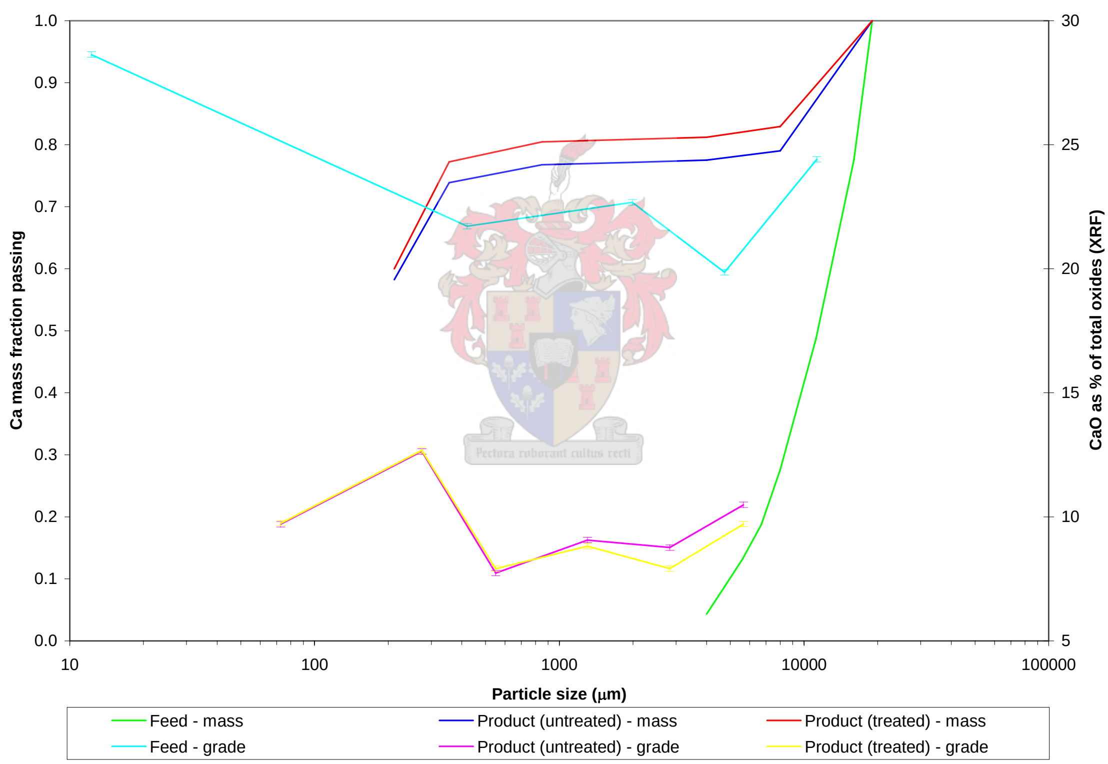

Figure 5.5 - Grade and mass distribution of calcium

From Figure 5.5 it can be seen that more of the calcium is present in the smaller sizes of the rod mill product for microwave treated ore than for untreated ore. Since 62% of the calcium in the ore exists in the form of calcite and 30% as apatite, this would indicate that the mineralogy of Palabora ore allowed for microwave induced fracture to occur specifically in these two gangue minerals (which contain neither magnesium, nor silicon).

For the distribution of magnesium in the rod mill products, it is seen that there is more of this element present in the smaller particle sizes for material which has not been subjected to microwave pretreatment (see Figure 5.6). As most of the magnesium present in the ore is contained within the minerals dolomite, serpentine, talc and orthopyroxene, it can be concluded that microwave treatment was produced a fracture pattern within the ore which has in some way shielded either these minerals from subsequent breakage during milling. The most likely explanation for this would be the introduction of intergranular fracture around either these minerals, or the minerals with which they are closely associated in the ore, which tends to preserve minerals at larger particle sizes. This result then supports the claim that microwave treatment can bring about the liberation of gangue material at larger particle sizes.

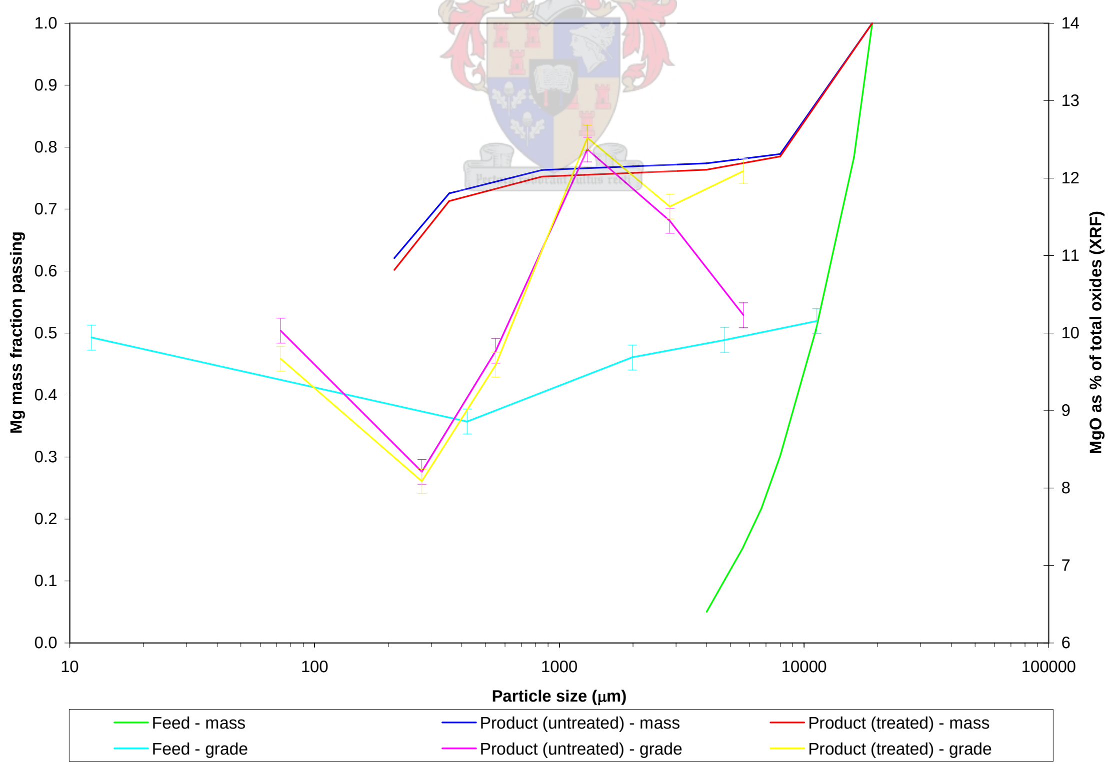

Figure 5.6 - Grade and mass distribution of magnesium

Figure 5.7 shows that microwave pretreatment produces less silicon containing material, after milling, in the -212 µm size range, and more in the +212 µm range than is the case for the untreated ore. As most of the silicon present in the ore exists in the form of orthopyroxene, it follows that more orthopyroxene exists in particles larger than 212 µm in the microwave treated ore than in the untreated ore. Similar to what was seen for the magnesium containing minerals, this result points towards a change in the fracture pattern associated with the ore after microwave treatment, in this case one which most likely causes intergranular fracture around orthopyroxene grains (or their associated minerals) and shields the orthopyroxene containing particles from further breakage below 212 µm. Similar to the results for the magnesium containing minerals, this result also supports the claim that microwave treatment can bring about the liberation of gangue material at larger particle sizes, a claim which is investigated further in section 5.5.

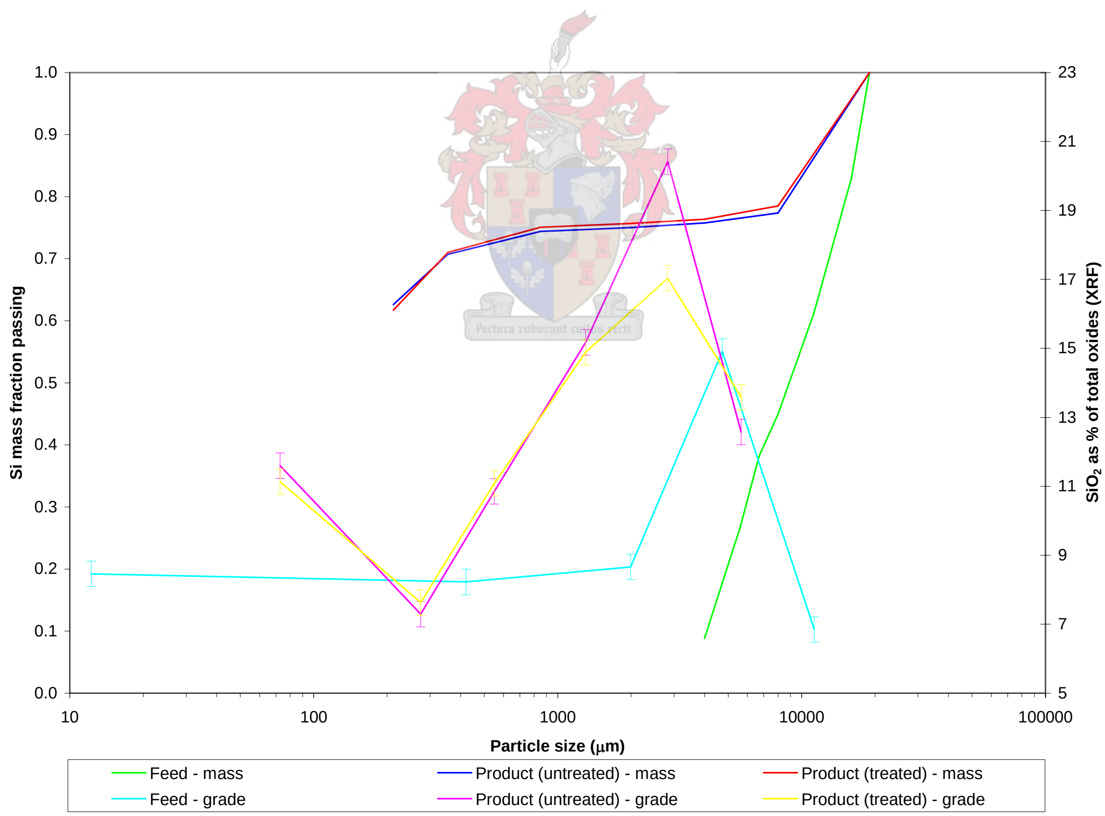

Figure 5.7 - Grade and mass distribution of silicon

5.4. CALCULATION OF THE BREAKAGE CHARACTERISTICS FOR ROD MILLING

It was noted that the time-dependent cumulative size distributions (Figure 4.4) for both the microwave treated and untreated ores tended to flatten out over a large intermediate size range, with this flat portion becoming more noticeable with increasing grinding times. It was also seen that this effect was more pronounced in the size distributions of the treated material, where at each grinding time this flat portion always extends over a wider size range than that seen for the corresponding size distribution of the untreated material.

Austin and Weller, 1982, note that the breakage rate of larger particles is often not first order, but that after showing a quick initial rate of breakage, it tends to drop off with time. There are two reasons for this:

- Some particles are too large to be nipped properly between the grinding media, resulting in less impact energy being conveyed to these particles
- The accumulation of finer material with time tends to cushion the breakage of the larger particles

Thus, some particles will be too strong to break due to these attenuated impact forces. Initially, however, the existence of several brittle, large particles (containing many flaws) would still allow for comminution through impact breakage, after which the main mechanism of particle breakage in the larger size classes would be attrition.

It should be noted that the level of the applied impact forces will depend strongly on mill size as well, with a mill of larger diameter delivering more impact force than a mill of smaller diameter. Thus this phenomenon will not be as noticeable in larger mills.

Since this effect was more pronounced in the treated material, it is reasonable to assume that many of the larger particles had been weakened through microwave treatment, as a result of either new fracture formation, or extension of the existing fracture network, and broken rapidly.

Figure 5.8 shows a comparison of the results of grinding tests on the treated and untreated ores (see Figure 4.4) and is thus based on data obtained from 4 separate tests (i.e. two for both treated and untreated material). The colour bar on the plot indicates the change in the mass fraction passing a certain particle size, after a specific milling time, between microwave treated and untreated material. Thus, for instance, the positive change of 0.06 in mass fraction passing observed at a grinding time of 3 minutes and a particle size of $3x10^3$ μm (3 mm), means that 6% more of all the ore is now smaller than 3 mm after grinding for 3 minutes due to the microwave pretreatment. As will become obvious from the simulation results in section 6, and the subsequent economic analyses in section 7, when processing up to 80 000 tons per day of ore as is the case at Palabora, even small increases in the grindability of an ore (which can be directly related to changes in passing fraction of an ore) at the same grinding time lead to significant savings in terms of grinding times, and thus grinding energy. Several points concerning Figure 5.8 should be noted:

- The scatter in the data noted for particle sizes greater than around 10^4 micron (10 mm) can be attributed to the errors associated with sizing small quantities of large particles through sieving (where the passing of only one or two extra particles at this size can have a large influence on the results of the data for this size class).
- More fine material (i.e. material smaller than around 40 μm) is produced in microwave treated ore, than in the untreated ore, for the same grinding time. This effect is seen to increase sharply after around 8 minutes of grinding.

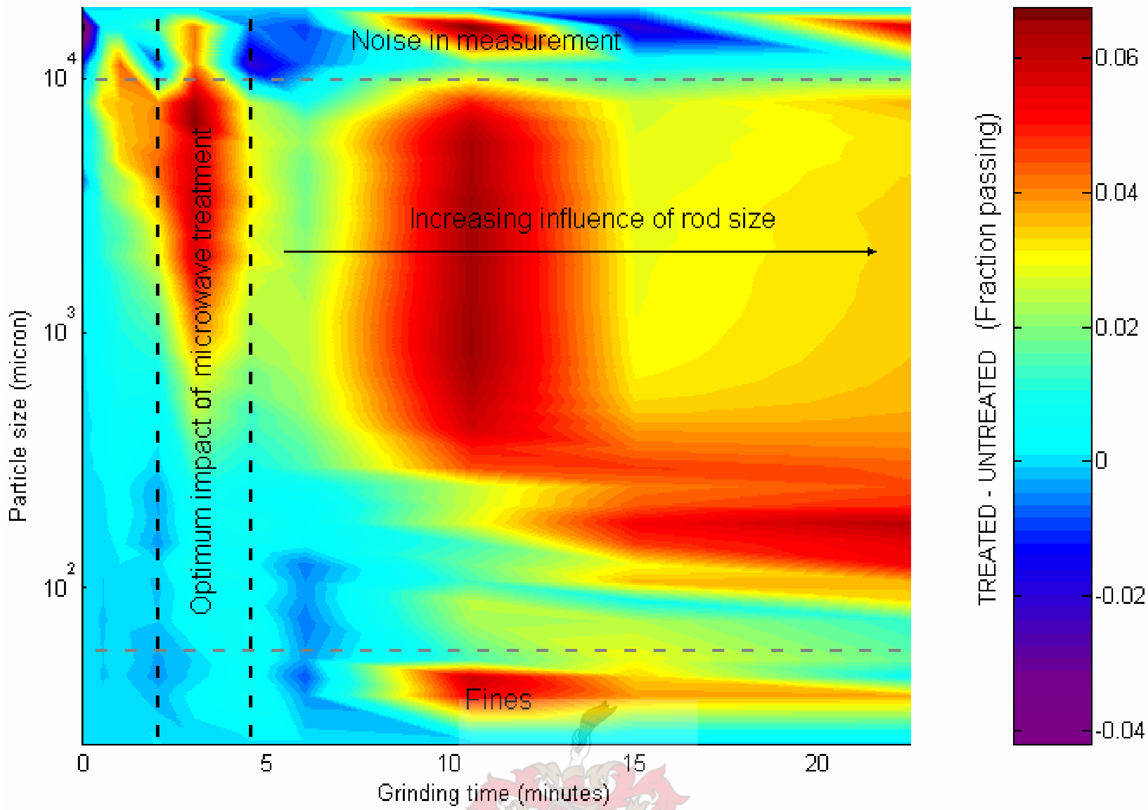

Figure 5.8 - Contour plot of difference in passing fraction between treated and untreated material

- A small range of grinding times (between 2 minutes and 5 minutes) exist where the effects of microwave treatment are best exploited (in terms of differences in grind size between treated and untreated material) *without a large increase in the production of fines*. The optimum grinding time in this region lies at around 3 minutes for the conditions prevailing in the test mill.
- At larger grinding times, the effects of rod size on the size distributions become more pronounced (also see Figure 4.4), culminating in a plateau region where the differences in passing sizes remains more or less constant after the brittle large particles have broken. It is thought that this effect tends to hide the effects of the microwave treatment in terms of liberation.

Figure 5.8 then allows for important decisions to be made on how the grinding of microwave treated ore should differ from that of the untreated ore to best make use of the advantages provided by microwave pretreatment, and thus has major implications in the design, or adaptation, of any milling circuit employed to grind this ore to the correct liberation size. It is obvious from Figure 5.8 that overgrinding of the microwave treated ore should be minimized to prevent an increase in the loss of valuable minerals to slimes (fine material from which valuable minerals are not recoverable), and as the major benefits (in terms of differences in grind size between treated and untreated material) from the microwave treatment appear at shorter grinding times, the residence times in the mills should be lower to remove the liberated material before overgrinding occurs. These results were then used extensively as guidelines, for the adaptation of the flowsheet for the processing of Palabora ore after microwave treatment, during the simulation phase of the work (section 6).

In order to obtain accurate parameters for the selection and breakage functions particular to the treated and untreated material for simulation, the effect of rod size on changing breakage rates with time would have to be eliminated, since the form of the selection function would not be able to model this phenomenon. Since this effect is not expected, and was not observed, at short grinding times for either the untreated or the treated material, it was decided to estimate the model parameters from these distributions only.

The procedure of Das, 2001 (see section 3.3.5), was incorporated into a MATLAB program to optimize the breakage parameters for rod milling from the measured size distributions. This was done through a minimization of the sum of squares of the errors between the measured data and the model results.

Due to the fact that the parameters obtained from this model are only pseudo-parameters (which means that while they can correctly predict the breakage response of the ore during milling, in most cases the parameter values themselves are not of any value in interpreting differences between the treated and untreated ores) it was decided to use the breakage function obtained for the untreated material for the treated case as well, and perform the back-calculation to determine a new selection function only. Even though one would expect a different breakage function for material which undergoes preferential breakage, this method ensures a degree of continuity between the results for the treated and untreated ore, and its simplicity does not affect the reliability of the model in terms of predicting size distributions.

After running several simulations, it was found that the best model fits were obtained when only the size distributions associated with the grinding times of 0 minutes (initial), 0.5 minutes, 1 minute, 2 minutes and 3 minutes were used (see Figure 5.9 and Figure 5.10). These grinding times were then those at which the resulting product size distributions obtained during the milling tests were least affected by the influence of rod size (as discussed previously in this section). The last time of 3 minutes also coincides with the optimum grinding time for exploiting microwave fracturing (see Figure 5.8).

The resulting breakage and selection function parameters (refer to section 3.3.3) for the untreated and the treated ore appear in Table 5.2, while the selection functions are plotted in Figure 5.11.

Table 5.2 - Pseudo-parameters for selection and breakage functions for rod milling

Material	S_1	α	μ	λ	ϕ_{5mm}	γ	β	δ	SSE
Untreated	0.289	0.525	13.281	0.690	0.392	0.996	0.736	0.518	0.255
Treated	1.088	1.004	1.447	1.149	0.392	0.996	0.736	0.518	0.202

Comparisons of all the experimental size distributions with model predictions at the same batch grinding times appear in Figure 5.9 for the untreated ore, and in Figure 5.10 for the treated ore.

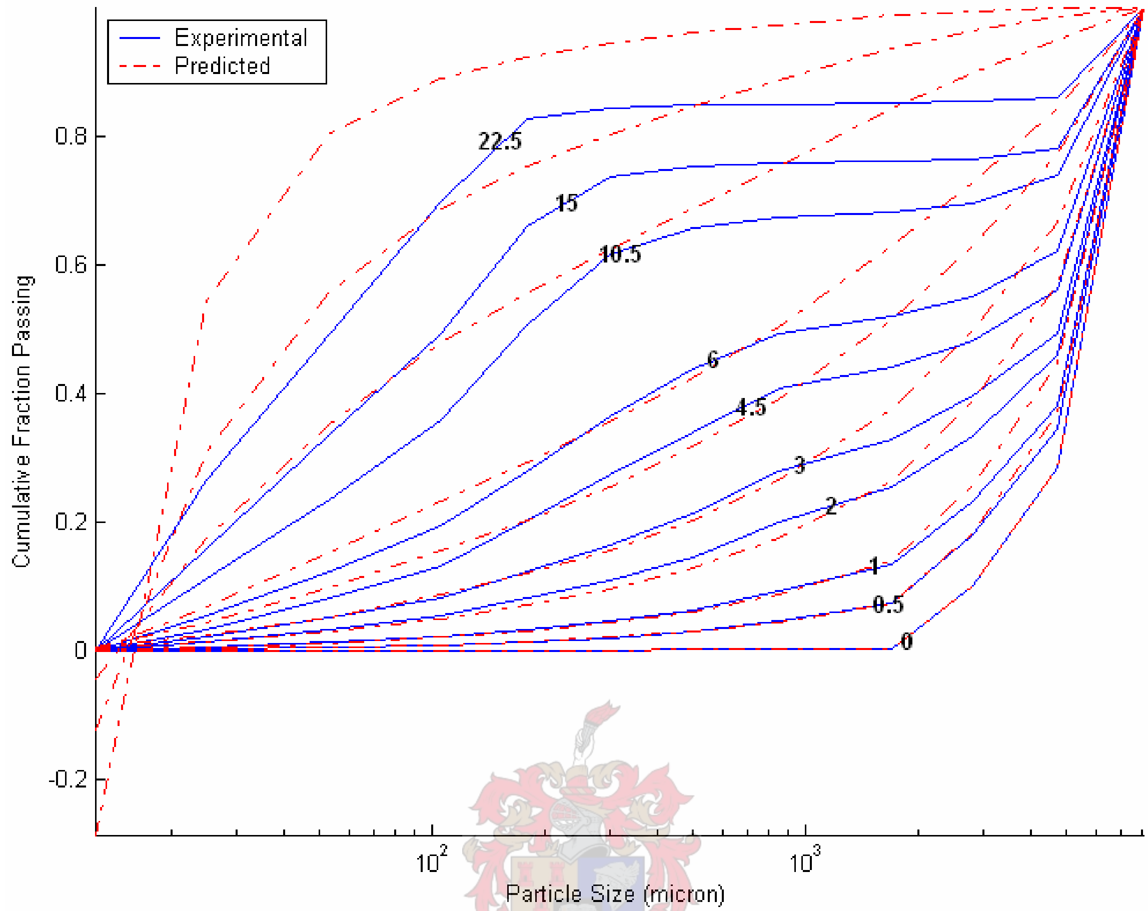

Figure 5.9 - Comparison of predicted and experimental size distributions for untreated ore

It can be seen that, for both treated and untreated ore, the model only predicts the size distribution at 0.5 minutes of grinding accurately over the entire size range. At longer grinding times, the effect of rod size on the slowing of the initial breakage rates of the larger particles begins to skew the data in these size ranges, until the model breaks down completely after about 10.5 minutes for the untreated ore, and earlier still at around 6 minutes for the treated ore, leading to the prediction of negative passing fractions.

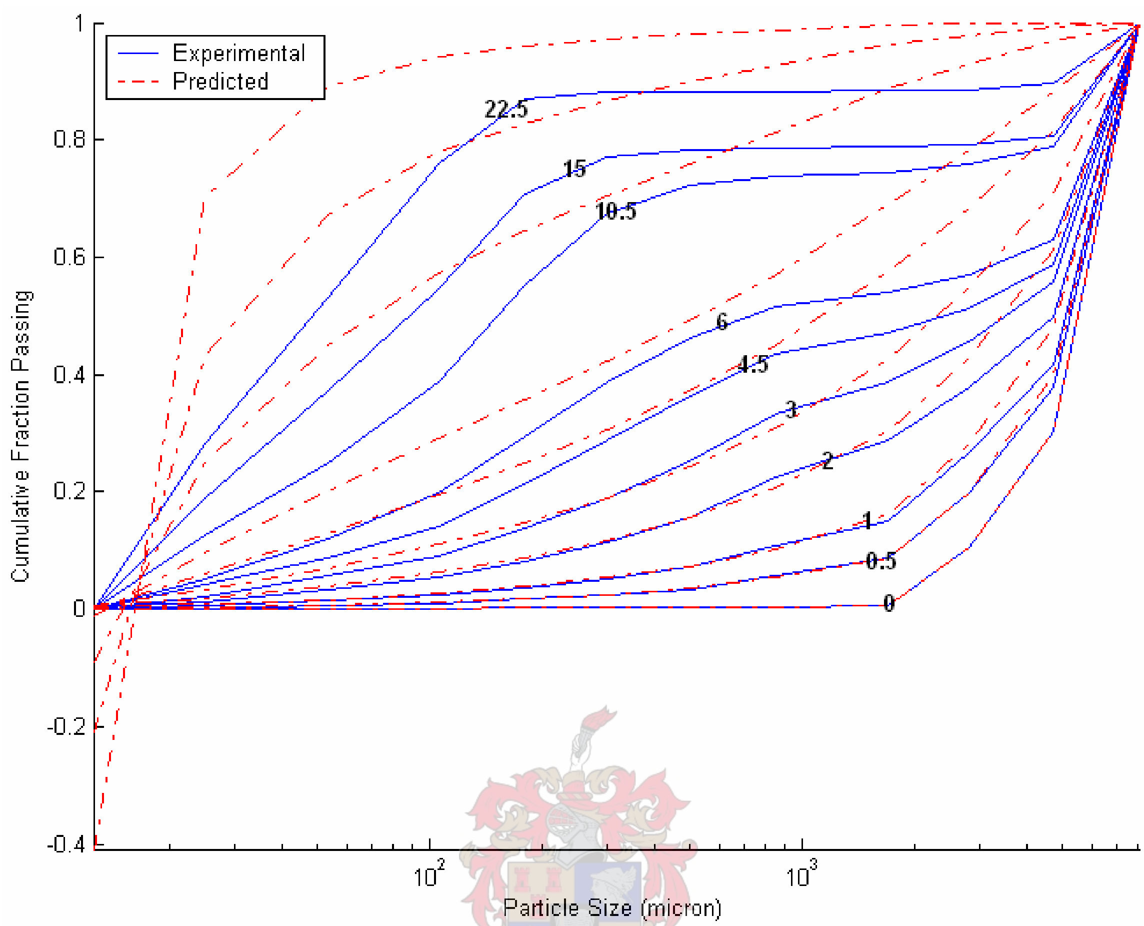

Figure 5.10 - Comparison of predicted and experimental size distributions for treated ore

Since the values for the selection of particles for breakage is fitted to a functional form, this prevents the prediction of nonsensical values, and does to some extent compensate for the slowing down of the breakage rate by ensuring that the predicted selection function values in the larger size classes are realistic. Since the selection function is chosen from a comparison of the errors between measured and predicted data for around 35 points, the relatively few measurements which experience the slowing down of the breakage rates will affect the outcome of the final selection function only slightly. This, together with the fact that the conditions under which the model breaks down in the situation of batch milling will not occur during the simulations, ensures that the pseudo-parameters obtained from these back-calculations will provide reasonably accurate predictions during the modelling of the milling circuit.

Following the method of Austin and Weller, 1982, these selection functions were then scaled up to suit the size of rod mill used at Palabora (refer to section 3.3.6). The parameter values obtained after scale-up are shown in Table 5.3, while the full selection functions for both treated and untreated ores, before and after scale-up, are shown in Figure 5.11.

Table 5.3 - Breakage parameters for treated and untreated ore after scale-up

Material	S_1	α	μ	λ	ϕ_{5mm}	γ	β	δ
Untreated	0.2890	0.5254	13.2808	0.6901	0.3920	0.9960	0.7360	0.5180
Treated	1.0880	1.0038	1.4469	1.1492	0.3920	0.9960	0.7360	0.5180

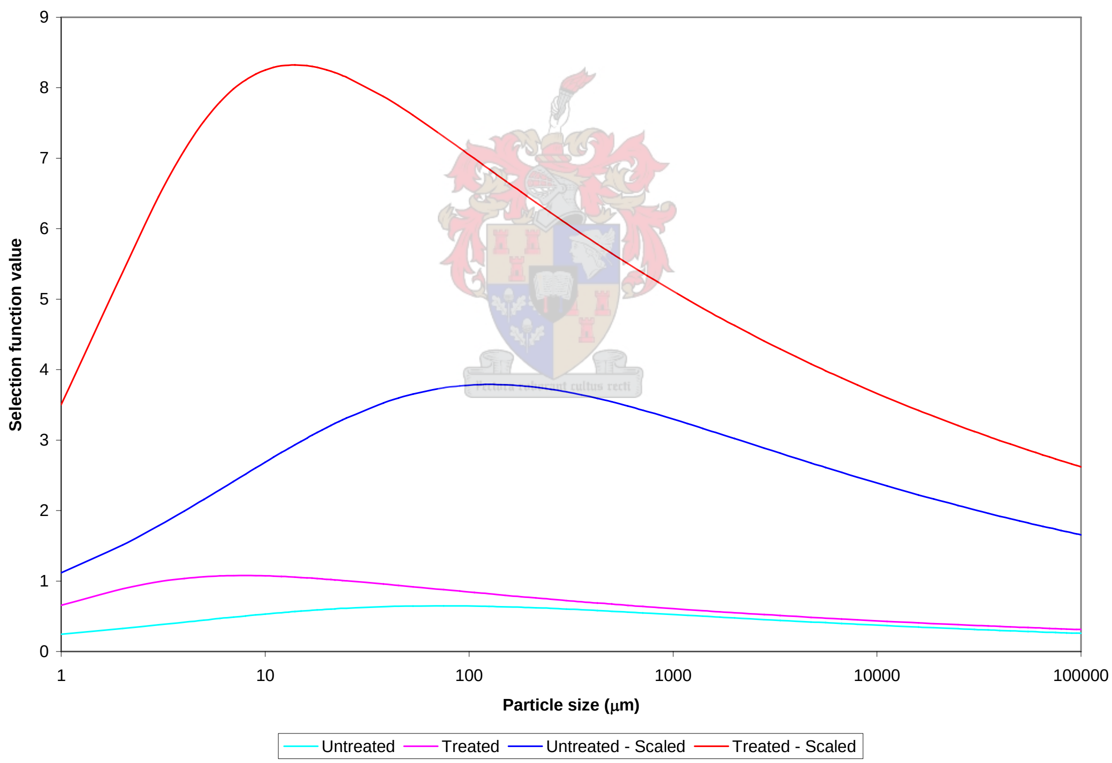

Figure 5.11 - Plot of selection function values for treated and untreated ore for rod milling

Even though the parameters used in the calculation of these selection functions are pseudo-parameters, the fact that these functions describe the behaviour of the treated and untreated ores means that their forms will have meaning. It can be seen that the selection function values (which have associated units of minute^{-1}) are always higher for the treated ore than for the untreated ore at all particle sizes, indicating that the microwave treatment has induced weaknesses into the ore at all particle sizes.

5.5. GRAVITY SEPARATION

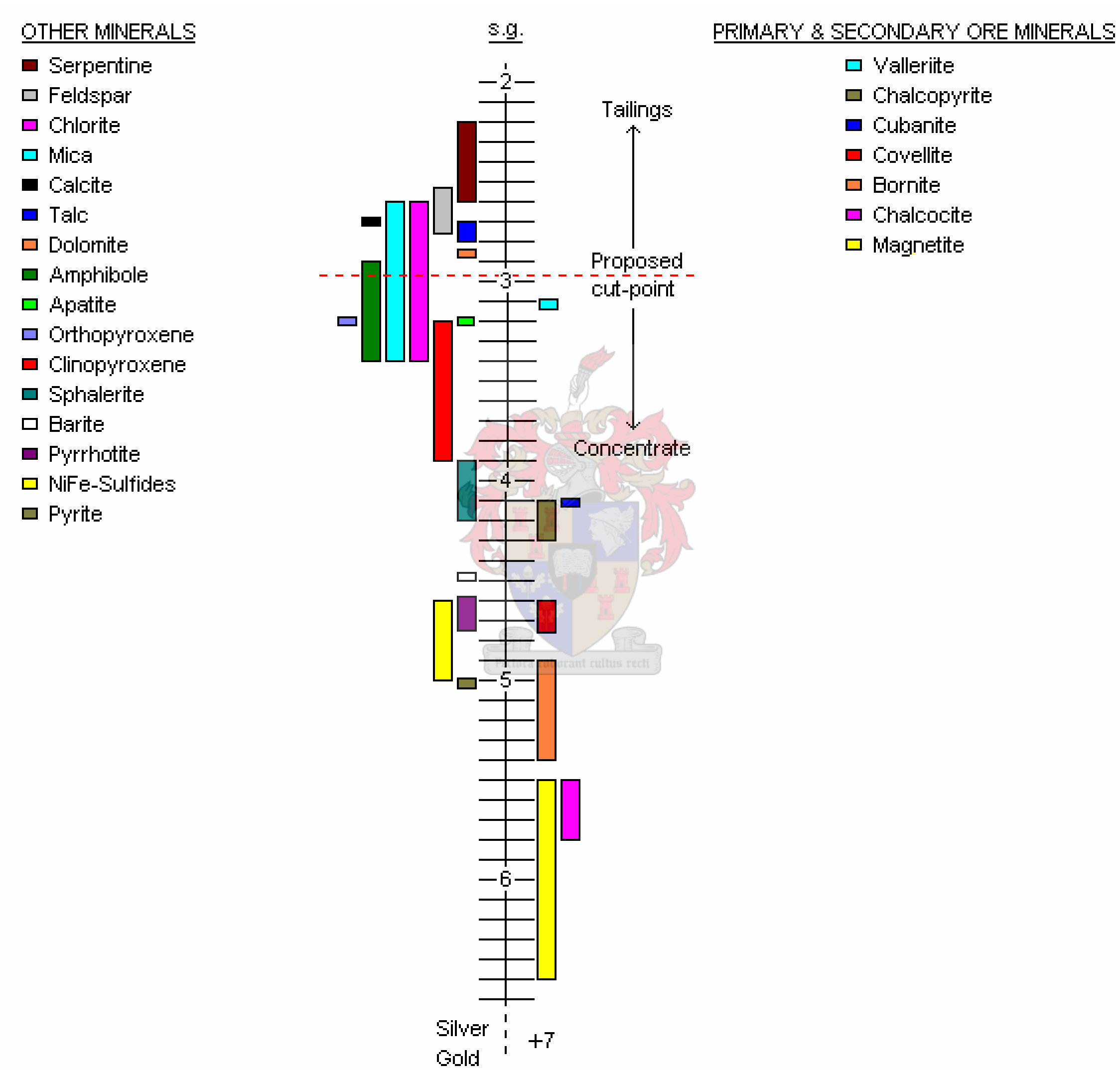

Figure 5.12 - Density distribution of minerals in ore

From the known mineral content of the ore, Table 5.1 was constructed to show the possible effect of the proposed split point on the resulting concentrate and tailings of a gravity concentration process. This represents what would result from a perfect split of fully liberated minerals, given the range of their associated densities.

Table 5.4 - Gravity concentration criterion for the splitting of Palabora ore

Mineral	Silver	Magnetite	Chalcocite	Bornite	Pyrite	NiFe-sulfides	Covellite	Pyrrhotite	Barite	Chalcopyrite	Cubanite	Sphalerite	Clinopyroxene	Apatite	Orthopyroxene	Valeriite	Amphibole	Chlorite	Mica	Dolomite	Talc	Calcite	Feldspar	Serpentine
Gold	2.2	5	6	7	8	9	10	10	11	13	14	15	38	70	70	110	161	495	220	153	75	61	50	29
Silver	-	2.5	2.8	3.5	3.7	4.1	4.4	4.6	5	6	7	7	17	32	32	51	74	228	102	70	35	28	23	13
Magnetite	-	-	1.1	1.4	1.5	1.7	1.8	1.8	2.0	2.5	2.7	2.8	7	13	13	20	30	92	41	28	14	11	9	5.3
Chalcocite	-	-	-	1.2	1.3	1.5	1.6	1.6	1.8	2.2	2.3	2.5	6	12	12	18	26	81	36	25	12	10	8	4.7
Bornite	-	-	-	-	1.1	1.2	1.3	1.3	1.4	1.8	1.9	2.0	5	9	9	15	22	66	29	20	10	8	7	3.9
Pyrite	-	-	-	-	-	1.1	1.2	1.2	1.4	1.7	1.8	1.9	4.7	9	9	14	20	62	28	19	9	8	6	3.6
NiFe-sulfides	-	-	-	-	-	-	1.1	1.1	1.2	1.5	1.6	1.7	4.2	8	8	12	18	56	25	17	8	7	6	3.2
Covellite	-	-	-	-	-	-	-	1.0	1.1	1.4	1.5	1.6	4.0	7	7	12	17	52	23	16	8	6	5	3.0
Pyrrhotite	-	-	-	-	-	-	-	-	1.1	1.3	1.4	1.5	3.8	7	7	11	16	50	22	15	8	6	5	2.9
Barite	-	-	-	-	-	-	-	-	-	1.2	1.3	1.4	3.5	6	6	10	15	46	20	14	7	6	4.7	2.7
Chalcopyrite	-	-	-	-	-	-	-	-	-	-	1.1	1.1	2.8	5	5	8	12	37	16	11	6	4.6	3.8	2.2
Cubanite	-	-	-	-	-	-	-	-	-	-	-	1.1	2.6	4.9	4.9	8	11	35	15	11	5	4.3	3.5	2.0
Sphalerite	-	-	-	-	-	-	-	-	-	-	-	-	2.5	4.6	4.6	7	11	33	15	10	5	4.1	3.3	1.9
Clinopyroxene	-	-	-	-	-	-	-	-	-	-	-	-	-	1.9	1.9	2.9	4.3	13	6	4.0	2.0	1.6	1.3	0.8
Apatite	-	-	-	-	-	-	-	-	-	-	-	-	-	-	1.0	1.6	2.3	7	3.1	2.2	1.1	0.9	0.7	0.4
Orthopyroxene	-	-	-	-	-	-	-	-	-	-	-	-	-	-	-	1.6	2.3	7	3.1	2.2	1.1	0.9	0.7	0.4
Valeriite	-	-	-	-	-	-	-	-	-	-	-	-	-	-	-	-	1.5	4.5	2.0	1.4	0.7	0.6	0.5	0.3
Amphibole	-	-	-	-	-	-	-	-	-	-	-	-	-	-	-	-	-	3.1	1.4	0.9	0.5	0.4	0.3	0.2
Chlorite	-	-	-	-	-	-	-	-	-	-	-	-	-	-	-	-	-	-	0.4	0.3	0.2	0.1	0.1	0.1
Mica	-	-	-	-	-	-	-	-	-	-	-	-	-	-	-	-	-	-	-	0.7	0.3	0.3	0.2	0.1
Dolomite	-	-	-	-	-	-	-	-	-	-	-	-	-	-	-	-	-	-	-	-	0.5	0.4	0.3	0.2
Talc	-	-	-	-	-	-	-	-	-	-	-	-	-	-	-	-	-	-	-	-	-	0.8	0.7	0.4
Calcite	-	-	-	-	-	-	-	-	-	-	-	-	-	-	-	-	-	-	-	-	-	-	0.8	0.5
Feldspar	-	-	-	-	-	-	-	-	-	-	-	-	-	-	-	-	-	-	-	-	-	-	-	0.6

Table 5.4 shows the gravity concentration criterion (determined using equation 3.62) for the splitting of each mineral found in the ore from every other mineral. Over the size ranges used for gravity separation in this project (i.e. -850+212 μm), a gravity concentration criterion of around 1.8 (Burt, 1984) is known to indicate a probable mineral separation, and this value was thus used in the construction of the table. All values marked in red show splits which are highly unlikely, while green shows those which should be possible.

It can be seen that apart from valeriite, it should be possible to separate all the valuable minerals from a large portion of the gangue material, provided that sufficient mineral liberation has occurred.

Figure 5.13 and Figure 5.14 show the distribution of various minerals in particles of a certain density as a result of their mineral associations. These associated densities are calculated from QEMSCAN data on the -850+212 µm size class.

It thus appears that a good split of high efficiency may provide a good separation for both treated and untreated ore, and that slightly more carbonate gangue may be removed in the floats of the treated material.

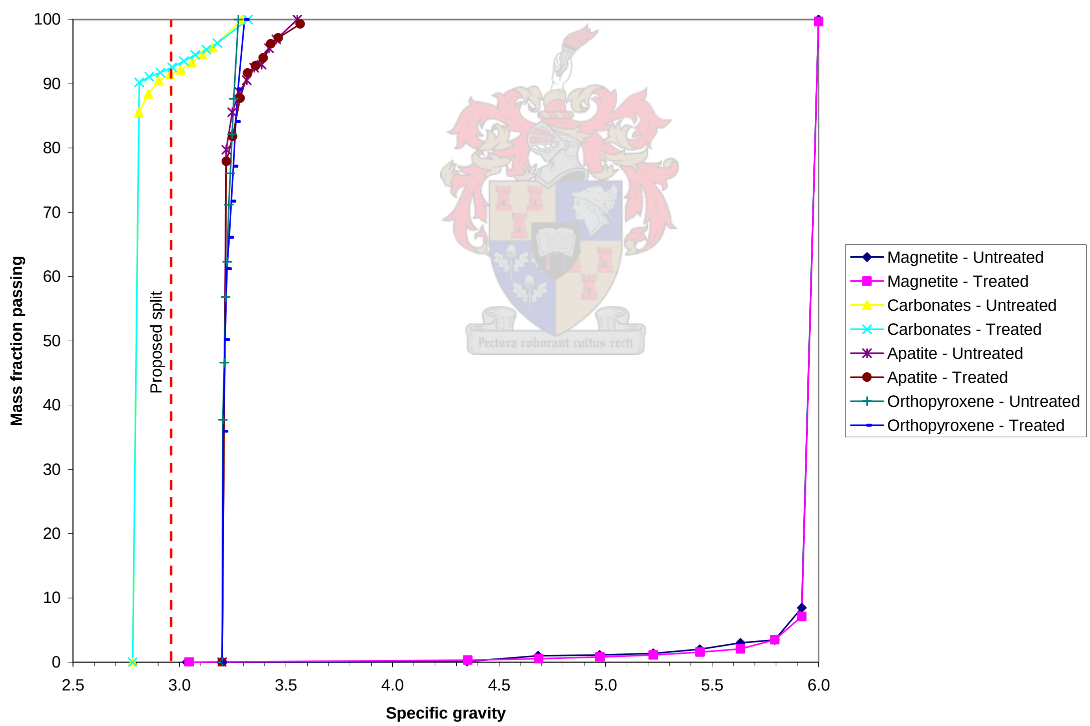

Figure 5.13 - Distribution of major minerals with particle density

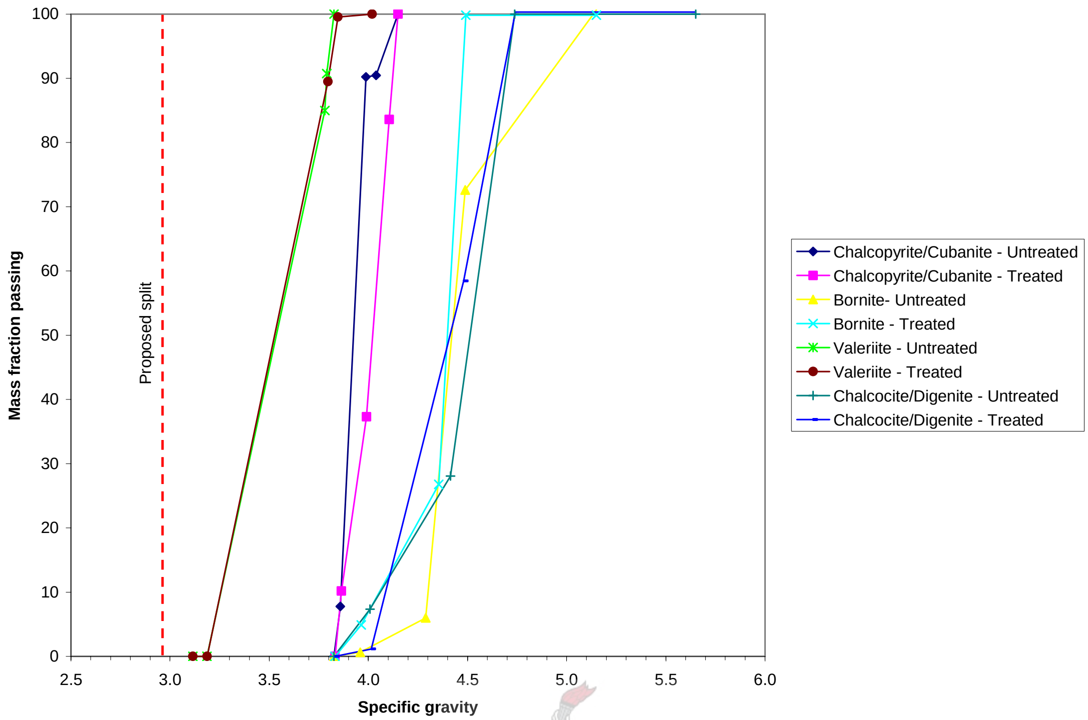

Figure 5.14 - Distribution of copper bearing minerals with particle density

The differences between the data for the treated and untreated ore do appear small, however, and it is likely that the most benefit would come from the higher tonnages of treated ore reporting to the -850+212 µm size class for gravity concentration (see Figure 6.16).

The experimental results obtained from the sink-float testing performed on the -850+212 µm size class are presented in Figure 5.15. There appears to be very little difference between the mass fractions reporting to the floats and sinks in the treated and untreated ore.

One would expect that a different pattern of liberation would result in different particle densities between treated and untreated ore. If this were to occur around minerals which are present in small amounts, such as the copper minerals in this case, not much difference would be seen in the splits. However, selective breakage around minerals which occur in greater quantities in the ore, such as magnetite, would result in more light and heavy particles, with fewer minerals of the middling densities composed of magnetite associated with gangue.

Figure 5.15 - Split between floats and sinks for treated and untreated ore

This result may then indicate one of two things: either the MW treatment of the material has not induced a fracture pattern which is significantly different in terms of selective breakage, or that a more selective breakage pattern is occurring, but that this effect is being hidden as a result of the treatment process chosen up to this point, possibly through over grinding which had been observed.

In an attempt to model the results of the gravity separation, the modal composition and liberation data of the gravity separation feed obtained from QEMSCAN were compared with the elemental assays for the float and sink products from XRF. A model of this nature would allow for the prediction of the split of each mineral between the heavy and light fractions resulting from gravity concentration, based upon the densities of the particles with which these minerals are associated.

By choosing a functional form of an equation for the split between floats and sinks, and by minimizing the sum of the squared errors from these two data sets, the following selection function for displacement of floats to sinks (ρ < 2.967 s.g.) and from sinks to floats (ρ > 2.967 s.g.) for a cut-point of 2.967 s.g. was obtained.

$$S_f = \begin{cases} 0.285 \cdot \exp\left(\dfrac{\rho - 2.967}{0.15}\right) & \rho < 2.967 \\ \\ 0.285 \cdot \exp\left(\dfrac{2.967 - \rho}{1.978}\right) & \rho \geq 2.967 \end{cases} \qquad \textbf{5.1}$$

Figure 5.16 shows the selection function for misplaced material graphically.

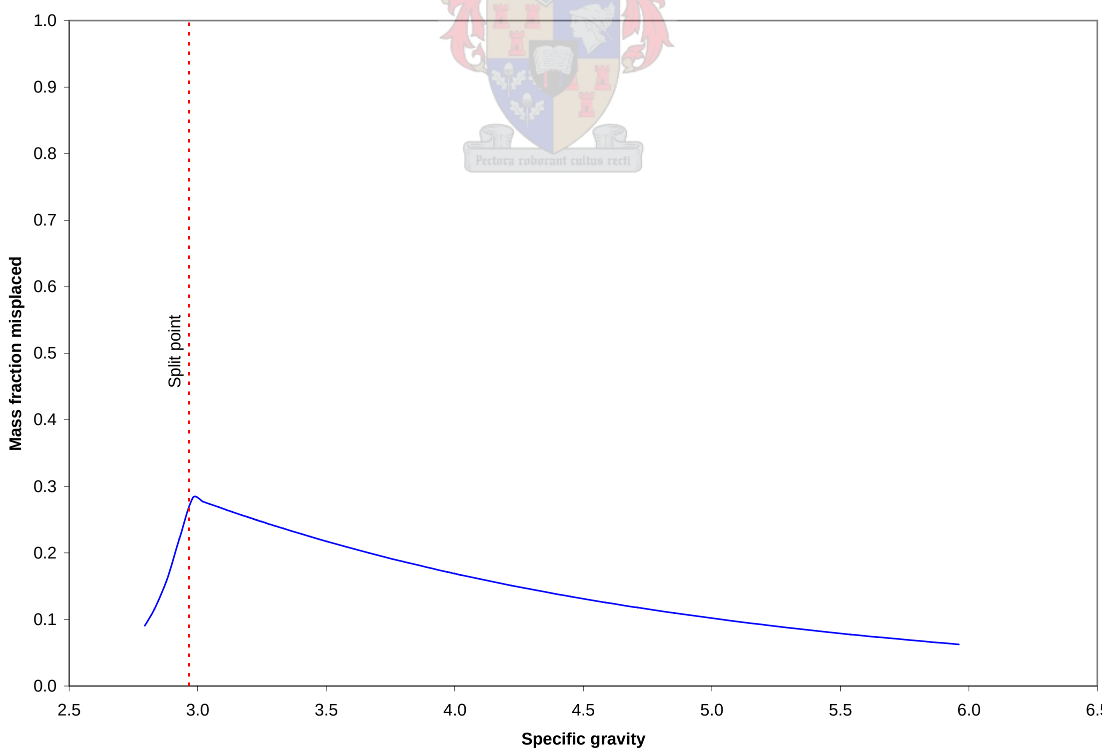

Figure 5.16 - Selection function for gravity separation

The criteria used in this optimization were:

- split masses reporting to the floats and sinks (Table 5.5)
- the distribution of the valuable ore elements iron and copper between floats and sinks (Table 5.6 and Table 5.7)
- the distribution of the primary gangue element calcium between floats and sinks (Table 5.6 and Table 5.7)

Table 5.5 - Split fractions between floats and sinks (split point at s.g. of 2.967)

Material	Floats		Sinks	
	Exp	Model	Exp	Model
Untreated	0.272	0.232	0.728	0.769
Treated	0.265	0.236	0.735	0.761

Table 5.6 - Comparison of experimental and model data for untreated material

Element	Floats		Sinks	
	Exp	Model	Exp	Model
Fe	0.02	0.06	0.98	0.94
Ca	0.67	0.66	0.33	0.34
Cu	0.11	0.17	0.89	0.83

Table 5.7 - Comparison of experimental and model data for treated material

Element	Floats		Sinks	
	Exp	Model	Exp	Model
Fe	0.02	0.06	0.98	0.94
Ca	0.65	0.66	0.35	0.34
Cu	0.11	0.16	0.89	0.84

The minerals used in this analysis comprise around 91% of the total material found in the -850+212 μm size range by mass, and in total, 96.3% of the Cu, 98.3% of the iron and 97.5% of the calcium exists in these minerals, thus supporting the use of this method to determine the selection function for the gravity separation. The majority of the balance of the material is accounted for by mostly the other gangue minerals present, in this case: serpentine, talc, mica, feldspar, amphibole, clinopyroxene and chlorite.

Table 5.8 - Predicted split fractions for all minerals

Mineral	Untreated		Treated	
	Floats	Sinks	Floats	Sinks
Bornite	0.13	0.87	0.14	0.86
Covellite	0.12	0.88	0.12	0.88
Pyrite/Pyrrhotite	0.11	0.89	0.11	0.89
Chalcocite/Digenite	0.14	0.86	0.14	0.86
NiFe-sulfides	0.11	0.89	0.11	0.89
Chalcopyrite/Cubanite	0.17	0.83	0.17	0.83
Valeriite	0.22	0.78	0.22	0.78
Magnetite	0.06	0.94	0.06	0.93
Apatite	0.25	0.75	0.25	0.75
Calcite/Dolomite	0.85	0.15	0.86	0.14
Orthopyroxene	0.25	0.75	0.25	0.75
Amphibole/Clinopyroxene	0.20	0.80	0.20	0.80
Sphalerite	0.14	0.86	0.14	0.86
Chlorite	0.22	0.78	0.21	0.79
Mica	0.24	0.76	0.24	0.76
Serpentine/Talc	0.32	0.68	0.31	0.69
Feldspar	0.30	0.70	0.30	0.70
Gold/Silver	0.07	0.93	0.07	0.93
Barite	0.12	0.88	0.12	0.88
Other	0.50	0.50	0.50	0.50

The predicted split of minerals between sinks and floats using the calculated selection function appears in Table 5.8. The distribution of the unknown material (described as 'other') which comprises around 0.3% of the material in this size range, is assumed to follow a 50/50 split between floats and sinks. It can be seen that there is very little difference between the composition of the material reporting to the floats and sinks for the treated and untreated material, and it can once again be concluded that the main benefit from microwave treatment, to any gravity separation process added to the

Palabora process flowsheet as a preconcentration step, is most likely to come from the slightly higher tonnages of treated material reporting to the size classes which are amenable to gravity separation (refer to Figure 6.16).

This selection function then also allows for an investigation into what effect trying to split at different densities may have on the resulting division of material between floats and sinks.

Since there is a variation in the split point of gravity concentration devices from that obtained in a sink-float analysis, this could now be taken into account by investigating the upper and lower limit of recovery during simulation.

5.6. FLOTATION

5.6.1. EXPERIMENTAL RESULTS

Due to the small quantities (i.e. less than 0.5% of the ore) of floatable minerals present in the low-grade Palabora ore, no meaningful results were produced from the micro-flotation testing (see discussion in section 4.9). Thus, as no flotation results were generated from this work, the flotation data collected by other workers (Sahyoun et al., 2004) on the same ore, and at similar microwave treatment conditions, was used to support any claims made about the possible benefits of microwave pretreatment to the increased recovery of valuable minerals during flotation.

The QEMSCAN analyses on the -212+25 μm size range, however, do indicate changes in the liberation of the copper bearing minerals in this ore after microwave pretreatment. From Figure 5.17, it can be seen that the amount of copper minerals considered to be easily recoverable by flotation (i.e. fully liberated minerals, or minerals attached to other recoverable sulfides) increases significantly by 13.6% for material which has been microwave treated before grinding. These copper minerals include: chalcopyrite, cubanite, bornite, chalcocite, digenite and valeriite (see Table 5.9 for the relative mass fractions of these copper minerals).

Table 5.9 - Copper minerals found in the -212+25 μm size range

Mineral phase	Mass fraction	
	Untreated	Treated
Chalcopyrite/Cubanite	0.52	0.62
Bornite	0.26	0.23
Chalcocite/Digenite	0.05	0.03
Valeriite	0.16	0.13

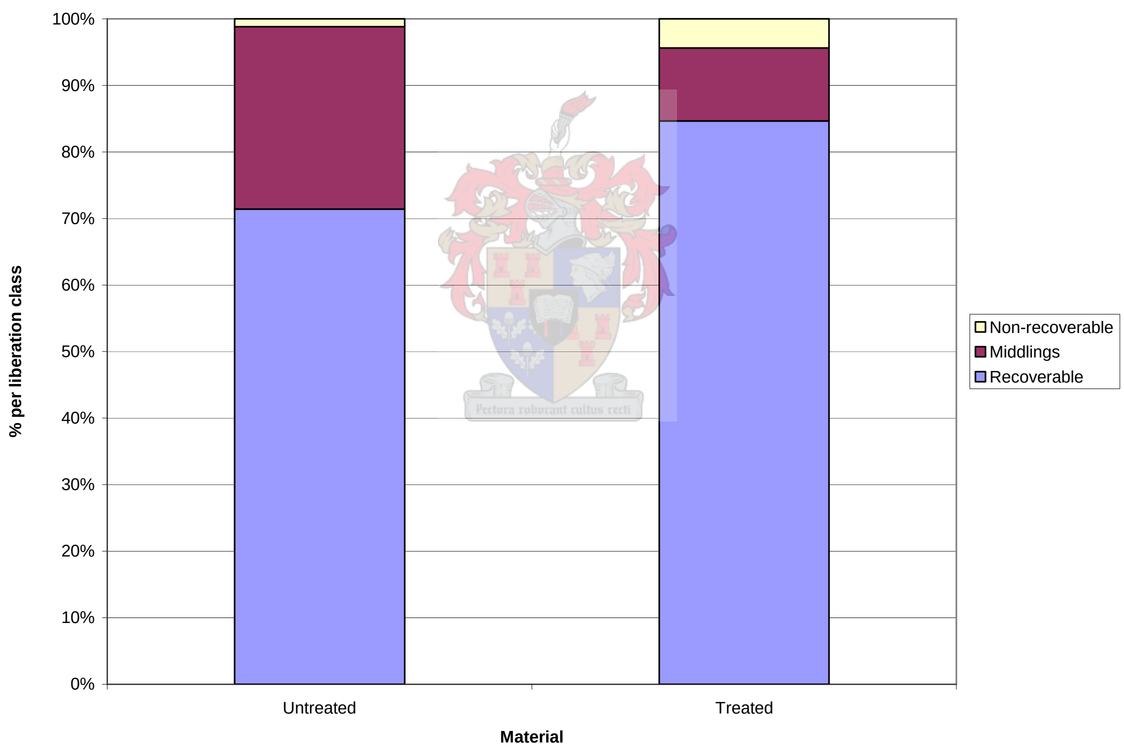

Figure 5.17 - Potential for copper recovery (all copper minerals considered floatable)

The slight increase in locked copper minerals (see Figure 5.17) in material which has been treated can have two possible explanations:

- It is possible that the material has been liberated by the microwave treatment, but that localized hot spots occurring within the absorbing phases results in the sintering of some of the liberated minerals back onto the gangue.
- Due to the small samples used in the QEMSCAN analysis, it is also possible that this is scatter in the observed data.

Since the total amount of locked copper minerals in both the treated and untreated material is relatively small, and since the difference in the amount of locked material between the two is only 2.7%, it is likely that this will not impact much on the increased recovery after microwave pretreatment, given the much higher increase in the amount of liberated valuable minerals in the treated ore.

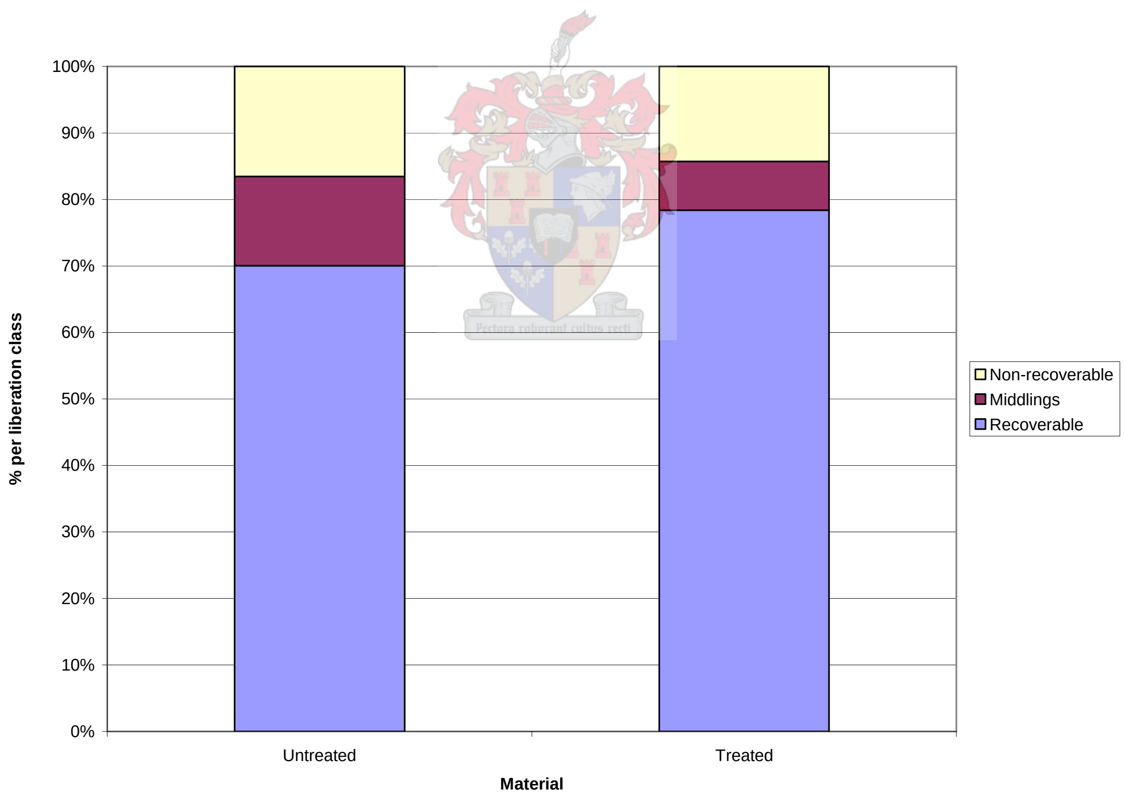

Figure 5.18 - Potential for copper recovery (valeriite not considered floatable)

While valeriite itself is not easily recovered by flotation, 97.5% of the valeriite in the untreated material, and all the valeriite in the treated material, is attached to other sulfides which are readily floatable.

Thus, even for the worst case scenario where all the valeriite is considered to be non-recoverable, the ideal flotation recovery of copper minerals at this grind size would still increase by 8.4% (Figure 5.18).

From the comparison of the QEMSCAN data for microwave treated and untreated material in this size range, it is concluded that microwave pretreatment significantly increases the liberation (which in turn directly influences the recovery) of valuable minerals in the size range associated with the selective recovery process of flotation.

5.6.2. FLOTATION DATA TO BE USED IN THE ECONOMIC ANALYSIS

Since no conclusive experimental results were obtained to quantify the effects of microwave treatment on the flotation of the ore used in this work, the known recoveries from the existing Palabora flowsheet will be used in any calculations involving the untreated material.

Plant data shows that 82.72% of the copper sent to flotation is recovered in the concentrate stream. If we assume that all the material considered as 'recoverable' will float, then we can determine what proportion of the middlings fraction in the untreated material can also be recovered. If we further assume that the same proportion of middlings in the treated material will also float, the total recovery of minerals from the flotation circuit after microwave treatment can be estimated as well.

Table 5.10 shows the estimated copper recovery (from the liberation data obtained by QEMSCAN) given the case of all the copper minerals being floatable, and also the case of valeriite being considered unrecoverable. This gives the probable range for the copper recovery after microwave treatment, which then lies between 84.98% and 89.43%.

Table 5.10 - Estimated recoveries of copper minerals from flotation

Minerals considered floatable	Recovery (%)	
	Untreated	Treated
All copper minerals	82.72	89.43
Not including valeriite	82.72	84.98

The independent batch flotation work performed by Sahyoun et al., 2004, on Palabora ore treated at 10 kW for 0.5 seconds in the same cavity used to treat the material in this work, showed an increase in final recovery of copper from 81% for the untreated material, to 88% after microwave treatment. These values then correspond well to the first case in which much of the valeriite is recoverable by association with other sulfides, and also to the actual plant recovery for untreated ore. A conservative value of 88% in recovery will be used for any calculations involving treated material.

Plant data from Palabora shows the recovery of copper with particle size (Figure 5.19). It can be seen that the recovery peaks at a particle size of around 45 μm. Below this particle size, the recovery begins to drop off again.

This means that if the feed to the flotation circuit includes a greater amount of -45 μm material, the recovery of copper will likely drop. Care will be taken when designing the process flowsheets to ensure that over grinding does not occur, especially when dealing with the softer microwave treated ore.

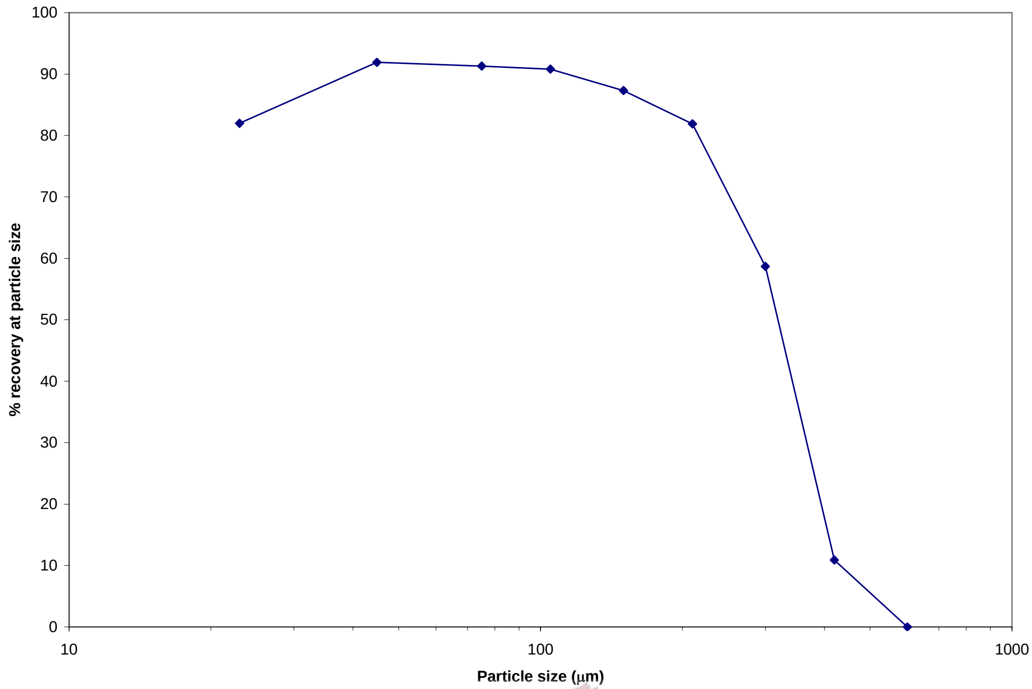

Figure 5.19 - Recovery of copper with particle size at Palabora

6. FLOWSHEET SIMULATION

In order to investigate the impact of microwave pretreatment on a process flowsheet, the milling section employed by Palabora was modelled with the aim of determining what changes occurred in the milling circuit performance in terms of grind size and possible increases in throughput. These investigations were performed using the flowsheet simulation package MODSIM. The downstream benefits of any such changes in milling performance on mineral recovery and plant profitability were also investigated (refer to section 7).

By first modelling and simulating the performance of each individual item in the flowsheet (see Figure 6.4 for a representation of the milling section), using the known feed and product size distributions, tonnages and in some cases the actual equipment dimensions, provided by Palabora Mining Company, it was possible to determine the model parameters required by the simulator to describe the working of each. This was done by varying the unknown parameters in the equipment model and minimizing the error between the model prediction and the actual plant data for each item of equipment (see APPENDIX C for the model parameters used in the simulations).

The breakage parameters used to describe the rod milling behaviour of the ore (which were developed in section 5.4), before and after microwave treatment, were incorporated into the rod mill model in MODSIM and tested against the plant data. After these initial investigations, it was found that by retaining the breakage parameter values as they are before scale-up (see Table 6.1), and varying the residence times for the rod mill and the variation of particle speed through the mill with size, very good fits between the product size distributions from the simulations and the actual plant data could be obtained (see Figure 6.2).

Table 6.1 - Parameters used for modelling of the rod mill in simulations

Material	S_1	α	μ	λ	ϕ_{5mm}	γ	β	δ
Untreated	0.2890	0.5254	13.2808	0.6901	0.3920	0.9960	0.7360	0.5180
Treated	1.0880	1.0038	1.4469	1.1492	0.3920	0.9960	0.7360	0.5180

For the two cyclones, Palabora reported most of the data required for accurate modelling of the equipment (including most of the important equipment dimensions) and very few parameters needed to be varied in these initial simulations in order to achieve the same separations as the plant.

For the modelling of the two ball mills, the known model parameters (such as the residence time in the mills) were input into the simulator models. Since little was known about the breakage and selection functions required to model the ball milling of the ore, an approach similar to that used for obtaining these parameters for rod milling was used. Starting from the known grinding parameters for a copper ore given by MODSIM, and then varying these breakage parameters until the error between the model predictions and actual plant data were minimized, it was possible to arrive at a set of pseudo-parameters, similar to those obtained for the rod mill, which could be used to describe the performance of the two ball mills in the milling circuit.

An important aspect of the modelling concerned the grinding energy savings brought about by the microwave pretreatment of the ore. As this is related to the hold-up in the mills, which in turn will affect the power draw, it was necessary to determine how accurate the calculations of the mill hold-up were, in order to ensure accurate predictions of energy savings. Palabora reports the charge of media in their mills as follows:

- Rod mill charged with 116 tons of media
- Ball mills charged with 80 tons of media

Since no information was supplied as to the ratio of media to ore, it was assumed that around 20% of the total charge in the rod mill, and around 35% of the total charge in each of the ball mills would be ore. This assumption would mean that the rod mill is charged with 29 tons of ore, and the ball mills with around 43 tons of ore.

The hold ups calculated by the simulator were:

- Rod mill hold up of 22 tons
- First ball mill hold up of 38 tons
- Second ball mill hold up of 43 tons

The deviations of the model hold ups from the plant data (around 24% for the rod mill and 11% for the first ball mill) will mean that the direct energy costs of milling calculated from the simulations will be slightly lower than those of the actual plant. Simple calculations show that the total energy consumption of the three mills will be under-predicted by between around 14% and 18%, thus any results in terms of energy savings from the model will also be under-predicted and can therefore be considered conservative estimates for the plant.

However, since the energy savings calculated will be between two models of the plant using the calculated hold-ups, this will not be of concern there. Once these values are converted to values of percent savings between treated and untreated material, these values can be used with reasonable accuracy in cost estimations on the actual plant itself.

In terms of grinding media consumption, the differences in hold-up will have no effect as the values are calculated from the actual tonnages milled.

The work index provided by Palabora for rod milling was 13.5 kWh/t, and this value was used for simulations involving the untreated material. This was considered a reasonable assumption as the composition of the ore being milled does vary with time and the composition as measured for the ore used in our test work would not be fully representative of the bulk properties of that processed at Palabora.

It was also necessary to obtain a value of the work index for the treated ore, which reflected the effect of a reduction in ore strength on the power required for milling. Simulations were run using the breakage parameters for the treated material to determine what grinding time and throughput provided the same 80% passing product size, and the same hold-up, as was achieved for the untreated material (see APPENDIX B). Equating the power requirements for these two situations then allowed for the calculation of the work index for the treated ore, based on the known value of the work index for the untreated ore supplied by Palabora. A value of 5.29 kWh/t (39% of the work index for the untreated ore) was obtained, and this value was to be used in the simulations to follow.

It was assumed that by the time the material is ground to the sizes associated with the ball milling section, all the fractures which had been induced by the microwave treatment would have been exploited. Under these circumstances, the same breakage parameters can be used for both treated and untreated ore. Palabora Mining Company also reported a work index of 12 kWh/t for both ball mills in the milling circuit.

For the energy input of the microwave treatment, an efficiency of 90% in the conversion of electrical power into microwave power was assumed. This meant that to supply the 1.46 kWh/t of energy used in the process, an electrical energy input of 1.62 kWh/t was required.

The parameters used for each item in the flowsheet during simulation, are listed in APPENDIX C. These could then be used to investigate what effect microwave treatment could have on the flowsheet.

6.1. EXISTING FLOWSHEET

6.1.1. PRESENT OPERATION

Following from the work performed in the first part of section 6, it became possible to model the existing conventional milling flowsheet (Figure 6.1) used at Palabora, by using the model parameters listed in APPENDIX C.1 in the flowsheet simulator MODSIM.

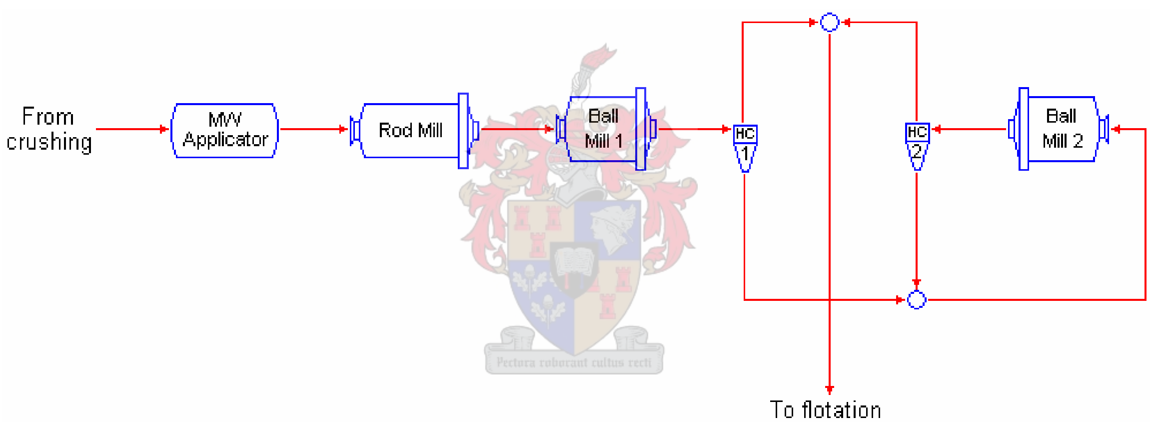

Figure 6.1 - Existing Palabora milling circuit with the addition of microwave pretreatment

The resulting size distributions of the material sent to flotation (Figure 6.2) shows that the model slightly over-predicts the grinding at the larger sizes, and under predicts the grinding at smaller sizes. This similarity between plant data and model predictions is sufficient to draw conclusions made from the simulations back to the plant with only slight error, and since the comparisons between the treated and untreated material is not reliant on the actual plant data at all, this will not be of concern there.

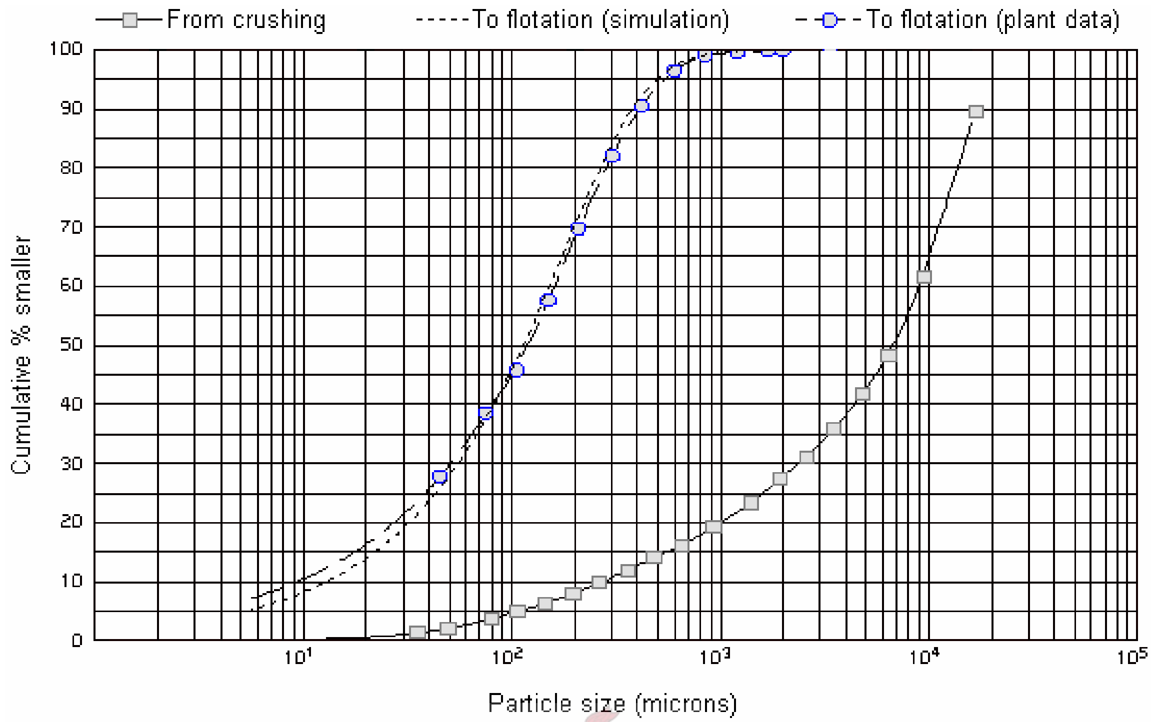

Figure 6.2 - Comparison of material sent to flotation from model simulations and plant data

Two cases were investigated for the existing plant, to observe what effects microwave treatment can have on grind size for the same mill throughputs, and what effect can be seen on the same final grind size to flotation by increasing the throughput.

6.1.2. MICROWAVE TREATMENT

For this investigation, the same circuit parameters were used as for the untreated case, with the only exception being that the breakage and selection parameters, used to describe the behaviour of the ore during rod milling, were changed to reflect the differences between microwave treated and untreated ores which were observed during our grinding experiments (refer to section 5.4).

Initial simulations showed that this caused the 80% passing size of the material sent to the flotation section to decrease from 277 µm to 210 µm, though more fine material was produced. At the same time, the circulating load over the second hydrocyclone (and thus through the second mill) increased slightly from 249% to 253%. It is known that increasing the circulating load decreases the production of fine material by preventing over grinding (JKMRC, 1999). Since a lower tonnage passes through the second mill after microwave treatment of the ore, scope exists for optimizing the plant operations by raising the circulation ratio further to provide a flotation feed containing less fine material.

The plant parameters were then optimized to produce the same size distribution of material in the flotation feed as for the untreated case

6.1.3. EFFECT OF INCREASED THROUGHPUT ON FLOTATION FEED

A series of simulations were run to investigate the minimum 80% passing grind size achievable at a given throughput after microwave pretreatment. At the same time, the corresponding maximum 20% passing grind size associated with these 80% passing sizes were produced (Figure 6.3).

This was achieved by ensuring that the hold-up in each mill was kept the same as for the untreated case, thus ensuring the finest grind possible without overloading the capacity of any of the mills.

Figure 6.3 also shows the recovery of copper with particle size as was measured by Palabora Mining Company at their plant after flotation. It can be seen that any extra production of fines will lead to increased copper losses. Using the current 20% passing size sent to flotation in the Palabora plant as the design target, it can be seen that after microwave pretreatment it is theoretically possible to increase the amount of material processed in each milling circuit from 388 t/h to around 565 t/h, a significant increase in throughput of 46%, while not violating the required 80% passing size of the flotation feed.

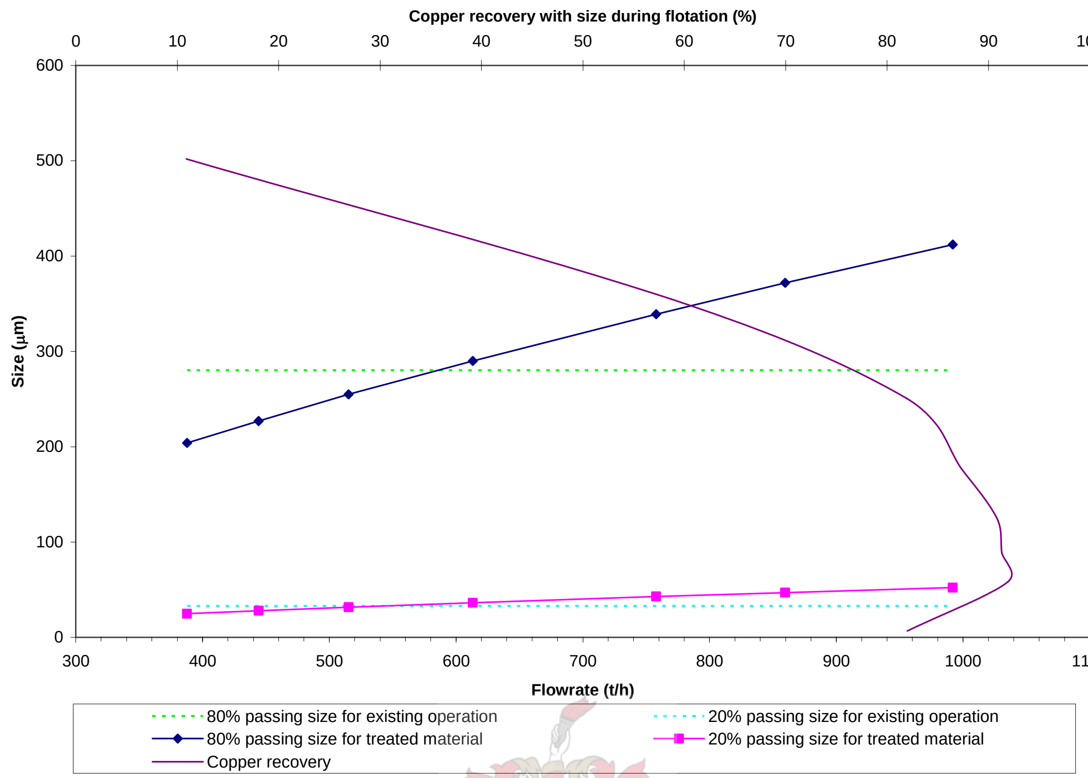

Figure 6.3 - Limitations on grind size with throughput for the existing plant flowsheet

Since Figure 6.3 shows the maximum grinds possible at each flowrate, it should be obvious that the circuit parameters can be changed to optimize the grind to a suitable size at any throughput lower than this value.

6.1.4. 10% INCREASE IN THROUGHPUT AT THE SAME FINAL GRIND SIZE

From an investigation of the flowsheet, it was found that the major limitation in terms of throughput would be on the slurry pumps feeding the material to the first of the two hydrocyclones, both of which have a diameter of 27” (686 mm). For the first hydrocyclone, a feed pressure of around 6 m of slurry is required for correct operation at the current plant flowrate of 306 m^3/h (Ruhmer, 1991). Assuming an increase of 10% in throughput means that the pump feeding the first hydrocyclone would be required to handle a head of around 6.7 m of pulp. This was assumed to be reasonable and the effect of a 10% increase in throughput, with the same final grind size of material sent to flotation, on the energy and grinding media consumption in the milling circuit was investigated.

The grinding time in the rod mill was reduced to achieve the same hold-up as for the untreated material, while the grinding times in both the ball mills were reduced until the same grind size could be achieved.

Figure 6.4 summarize the flowrates and the 20%, 50% and 80% passing sizes for the simulations of the treated and untreated material at the same throughput, and also of the treated material at the increased throughput, on the existing Palabora flowsheet. Figure 6.5 shows the associated energy and grinding media consumption per ton of ore treated for each item in the flowsheet, as well as the corresponding consumption per ton of feed to the milling circuit.

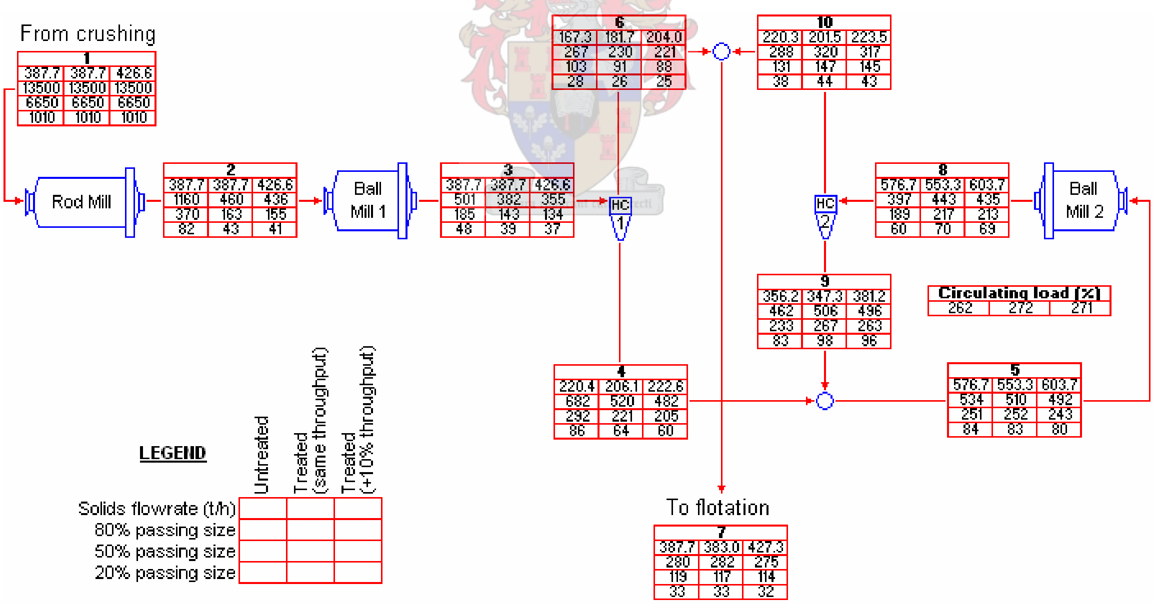

Figure 6.4 - Results obtained for various simulations of the existing flowsheet

The energy consumptions are predicted by the simulator itself, and are represented as a power factor which is multiplied by the work index of the ore to obtain the value in kWh/t. To convert these values to a consumption per ton of feed to the rod mill, the total energy consumption is divided by the flowrate to the rod mill.

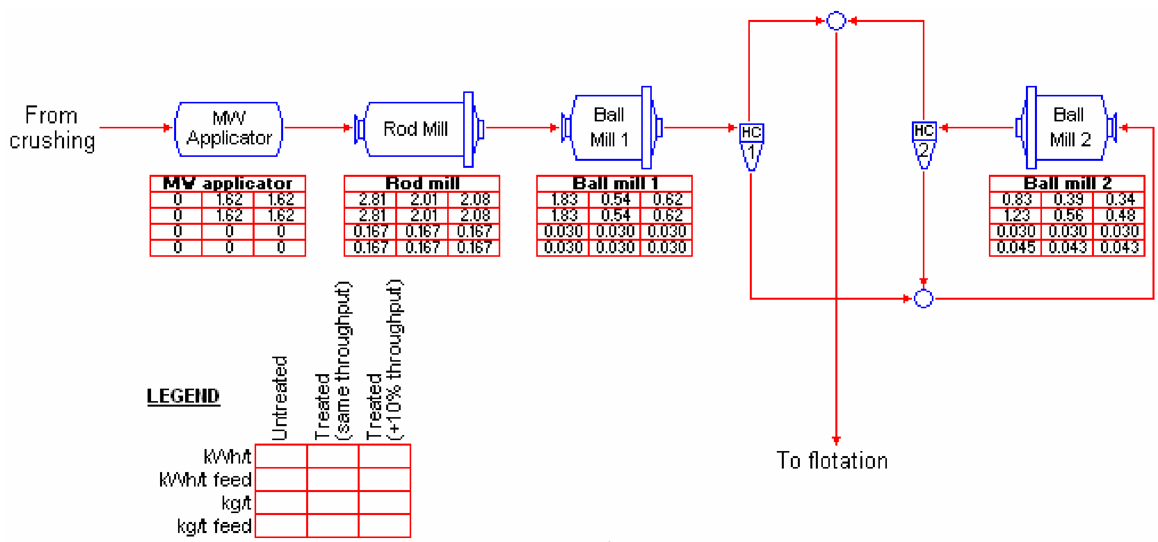

Figure 6.5 - Energy and steel usage obtained for various simulations of existing flowsheet

The grinding media consumptions obtained from the Palabora data were presented in the form of kg/t ore milled and these are the values which appear in Figure 6.8. For the calculation of the media consumption per ton of feed, the total media consumption is divided by the flowrate to the rod mill.

Table 6.2 summarizes the energy input (including microwave energy) per ton of ore fed to the milling circuit required to produce the feed to the flotation section for each of the three cases investigated. It should be noted that energy requirements for material conveying and pumping are not included, and will change with production rates. In comparison to the cost of grinding, however, these costs will be small. The grinding media consumption per ton of ore fed to the milling circuit is also summarized.

It can be seen that a reduction of 19% in energy usage per ton of feed (in the milling section) is possible from the most simple case of microwave treating the rod mill feed and then processing the material to produce the same final size distribution as for the untreated material. At the same time a small benefit in terms of a reduction in the use of grinding media is also predicted. The impact of these reductions in energy and grinding media consumption on the economics of the plant operation are studied in section 7.

Table 6.2 - Energy and grinding media used to produce feed to flotation in existing flowsheet

Treatment	Energy consumption	Consumption of grinding media
	kWh/t feed	kg/t feed
Untreated	5.86	0.242
Treated (same throughput)	4.73	0.240
Treated (+10% throughput)	4.81	0.240

Perhaps the most interesting result is that of the last case investigated. Even with a 10% increase in throughput, by making better use of the advantages created by the softer ore throughout the flowsheet, it is possible to produce the same grind size of the feed to the flotation circuit (Figure 6.4), while not exceeding the capacities of any of the mills or the hydrocyclones, and doing so with a reduction in energy usage per ton of ore fed to the milling circuit of 18%. Once again, a small reduction in the loss of grinding media is predicted. This possible increase in throughput, coupled with the reductions in energy and grinding media consumption which are still possible at this increased throughput, leads to a significant increase in the profitability of the plant (see section 7).

6.2. PROPOSED FLOWSHEET

Several simulations were then performed with the inclusion of a gravity separation circuit after the rod mill, in an attempt to remove some of the gangue before further grinding takes place (see Figure 6.6). The optimization of the circuits followed the same procedures as for the simulations of the existing plant.

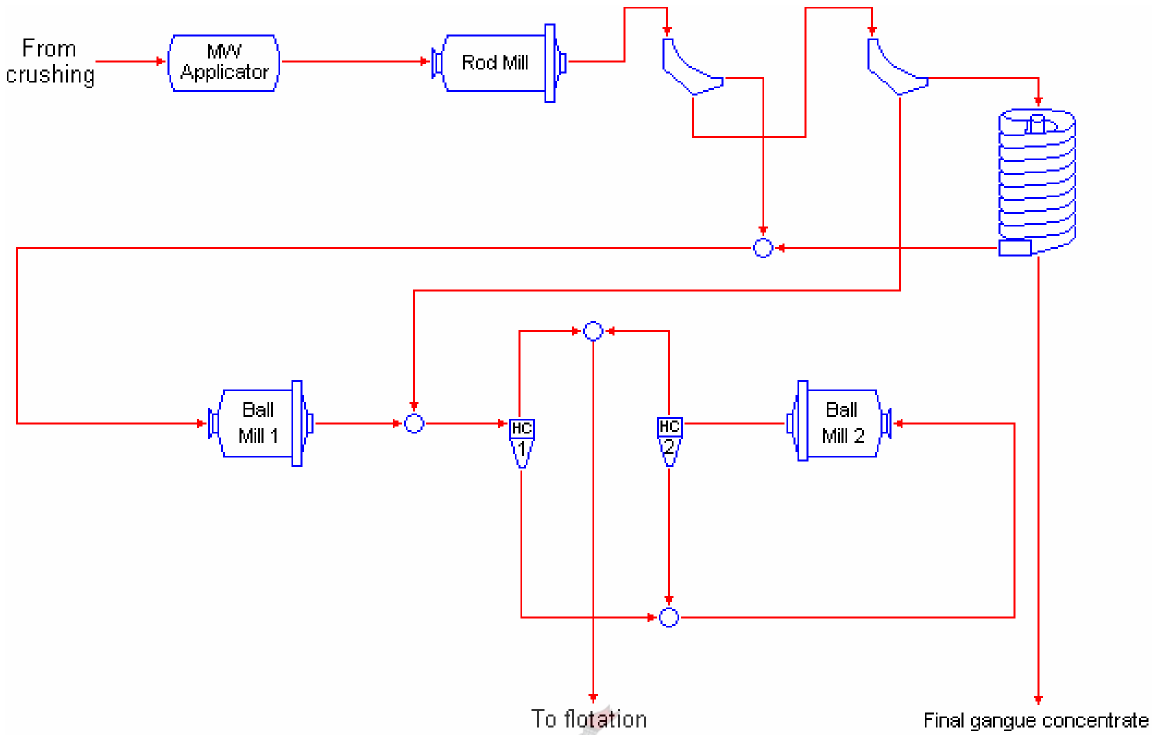

Figure 6.6 - Proposed Palabora flowsheet with gravity separation and microwave pretreatment

Since there would now be less soft gangue material being treated in the ball mills, it can be expected that the work index for these mills will increase. From the known mass, composition and work indices of the material lost to the gravity separation tails and recovered in the gravity separation concentrate, a new work index of 12.1 kWh/t was calculated for the material which would now be fed to the ball mills.

6.2.1. THE EFFECT OF DIFFERENT SEPARATION DENSITIES

Since it is known that the density of separation for spirals can deviate from the theoretical mean density determined in the sink-float testing by between 0.1 kg/dm^3 and 0.15 kg/dm^3 (Burt, 1984), it was decided to determine what effect a variation in the separation density would have on the proposed flowsheet.

Three case studies each for both the treated and untreated material were undertaken using separation densities of:

- 2.817 s.g. (lower boundary of deviation from theoretical mean)
- 2.967 s.g. (theoretical mean density of separation)
- 3.117 s.g. (upper boundary of deviation from theoretical mean)

To ensure that a comparison could be drawn between these simulations, the parameters of the equipment in the milling circuit were varied until the same 80% passing size in the flotation feed were obtained. The most important changes took place in the rod mill, where shorter residence times were used for the treated cases to ensure that the material was not ground too fine before the next stage of milling. The parameters used to model the individual items of equipment in the proposed flowsheet appear in APPENDIX C.2.

Table 6.3 summarizes the energy and grinding media consumption associated with splitting the material sent to gravity concentration at different separation densities. It can be seen that there is no difference in terms of savings in energy, and only slight savings of media, for the various splits The most notable differences apparent seem to be brought about by the microwave treatment itself, with a small reduction in energy use of 2.2%.

Table 6.3 - Energy and grinding media consumption at different separation densities

Treatment	Energy consumption	Consumption of grinding media
	kWh/t feed	kg/t feed
Untreated (split at 2.817 s.g.)	4.01	0.232
Untreated (split at 2.967 s.g.)	4.01	0.232
Untreated (split at 3.117 s.g.)	4.01	0.231
Treated (split at 2.817 s.g.)	3.92	0.233
Treated (split at 2.967 s.g.)	3.92	0.232
Treated (split at 3.117 s.g.)	3.92	0.231

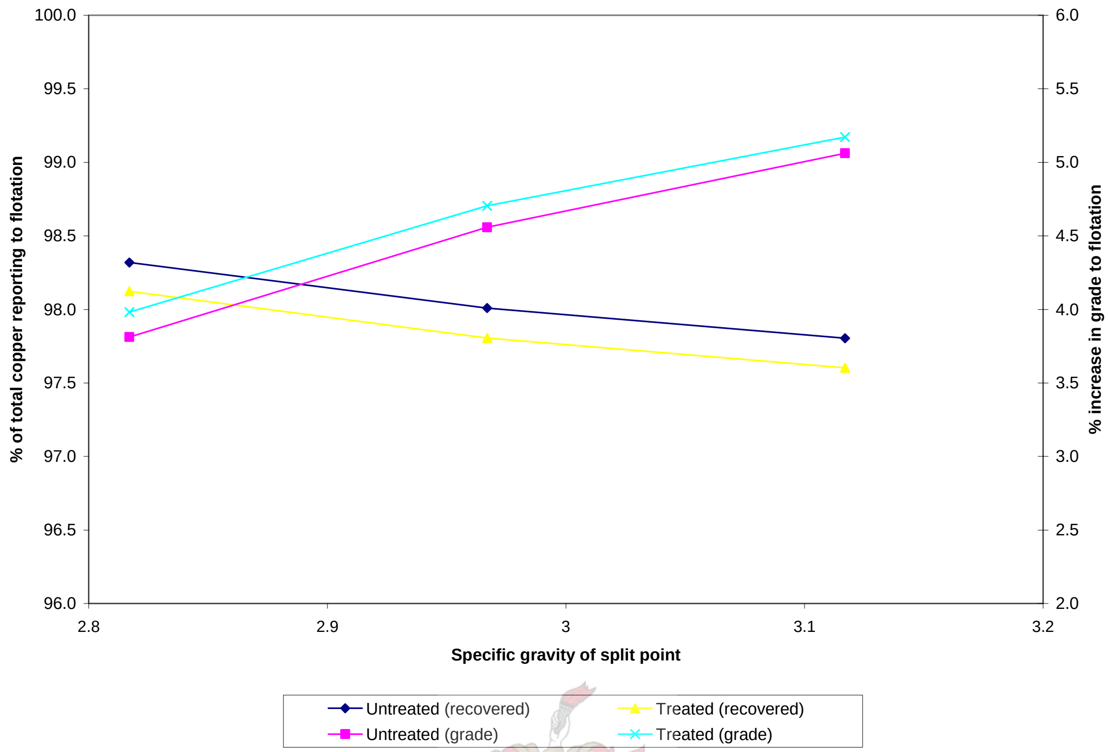

Figure 6.7 - Grade and recovery of copper in the flotation feed

It thus appears that the most important consideration, if any, between the different splits will be the effect on the grade of the material sent to flotation, and the total amount of valuable mineral lost in the gravity concentration tails.

Figure 6.7 shows the grade of the flotation feed, as well as the percent of the original copper in the rod mill feed reporting to the flotation circuit. It can be seen that while the grade of the microwave treated ore reporting to flotation is slightly higher than that of the untreated ore, a larger amount of the original copper is lost in the gravity separation tails.

This is due to the efficiency of gravity separation processes, where a certain amount of material is incorrectly classified, regardless of its density. While there is a slight increase in the liberation of copper minerals in the -850+212 μm size range with microwave treatment, more or less the same fraction of copper is misplaced to the floats for treated and untreated material. Since there is more copper reporting to the larger size classes in the treated material, the total amount of copper lost in this fashion therefore also increases.

The amount of copper lost also increases with a higher separation density. The associated increase in grade, even though there is more copper lost, is due to the greater amount of gangue removed in the gravity concentrate tails (see Figure 6.9).

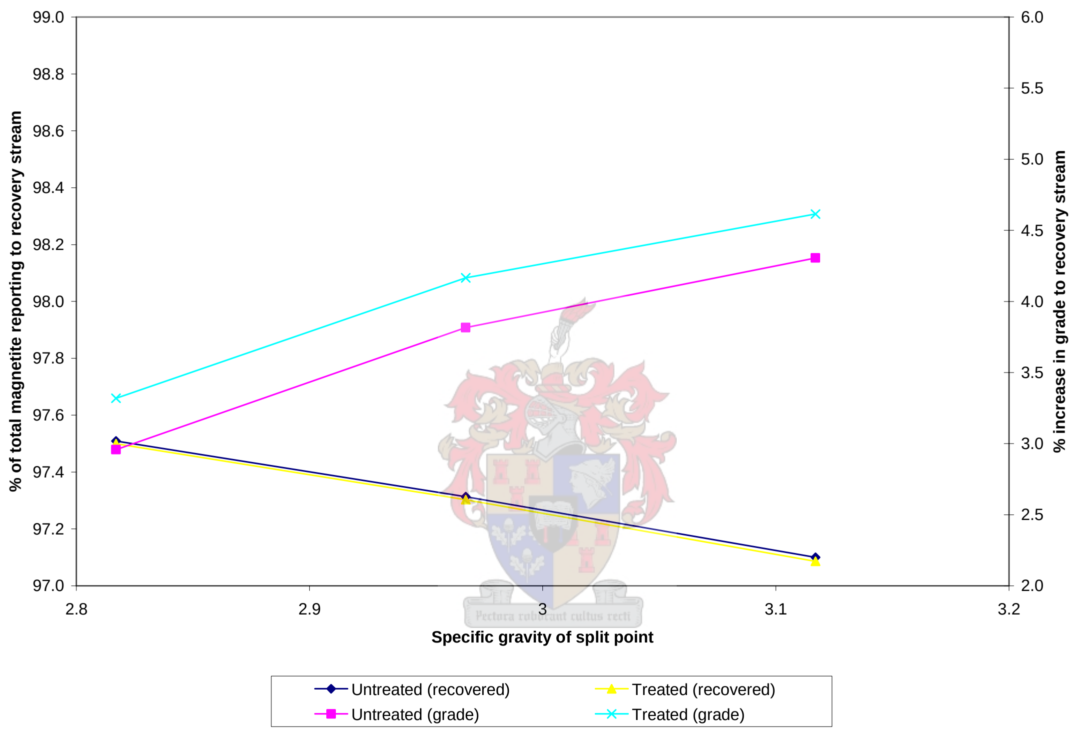

Figure 6.8 - Grade and recovery of magnetite in the flotation feed

If we look at the grade and recovery of magnetite to the flotation circuit (Figure 6.8), we see that while there is not much difference in the amount of material reporting to the flotation feed (the magnetite is later recovered through magnetic separation from the flotation tails and is thus an important mineral), the grade of the magnetite is higher after microwave pretreatment.

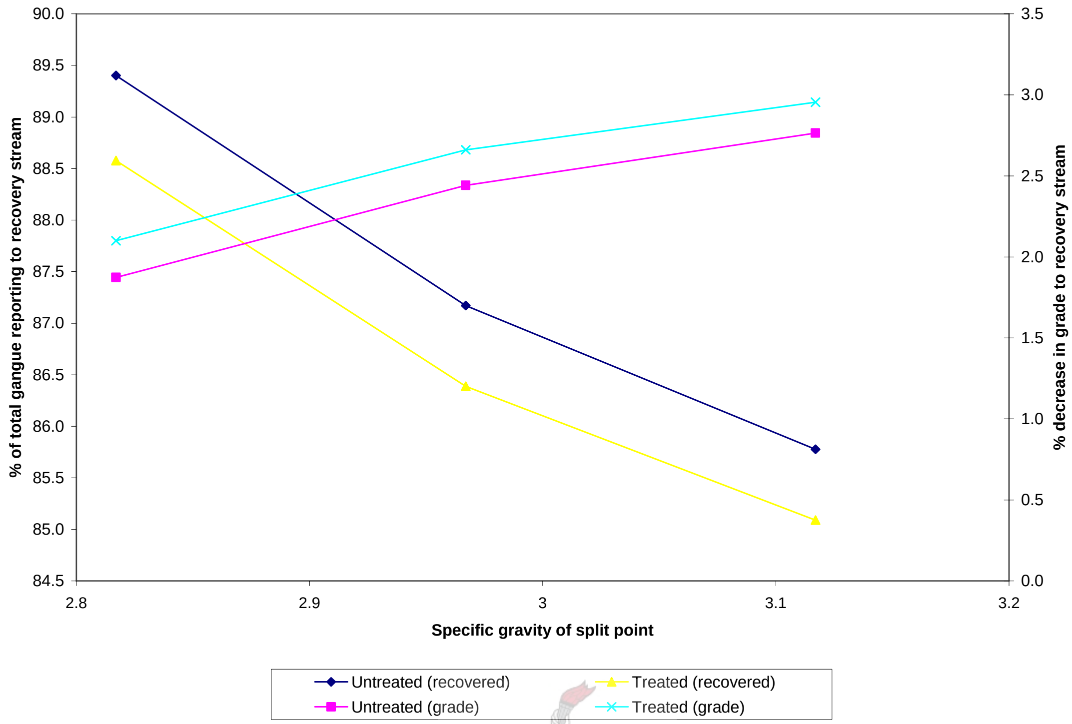

__**Figure 6.9 - Grade and recovery of gangue in the flotation feed**__

A similar comparison for the gangue material (Figure 6.9) shows that more gangue is removed during gravity separation after microwave treatment. It should be recalled that the gangue also consists of some minerals which can poison and complicate the flotation process (e.g. sphalerite). The removal of a larger amount of this material with microwave treatment will also benefit flotation, though this benefit is not at present quantifiable.

It is also reported by Palabora that the presence of numerous dolorite dykes which cut through the ore body causes severe decreases in grinding performance due the extremely high work index of the material, and its tendency to thus displace material from the mills and build up high circulating loads in the milling circuit. Even during times where the presence of dolorite is not a factor, the large amount of gangue removed should still be of significance to the present ore body being processed.

It is seen that by increasing the separation density to 3.117 s.g., up to 15% of the total gangue in the rod mill product can be removed before further grinding in the ball milling circuit.

6.2.2. MAXIMUM GRINDS AT VARIOUS DENSITIES

Similar to that done for the existing plant flowsheet, a series of simulations were then run to investigate the minimum 80% passing grind size achievable at a given throughput after microwave pretreatment. At the same time, the maximum 20% passing grind size associated with these 80% passing sizes were produced (Figure 6.10).

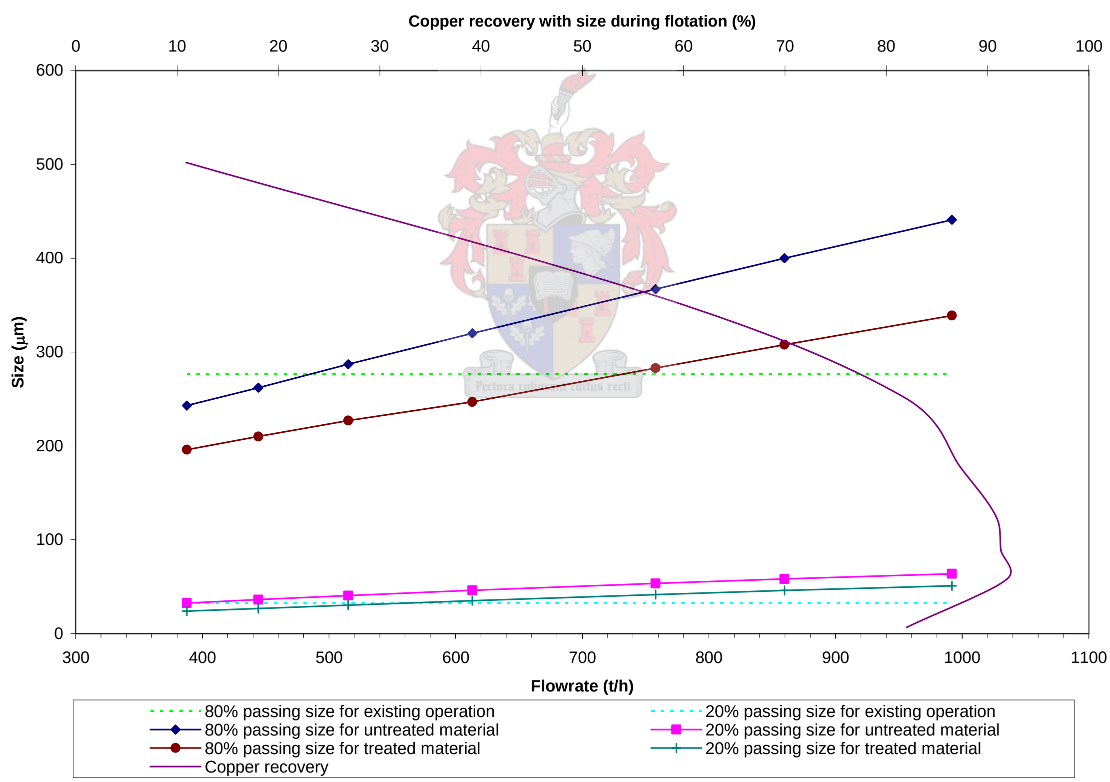

Figure 6.10 - Limitations on grind size with throughput for the proposed plant flowsheet

From the current 20% passing size sent to flotation in the Palabora plant, it can be seen that it is theoretically possible to increase the amount of material processed in each milling circuit to around 565 t/h after microwave treatment and the inclusion of a gravity concentration circuit. While this is the same maximum theoretical throughput as for microwaved material on the existing plant, the 80% passing size at this throughput decreases significantly to around 237 µm (with an associated copper recovery at this size class of around 85%), thus placing more material in the higher copper recovery zones prior to being sent to the flotation section.

Any effect caused by the inclusion of the gravity separation section, will be governed by the amount of material reporting to it. Due to the changes in the size distributions of the rod mill product with increased throughput and shorter residence times, different amounts of material are produced in the -850+212 µm size range and report to gravity separation (Figure 6.11).

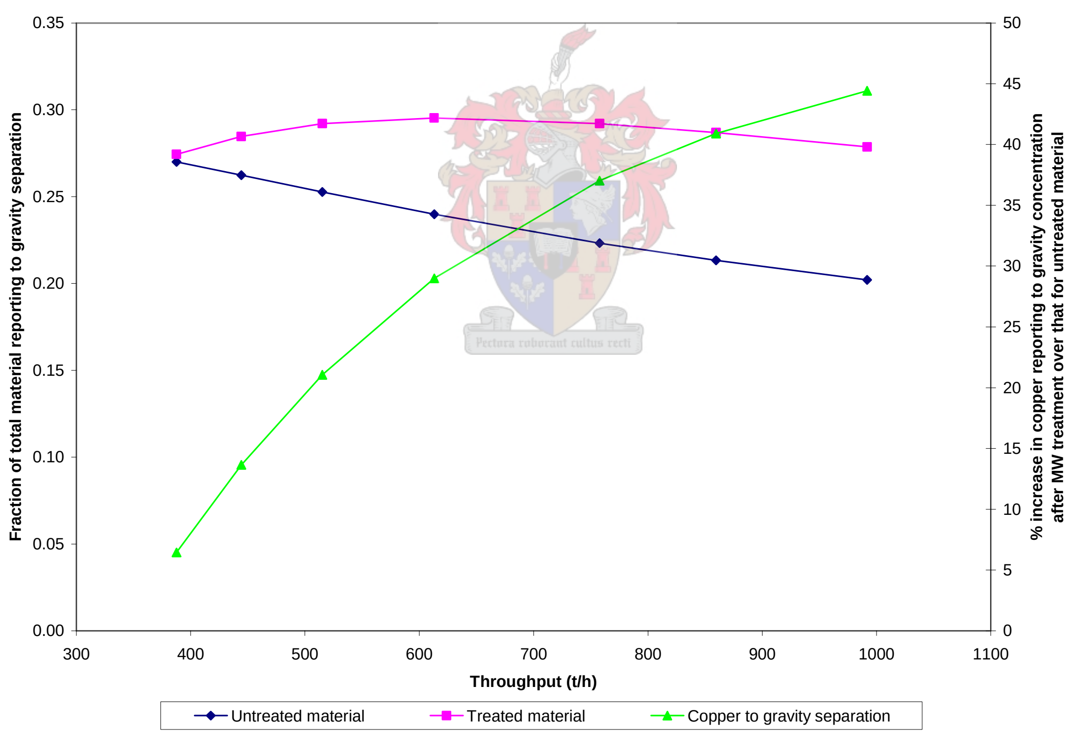

Figure 6.11 - Fraction of material reporting to gravity separation

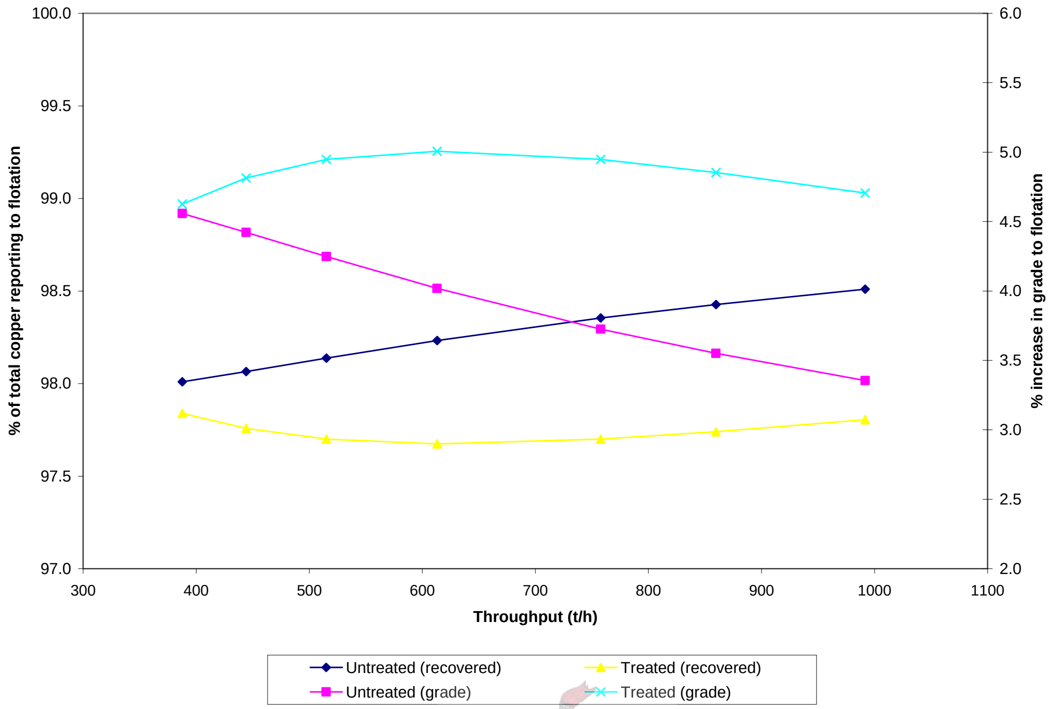

Figure 6.12 - Statistics for copper reporting to flotation

From Figure 6.12 it can be seen that the treated material has higher grades and lower recoveries of copper reporting to the flotation feed than the untreated material, for all throughputs. Further, it is seen that for the treated material, the maximum increase in grade of about 5% is accompanied by a loss of around 2.3% of the total copper in the rod mill feed to the gravity concentration tails, while the untreated material has a maximum grade increase of 4.6% with an associated loss of 2% of the total copper to the gravity separation tails. The implications of this result on the economics of the plant operation are explored in section 7.

This difference in recovery is explained by the larger amount of copper reporting to the gravity concentration circuit after microwave treatment (see Figure 6.11). Due to the inefficiencies associated with the gravity concentration process, there is thus more chance of copper being misplaced to the gravity concentration tails and being lost in the treated material.

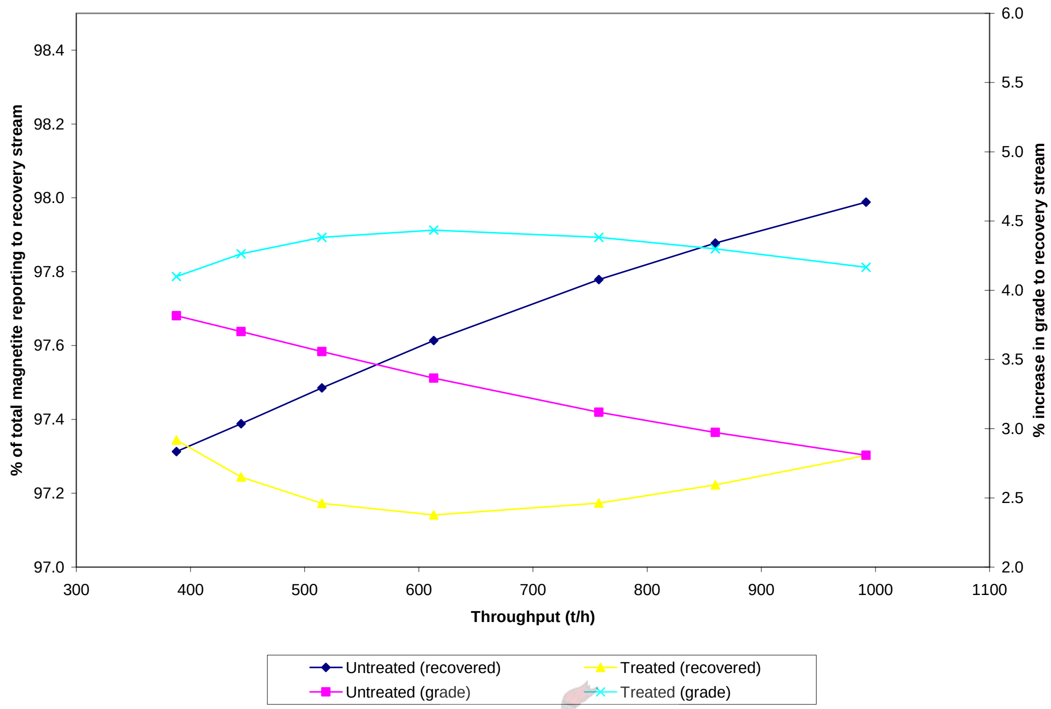

Figure 6.13 - Statistics for magnetite reporting to flotation

Since the copper is present in such small quantities, any amount of misplaced material can be detrimental to the final copper recovery after flotation, as can be seen from Figure 6.12.

Figure 6.13 and Figure 6.14 show the statistics for magnetite and gangue reporting to the recovery stream (i.e. flotation feed) respectively.

Calculations show that the amount of magnetite reporting to the gravity concentration circuit in the -850+212 μm class decreases after microwave treatment by 2.1%, while the amount of gangue increases by 1.6%. This is most likely due to the difference in the effects of microwave treatment on the strengths of these minerals. It would thus appear that the gangue material is weakened more by the microwave treatment than the magnetite.

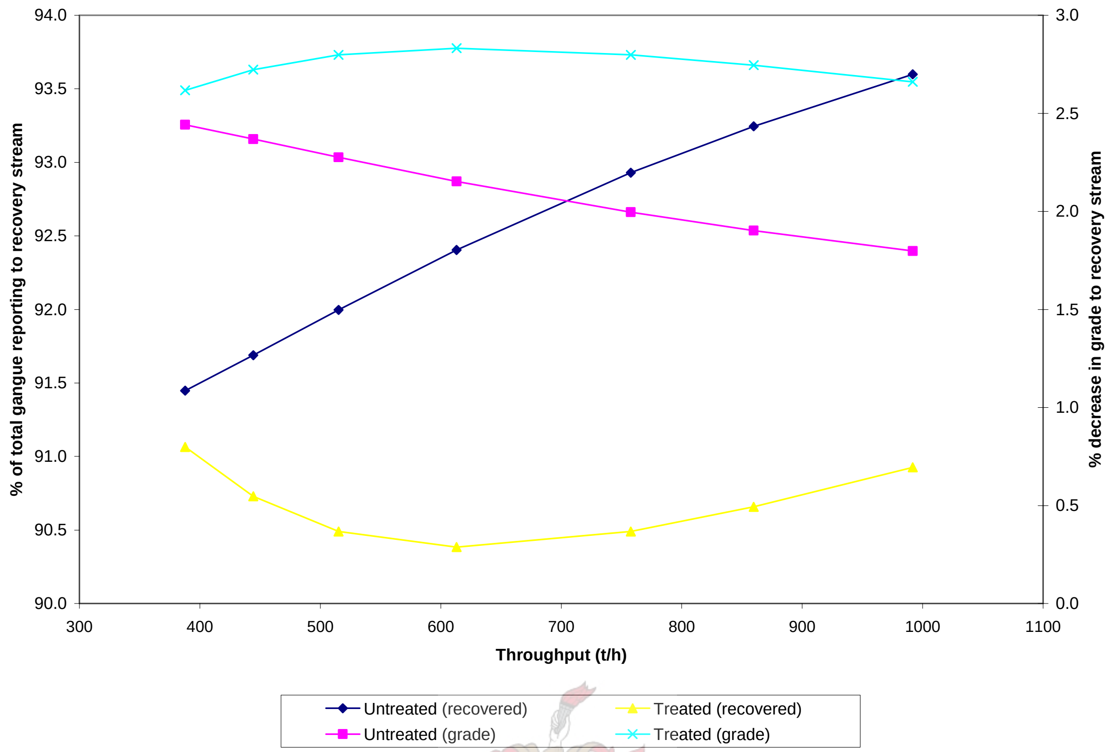

Figure 6.14 - Statistics for gangue reporting to flotation

Since magnetite is later recovered in the Palabora plant, losses of this material will also impact on the economics of the plant operation. From Figure 6.13, it is seen that for the treated material, the maximum increase in grade of about 4.4% over that in the existing plant for the material reporting to the recovery stream, is accompanied by a loss of around 2.9% of the total magnetite to the gravity concentration tails. The untreated material has a maximum grade increase of 3.8%, with an associated loss of 2.7% of the total magnetite to the gravity separation tails.

The statistics for the gangue thus show that the inclusion of the gravity separation circuit has a huge potential for the early removal of gangue. The highest removal of gangue from the treated material is 9.6%, while the largest potential removal of gangue from the untreated material is 8.6%.

It is seen that on average the total amount of material reporting to the flotation plant is 5.5% less in the case of the untreated material, and 6.8% less in the case of the treated material, than that initially reporting as feed to the rod mill.

If we further consider that the gravity concentration process removes around 77% of the gangue from the material reporting to it for both treated and untreated material, then the main force behind the improved results from microwave treatment would be the larger amount of material reporting to the gravity concentration process.

6.2.3. SAME FINAL 80% PASSING SIZE TO FLOTATION

The proposed flowsheet was simulated using the present flowrate in the existing plant for both treated and untreated material.

It was decided at this stage that in order to obtain a better comparison between the two cases that a similar product size distribution from the rod mill would be produced for both. This was done by keeping the residence time the same as in the existing plant, but then decreasing the residence time of the treated material in the rod mill until the product size distributions were similar.

For each case, the residence times in the ball mills were then varied and the results observed after each simulation. In this manner the final 80% passing size of the flotation feed from the proposed flowsheet was matched to that of the model of the existing flowsheet.

It was seen that shape of the product size distributions of the treated and untreated material sent to flotation differed from those of the existing flowsheet, with there being a greater fraction of material in the optimum recovery sizes for flotation (see Figure 6.15). This is as a result of the removal of large gangue particles in the gravity pre-concentration step, before further grinding take place in the ball milling circuit.

The impact on copper recovery of such a change in the feed to flotation should be large when combined with the increased liberation of copper minerals which has been observed in the -212 µm size range.

6.2.4. 10% INCREASE IN THROUGHPUT AT THE SAME FINAL GRIND SIZE

While there is a small possible increase in throughput for the untreated material with the addition of the gravity separation circuit, the maximum throughput is limited to around 400 t/h in each milling circuit. This translates to a possible maximum increase of just 3.2% in throughput. Since very little benefit in terms of increases in throughput were thus possible for untreated material after the addition of the gravity separation circuit, it was therefore decided to only study the valid case of an increase of 10% in the throughput for the treated material.

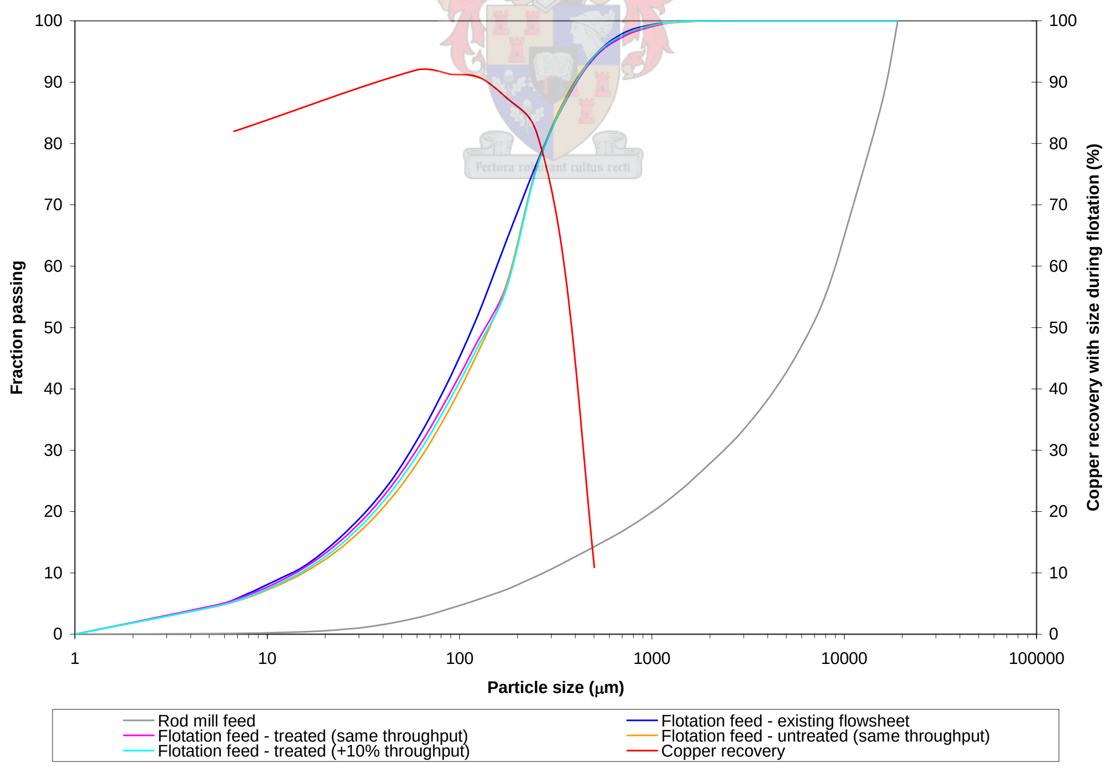

Figure 6.15 - Size distribution of product from milling section of plant (proposed flowsheet)

The residence time in the rod mill was decreased to ensure the same hold up in the mill as for the treated and untreated case at the existing plant throughput. Following the removal of material to the gravity concentration section and the return of the gravity concentrate to the milling circuit, the residence times of the ball mills were varied until the same size 80% passing size in the flotation feed was obtained as for the existing plant operation.

Figure 6.15 shows the resulting size distribution of the feed to the flotation section, for both the treated and untreated material with the same 80% passing size, as well as the size distribution of the treated material after the 10% increase in throughput, versus that of the existing plant. The copper recovery with size from flotation is also included for reference. On first glance, the fact that there is more material in the larger size fractions after the addition of gravity separation might lead one to believe that this could have a

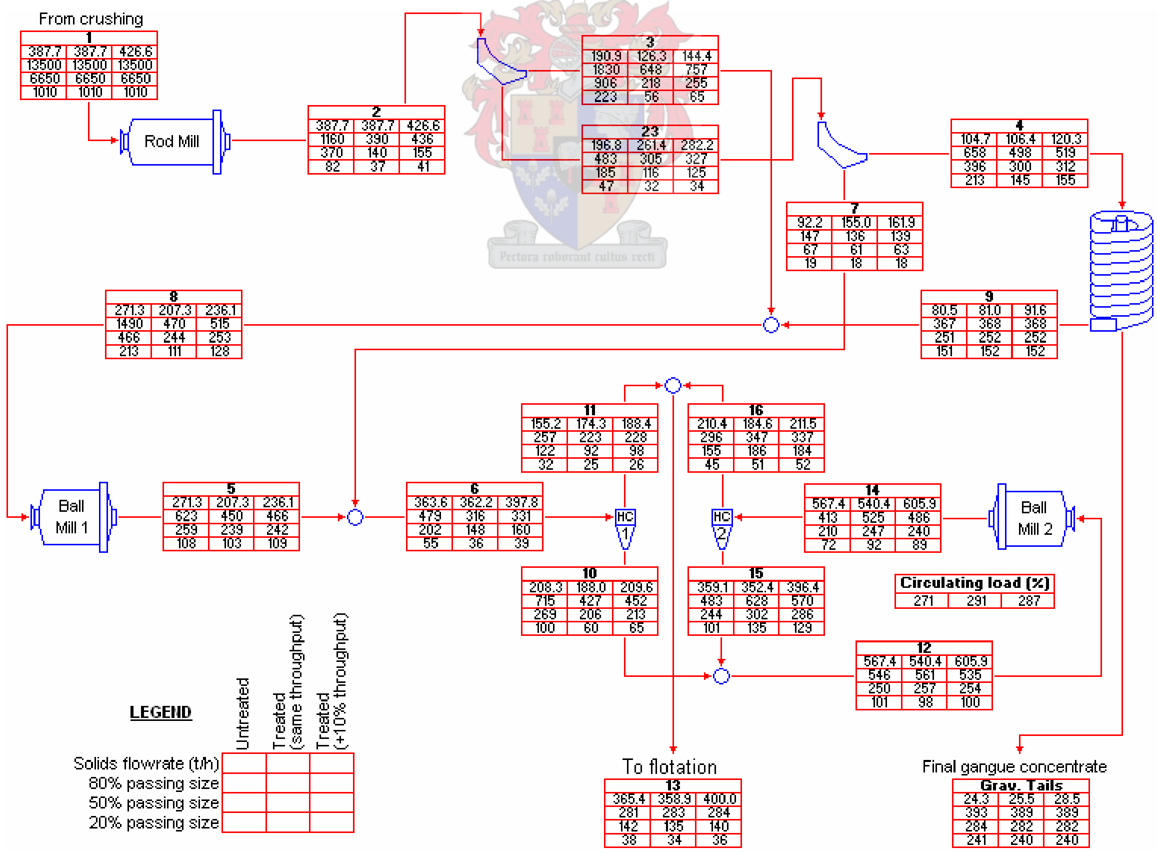

Figure 6.16 - Results obtained for various simulations of the proposed flowsheet

negative impact on the recovery of copper. However, given the smaller amount of fine particles and the fact that the flotation circuit also contains a classifier and mill to grind oversize material, it is much more likely that the recovery of copper will increase in this case, with a corresponding decrease in the grade of the flotation concentrate.

Figure 6.16 summarize the flowrates and the 20%, 50% and 80% passing sizes for the simulations performed on the proposed Palabora flowsheet, while Figure 6.17 shows the energy and grinding media consumption per ton of ore treated for each item in the flowsheet, as well as the corresponding consumption per ton of feed to the milling circuit.

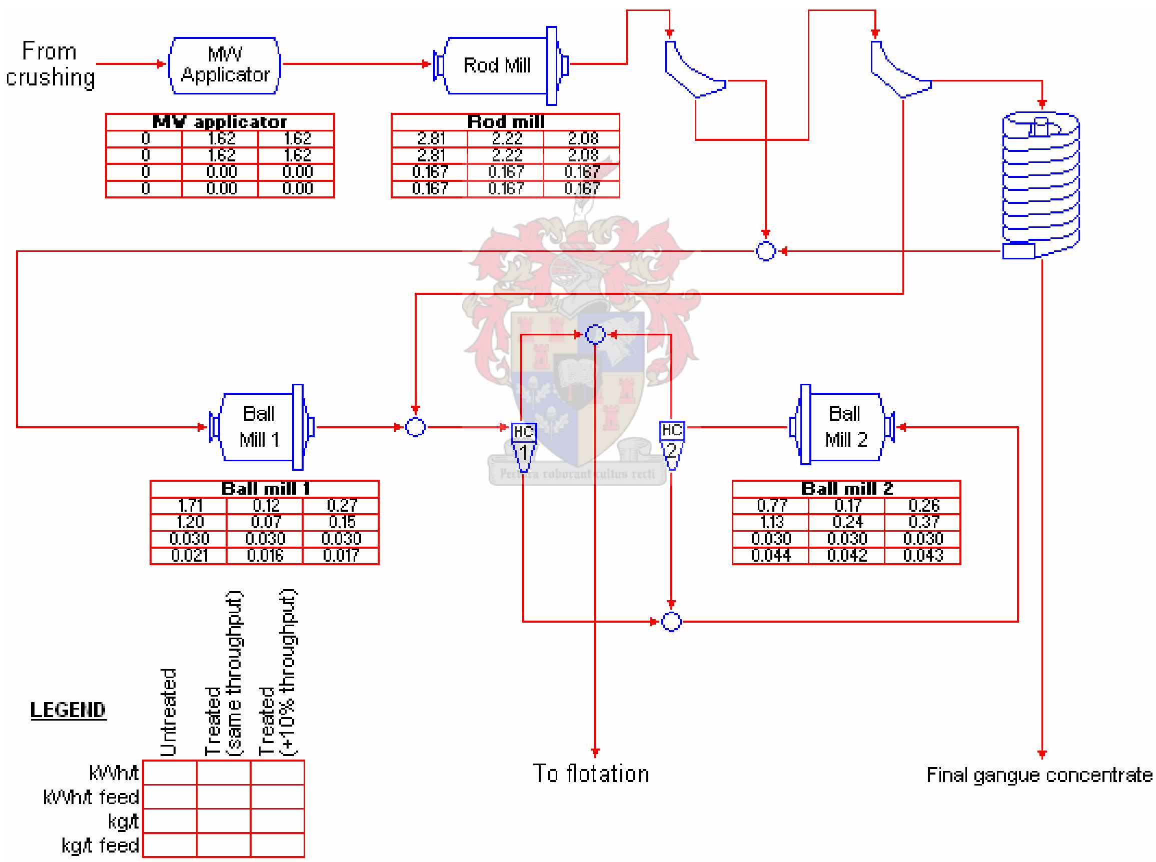

Figure 6.17 - Energy and steel usage obtained for various simulations of the proposed flowsheet

It appears that the largest energy and grinding media consumption occur in the rod mill for both treated and untreated material.

Since gravity separation is a very simple process, the only energy input required will be to the pumps which feed the slurry to the spirals. These costs will be ignored since they are, in general, small in comparison to the costs associated with the comminution of the ore.

Table 6.4 - Energy and grinding media used to produce feed to flotation in proposed flowsheet

Treatment	Energy consumption	Consumption of grinding media
	kWh/t feed	kg/t feed
Untreated	5.14	0.232
Treated (same throughput)	4.15	0.225
Treated (+10% throughput)	4.22	0.227

Table 6.4 summarizes the energy input (including microwave energy) per ton of ore fed to the milling circuit required to produce the feed to the flotation section for each of the three cases investigated for the proposed flowsheet. Once again, it should be noted that energy requirements for material conveying and pumping are not included. The predicted grinding media consumption per ton of ore fed to the milling circuit is also summarized.

It can be seen that a reduction of 19% in energy usage per ton of feed, over that for the untreated case, is possible by microwave treating the rod mill feed and then processing the material to produce the same final size distribution as for the untreated material. At the same time a reduction of 3% in the use of grinding media is also predicted.

For the case of a 10% increase in throughput (which is only made possible by the microwave pretreatment), the advantages created by the microwave treatment throughout the flowsheet make it is possible to still produce the same 80% passing size of the feed to the flotation circuit (Figure 6.15), together with a significant reduction in energy usage per ton of ore fed to the milling circuit of 18%.

These simulations also show a small reduction of 2.2% in the loss of grinding media for the case of microwave treatment at increased throughput over that of the untreated case.

6.3. SUMMARY OF RESULTS FROM FLOWSHEET SIMULATIONS

By comparing the results from the simulations we have performed, it is seen that in every case, microwave pretreatment shows benefits over that of the untreated cases. The base case of untreated material in the existing plant flowsheet is shown in blue in Table 6.5 and Table 6.6.

Table 6.5 - Comparison of energy consumption

Simulation	EXISTING FLOWSHEET		PROPOSED FLOWSHEET	
	Energy used (kWh/t feed)	% of existing energy consumption	Energy used (kWh/t feed)	% of existing energy consumption
Untreated	5.86	100.00	5.14	87.61
Treated (same throughput)	4.73	80.69	4.15	70.69
Treated (+10% throughput)	4.81	81.95	4.22	71.90

Table 6.6 - Comparison of grinding media consumption

Simulation	EXISTING FLOWSHEET		PROPOSED FLOWSHEET	
	Media loss (kg/t feed)	% of existing media consumption	Media loss (kg/t feed)	% of existing media consumption
Untreated	0.242	100.00	0.232	95.96
Treated (same throughput)	0.240	99.25	0.225	93.04
Treated (+10% throughput)	0.240	99.11	0.227	93.61

In terms of energy and grinding media savings, the reduced tonnages passed to the ball milling circuit after gravity separation shows definite improvement over that for the existing plant operation.

While it is likely that the proposed flowsheet would provide a greater copper recovery from the material sent to flotation due to the size of the flotation feed (where fewer losses are likely as a result of the smaller fraction of fine material), the improved copper grade and the smaller amount of gangue contaminants (i.e. gangue sulfides) present as a result of the gravity concentration of the flotation feed, it would however be necessary to consider the copper losses in the gravity concentration tailings before concluding whether the proposed flowsheet shows any benefits in money terms over the existing operation. This then forms part of the economic investigations performed in section 7.

7. ECONOMIC ANALYSIS

An investigation into the economic viability of the two proposed flowsheet changes was also performed in an effort to better gauge the impact of microwave pretreatment on the plant.

It was attempted to include as many of the major costs as possible to ensure reliable cost estimation. In the case of the existing flowsheet with the addition of microwave treatment to enhance flowsheet performance, the only major capital cost is that of the microwave applicator itself.

An installed cost of $4000/kW is known to be a reasonable assumption for microwave equipment (Bradshaw, 2004). Due to the layout of the Palabora plant, it is likely that separate microwave applicators and power sources will be required to handle each of the 6 conventional milling circuits in the plant. The required microwave power was also multiplied by a factor of 1.1 to allow for any disturbances which might occur in the steady-state operation of the plant.

The capital costs for the proposed flowsheet extend further to those of the sieve bends used in the two particle size classifications occurring before the gravity separation plant, as well as the costs associated with the spiral classifiers used for the gravity separation.

These capital cost were calculated using the metallurgical equipment cost tables published by Mintek, March 1991.

It was then necessary to scale these costs up to the present date. This was done using the Statistics South Africa Production Price Index for local commodities for the dates of March 1991 and November 2004 (Table 7.1).

Table 7.1 - Statistics South Africa Production Price Index for local commodities

Date	Index
1991, March	345.6
2004, November	939.3

While these are not the indices associated with the metallurgical industry itself, they will, none the less, provide a reasonable reflection of the price increases of these items of equipment. Since the price increase for imported commodities over the same time period is substantially lower, where any items of equipment need to be imported the indices used would over-predict the price increases. This would lead to more conservative estimates in terms of recouping any capital expenditure.

Estimates of the fixed capital costs associated with the full installation of each of the items of equipment, including such costs as erection, piping, electrical systems and instrumentation, are based upon the purchased costs of the equipment and are obtained by multiplying the purchased cost by a suitable Lang factor as follows:

$$C_{FC} = f_L \sum C_{EQ} \qquad \textbf{7.1}$$

where C_{FC} fixed capital cost

f_L Lang factor

C_{EQ} cost of equipment

Ruhmer, 1991, reports a suitable Lang factor for plants of this nature to be 3.89, and this value was used for the estimation of the costs of the gravity separation plant, as well as for the sieve bends required for the necessary alterations to the existing milling circuit.

Table 7.2 - Cost of energy and reagents used in the processing of the ore

Details	Price	Units
Exchange rate (Jan 2005)	6.0225	R/$
Copper (Cash buyer, Jan 2005)	3128.50	$/t
Energy (Jan 2005)	0.26	R/kWh
Grinding media (Nov 2004)	2.19	R/kg
S.I.B.X. (Jan 2005)	5.60	R/kg
Senfroth (Jan 2005)	4.20	R/kg
Coal (Jan 2005)	160.00	R/t
Naptha cost (Jul 2004)	117.75	USc/gal

The values used for the cost of the energy, reagents and fuels used in the process flowsheet are listed in Table 7.2.

For the microwave unit, the cost of the replacement of the magnetron must also be taken into account. The operating life of a magnetron is usually around 10 000 hours, and replacement costs are estimated at $100/kW (Bradshaw, 2004). It was assumed that replacements would then occur every 13 months during continuous operation.

In order to account for other costs which would be associated with the daily running of the plant, the financial statements for 2001 (the last year before the mining operation moved underground) were compared with the calculated running costs of the major equipment in the concentrating and refining departments, and the surplus monthly expenses calculated.

It is reported that the group profit for the year ended 2001 was R220 million. If we assume that this came only from the copper mining operation, then the calculated monthly expenditure, not including the main running costs which are estimated from flowsheet performance, is around R94 million.

While this would not be entirely a true representation of the financial situation given different operating conditions, it was assumed that these costs would to a large extent be independent of throughput, and were then assumed to be constant in the different economic evaluations performed.

Based upon plant data, as well as the data collected during the course of the work done in this project, the copper content and the recoveries associated with the various processes in the flowsheet were assumed to be as shown in Table 7.3.

Table 7.4 shows the various fuel and reagent consumptions used in the economic analysis.

Table 7.3 - Copper content and process recoveries

Details	%
Copper in rod mill feed	0.492
Total Cu lost in gravity tails - untreated (same throughput)	3.65
Total Cu lost in gravity tails - treated (same throughput)	4.02
Total Cu lost in gravity tails - treated (+10% throughput)	4.48
Copper recovery in primary concentrate - untreated	0.37
Copper recovery in primary concentrate - treated	82.82
Copper in smelter feed	88.00
Recovery of copper from electrolytic refining	97.00

Table 7.4 - Reagent use for various processes in the flowsheet

Reagent use	Amount	Relation
Coal (smelter)	0.222	$t_{coal}/t_{dry\ smelter\ feed}$
Electrolytic refining (electricity)	370	$kWh/t_{copper\ processed}$
Naptha (casting furnace fuel	75	$l/t_{copper\ processed}$
S.I.B.X. (flotation reagent)	25	$g/t_{flotation\ feed}$
Senfroth (flotation reagent)	30	$g/t_{flotation\ feed}$

Table 7.5 - Summary of capital costs, income and expenditure for each project

	EXISTING PLANT			PROPOSED PLANT		
	Untr.	**Tr.**	**Tr. (+10%)**	**Untr.**	**Tr.**	**Tr. (+10%)**
Capital costs (Rx10^6)	0	100.002	110.030	82.874	186.863	205.143
Microwave applicators		100.002	110.030		100.002	110.030
Sieve bends				9.948	10.288	11.248
Spirals				72.926	76.573	83.865
Periodic costs (Rx10^6)	0	2.500	2.751	0	2.500	2.751
Magnetron replacement (13 months)		2.500	2.751		2.500	2.751
Running costs (Rx10^6/month)	100.287	99.928	100.545	99.825	99.487	100.058
Comminution energy	2.555	2.062	2.304	2.239	1.807	2.022
Milling media	0.898	0.891	0.979	0.862	0.835	0.925
Flotation reagents	0.452	0.452	0.497	0.426	0.418	0.466
Smelter coal	0.663	0.704	0.775	0.638	0.676	0.740
Electrolytic refinery energy	0.657	0.698	0.768	0.633	0.670	0.734
Casting furnace naptha	0.943	1.002	1.103	0.909	0.962	1.053
Other costs	94.119	94.119	94.119	94.119	94.119	94.119
Income (Rx10^6/month)	126.465	134.377	147.852	121.855	128.977	141.235
Copper metal	126.465	134.377	147.852	121.855	128.977	141.235
NET INCOME BEFORE TAX (Rx10^6/month)	26.178	34.449	47.308	22.029	29.490	41.177
Depreciation - Straight line method	0	1.026	1.129	0.691	1.750	1.921
(over 10 years, no scrap value)						
Microwave applicators		0.833	0.917		0.833	0.917
Magnetrons (13 months)		0.192	0.212		0.192	0.212
Sieve bends				0.083	0.086	0.094
Spirals				0.608	0.638	0.699
COMPANY TAX (30%)	7.853	10.027	13.854	6.402	8.322	11.777
NET INCOME AFTER TAX (Rx10^6/month)	18.325	24.422	33.454	15.628	21.168	29.400

The capital costs and monthly income and expenditure, associated with each of the 6 cases studied, are summarized in Table 7.5 (refer to APPENDIX E for calculations of the required capital costs per milling circuit). It can be seen that the highest monthly expenditure in each project is that associated with the running costs for comminution.

Where microwave pretreatment is applied to the ore, the cost of this is included in the reported comminution energy costs.

It is assumed that the only tax allowances come from the depreciation of the capital investments stated. For the major items of equipment, the depreciation is calculated using the straight line method over a period of 10 years with no scrap value, while the depreciation on the magnetrons is also calculated using the straight line method with no scrap value and is assumed to run over the useful life of the magnetron, which is 13 months.

From the summarized monthly cash flows it would appear that the projects generating the highest monthly cash flows are those where microwave pretreatment is included in the milling circuit. It can also be seen that those projects where gravity concentration is used to remove gangue early on in the milling circuit, are less profitable than the existing operation.

It thus appears that while the addition of a combination of microwave treatment and gravity separation leads to slight savings in all running cost versus the corresponding cases for just the addition of microwave treatment, the losses of copper to the gravity concentration tailings cannot be justified.

By calculating the net present value (NPV) of the plant over a 10 year period (and discounted at 20% per year) the projected benefits afforded by each project can be compared with one another (Figure 7.1). The base case for the existing plant is shown in dark blue. All cases where changes to the plant flowsheet are made to include removal of gangue by gravity separation are represented by dotted lines of the same colour as the case for similar operation in the existing plant flowsheet. It can be seen that in every case the addition of the gravity separation circuit results in a decrease in the net present value of the plant, due to both the high capital costs associated with implementing the flowsheet changes, as well as the loss of income through lower overall copper recoveries.

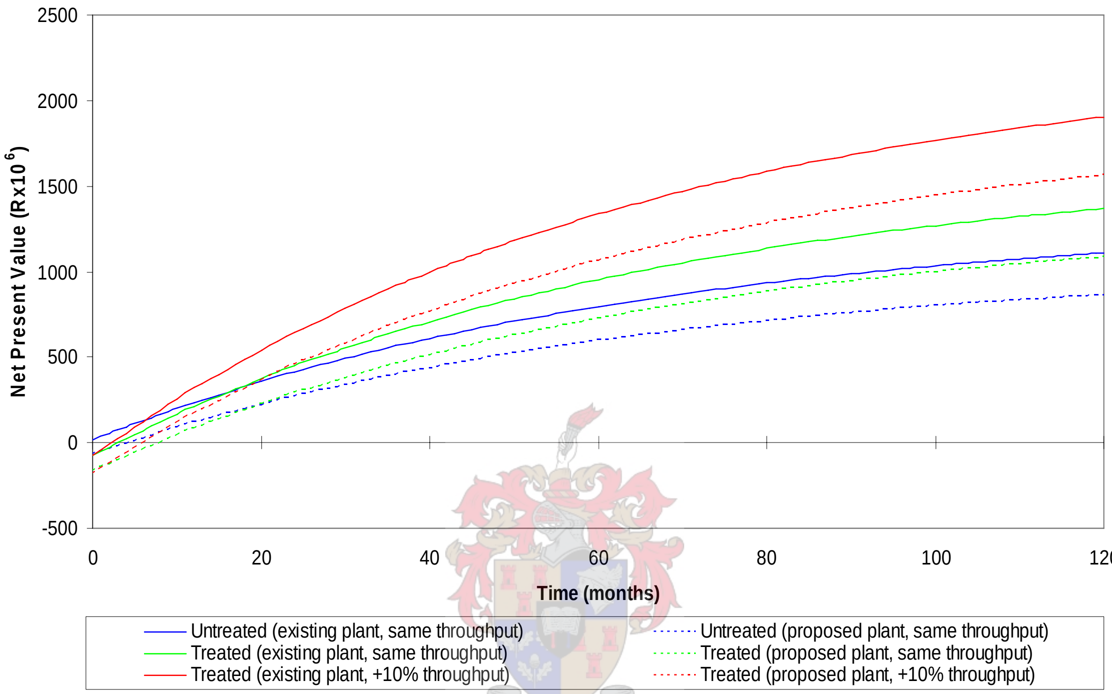

Figure 7.1 - Net present value of each project over a 10 year period

Due to the high monthly incomes already shown by the plant as well as the projected increases in plant profitability after the addition of microwave pretreatment (refer to Table 7.5), the capital costs associated with the addition of just microwave processing facilities are recouped over a period of 4 months, while after 16 months the addition of microwave treatment will begin to show benefits in NPV over conventional processing. The potential for an increase in the NPV of the plant with the addition of the microwave treatment is seen to be quite large. Furthermore, where the increases in throughput made possible by the addition of microwave pretreatment are exploited (as demonstrated in Figure 7.1 for a 10% increase in throughput), this results in further radical increases in the NPV of the plant.

It must be stressed, however, that the above analysis is based upon many assumptions and is therefore not a full picture of the actual income and expenses associated with the operation of Palabora Mining Company's copper recovery plant. It does however highlight the tremendous potential exhibited by the application of this technology.

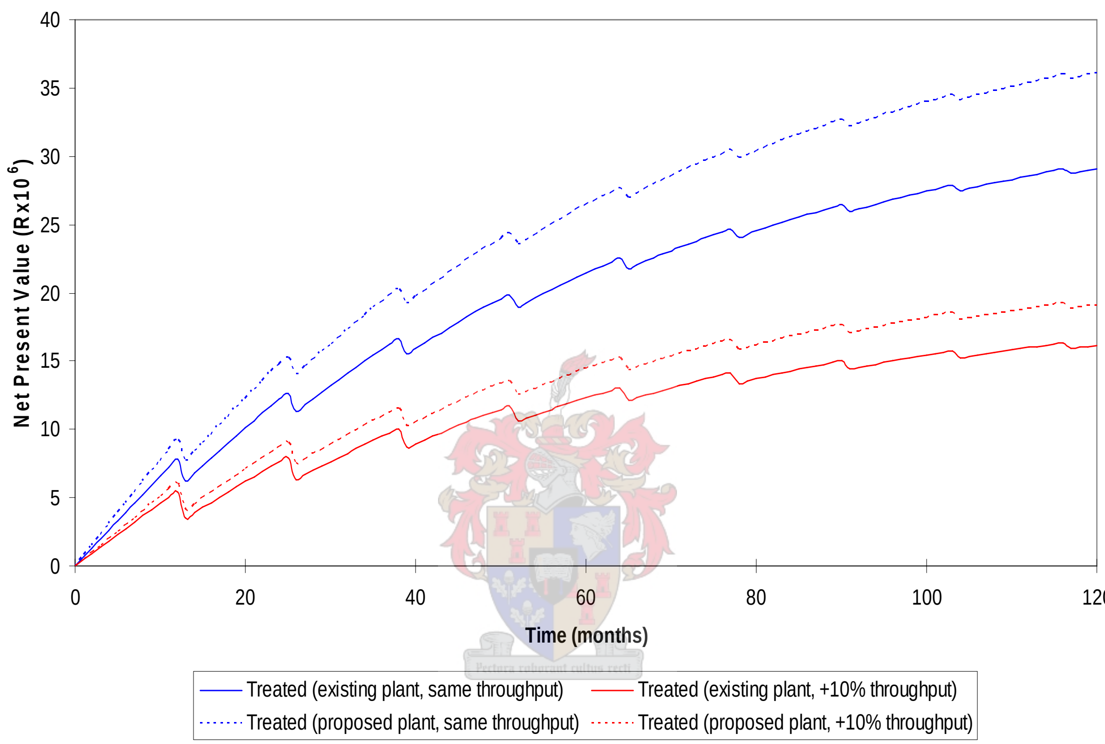

<u>Figure 7.2 - NPV of the plant alterations based upon energy and media savings alone</u>

A more impartial view of the benefits of microwave pretreatment is shown in Figure 7.2. This graph shows the NPV of the plant improvements, assuming that there is no income apart from the savings in grinding energy and milling media over the untreated case for both the existing and proposed flowsheets (and ignoring the respective initial capital outlay required for each of these cases). The dips in the plotted curves are due to the periodic replacement costs of the magnetrons. It is seen that operation of the plant using microwave pretreatment of the ore before grinding will lead to an increase of R29 million in NPV of the plant (over 10 years) based on savings in running costs alone. The 10%

increase in throughput which is investigated is associated with a higher energy and grinding media consumption over the same time period as for the existing throughput, and this explains the difference in savings between the two operating cases. As a result, savings from microwave pretreatment and a 10% increase in throughput will be in the region of R16 million over 10 years.

Though the savings in running costs generated as a result of implementing both microwave pretreatment of the ore, as well as gravity separation to remove gangue material before ball milling, are greater than those of the associated cases of just the addition of microwave pretreatment, unless the amount of copper lost to the gravity separation tailings can be reduced, operating under these conditions will still lead to decreases in the overall NPV of the plant (as seen in Figure 7.1).

It can also be seen that the value generated from savings in energy and grinding media alone cannot recoup the capital investments (Table 7.5), which is in the region of R100 million for the implementation of microwave pretreatment alone, and around R200 million for the combined implementation of microwave pretreatment with gravity separation, over the 10 year period investigated.

Table 7.6 shows the projected increases in NPV, for each of the 5 cases investigated, over the NPV for the existing plant operation at the end of a period of 10 years.

Table 7.6 - Increase in NPV over the existing plant operation without MW treatment over 10 years

Operating conditions	% increase in NPV	
	Existing operation	Proposed operation
Untreated (same throughput)	0	-22
Treated (same throughput)	23	-2
Treated (+10% throughput)	72	41

It is seen that after 10 years of operation, the implementation of microwave pretreatment before milling increases the NPV of the plant by 23% (or R259 million), and by 72% (or R795 million) when an increase in throughput of 10% (which is only made possible by the microwave treatment) is instituted. It can further be seen that in every case the NPV of the plant where the proposed combination of microwave technology with gravity separation is employed is much lower than the corresponding case at the same conditions for just the addition of the microwave treatment.

It is estimated that if a recycle stream over the rod mill ensured that all the material left the milling circuit and reported to gravity separation plant before being returned for subsequent rod milling, the characteristics of the ore could be drastically changed.

Table 7.7 - Ore characteristics after gravity concentration of all material

Description	Copper		Magnetite		Gangue	
	Untreated	Treated	Untreated	Treated	Untreated	Treated
% of total mineral lost	9.51	9.70	18.50	18.04	77.48	76.94
Original grade (%)	0.45	0.45	39.00	39.00	60.00	60.00
Grade after gravity concentration (%)	0.89	0.88	69.55	69.17	29.56	29.95

If all the ore could be processed in the gravity concentration plant, it is estimated that 23.19% of the untreated material, and 23.7% of the treated material, could be removed in the gravity concentration tails. The losses of the main minerals in the ore are listed in Table 7.7. While the grades of these minerals in the recovery streams can be vastly improved, the losses of the valuable minerals to the gravity separation tailings are substantial. It is assumed that improvements will have to be made to such an operation before it could become a viable option. It should also be noted that the differences between treated and untreated material resulting from the gravity separation would be slight, and thus no real benefit from the application of microwaving is found in terms of this operation. It would be possible to further scavenge the ore in an attempt to reclaim the lost valuable minerals, but it is assumed that losses would still be high unless some form of further size reduction was employed, though this would then negate the very benefits of not having to grind gangue material we are trying to exploit.

It must also be recalled that Palabora employs a very complex minerals beneficiation process, which covers much more than just the recovery of copper, and as such it is not known what effects the implementation of gravity separation, to remove gangue material early on in the process, may have on the rest of the plant.

It is thus suggested that only the combination of microwave technology with more selective recovery technologies, such as flotation (refer to section 5.6.1), shows potential for further exploiting the benefits of microwave pretreating the ore.

Due to the much lower capital costs associated with the implementation of just the microwave treatment section, versus the addition of both microwave treatment and subsequent gravity separation, the former seems to provide a reasonably risk-free method of utilizing the benefits associated with microwave treatment, and will result in large increases in plant profitability over several years. The ability of microwave treatment to drastically increase the plant throughput is also of major significance.

It is also likely that, due to the large changes which must be made to an existing plant to implement the use of microwave treatment combined with another technology, and the difficulty of such operations, only purpose built plants will incorporate this idea. The exception will be where this alternate technology already exists and the addition of microwave pretreatment can improve its performance (as is the case at Palabora which employs flotation to recover copper).

For any existing plant where the decision to implement microwave technology is taken, it would be recommended that microwave technology be added, and the benefits offered by it be put to their best use in the existing flowsheet without the implementation of other costly changes and additions, which may or may not further improve plant performance and profitability.

7.1. CURRENT OPERATING CONDITIONS AT PALABORA

The latest data from Palabora suggests very different operating conditions to those reported for 1989 and provided to us. The operations overview and production statistics for Palabora Mining Company for 2004 are shown in APPENDIX D.

In order to attempt to investigate what possible changes the implementation of the proposed flowsheet changes might have on the new operation at Palabora, these new production figures were used in the same financial calculations as for the 1989 plant operation. While it is not entirely correct to investigate the new operation in this manner without investigating what the changes in throughput and grade might have on the flowsheet first, this will none the less give an indication as to the suitability of microwave treatment in the new operation.

The copper content of the present ore body being mined is 0.791%, versus the value of 0.492% in 1989. The grade of the concentrate reporting to the smelter has decreased from 37.1% to 29%, while the reported average copper recovery over the entire plant increased from 84.8% to 87.1% in 2004. This equates to a recovery of around 85.1% in the primary copper concentrate.

Table 7.8 - Estimated copper losses to gravity concentration tails

Operating conditions	% of total copper lost	
	1989	2004
Untreated (same throughput)	3.65	5.48
Treated (same throughput)	4.02	6.04
Treated (+10% throughput)	4.48	6.73

Based on the same calculations as for the 1989 data, a copper recovery of 90.5% in the primary concentrate can be estimated for material which has been microwave treated to enhance liberation (refer to section 5.6.2). This is an increase in recovery of 6.3% over that of the existing operation. Copper losses in the gravity concentration tails, where this technology is used, will also increase due to the increase in grade. Estimates for the copper losses appear in Table 7.8.

Since the operation has moved underground, the tonnages mined have dropped severely. In total, 3 743 000 tons of ore were mined during this first half of the year at an average of around 20 800 tons per day, versus the 80 000 tons per day mined in 1989.

As the total amount of ore reporting to the conventional milling circuit in 1990 was around 55 000 tons per day, it is assumed that all the ore from the new operation reports to the conventional milling circuit.

Palabora posted a net loss of R158 million in the six months to June 2004 after production fell from the previous period, while first half sales were R1.03 billion. The average price of copper over this period was around \$2825/ton, while the average exchange rate was R6.685/\$.

By using these values to estimate the other costs associated with the mining, concentrating and refining operations which are not included in the study, a value of around R95 million per month was calculated to give the same losses as were reported in the financial statements for the 6 month period investigated.

It was assumed that this cost would not change if the microwave treatment units or the gravity separation section were added to the existing plant, as this would not influence the running of the plant significantly. Where the results from an increase in throughput are predicted, this cost was also used as not enough information was available to separate running costs from fixed monthly costs.

Figure 7.3 then shows the results obtained for the 1st half of 2004. With the introduction of the microwave pretreatment facility on the plant at a capital cost of R48 million, the NPV of the plant after 6 months of operation decreases by only 12.4% (or around R20 million) due to improvements in plant operating costs and increased revenues from higher copper recoveries. Even though the NPV of the plant decreases over this time period, the reclamation of over half the capital cost within these first 6 months means the NPV of the plant after the addition of microwave pretreatment will most likely rise above that of the existing operation after a reasonably short period of operation, even though the plant will still be running at a loss. It can also be seen that the addition of microwave pretreatment together with a 10% increase in plant throughput made possible by the pretreatment of the ore, has the greatest affect on the final NPV of the plant, with a reduction in losses over the 6 month period of 12.5% (approximately R20 million). It is likely, however, that in the new operation the throughput will be limited by the underground mining operation, and not by the flowrate through the comminution section of the plant. The predictions at the increased throughput may not be representative of possible plant operation then.

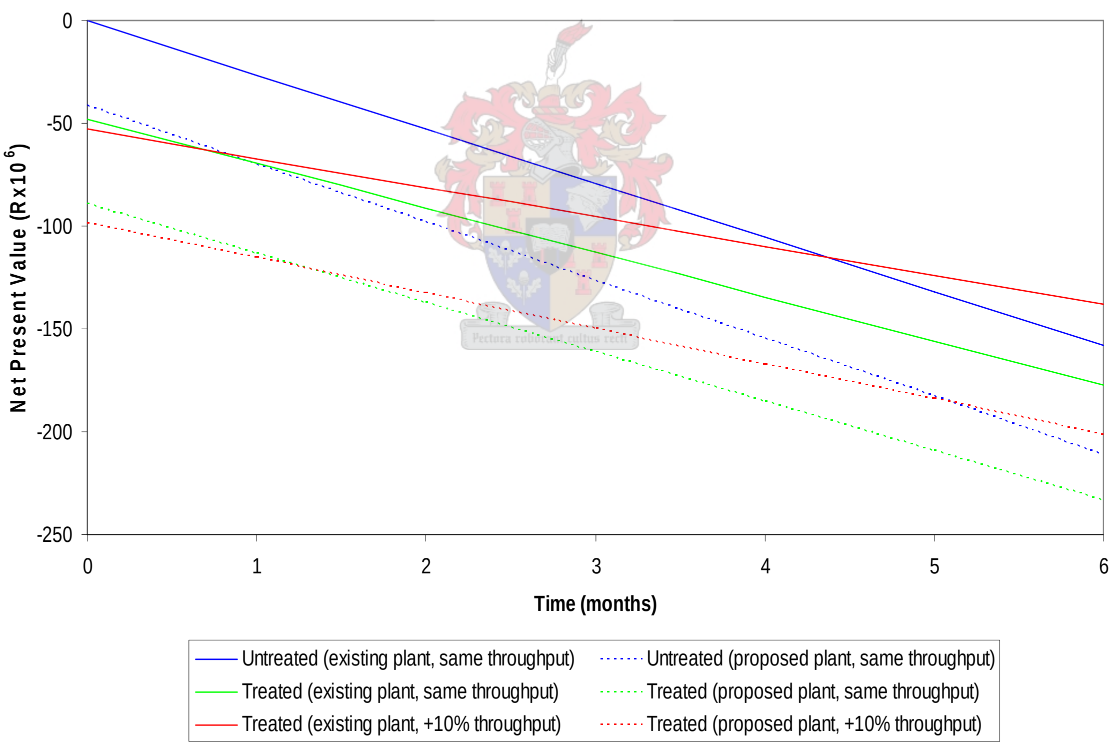

Figure 7.3 - NPV for Palabora over the 1st half of 2004 discounted to the beginning of the year

Furthermore, in all cases the large capital cost associated with the further addition a of gravity separation facility to remove gangue early on in the process, together with the increased losses in copper recovery occurring as a result of this process, is detrimental to the profitability of the plant and results in increases in the losses suffered during the 6 month period investigated. It appears that only an increase in throughput of 10% will see any benefit afforded to the plant if the combined technologies of microwave treatment and gravity concentration are implemented, though even this does not outperform any of the scenarios based around the exclusion of gravity separation from the plant.

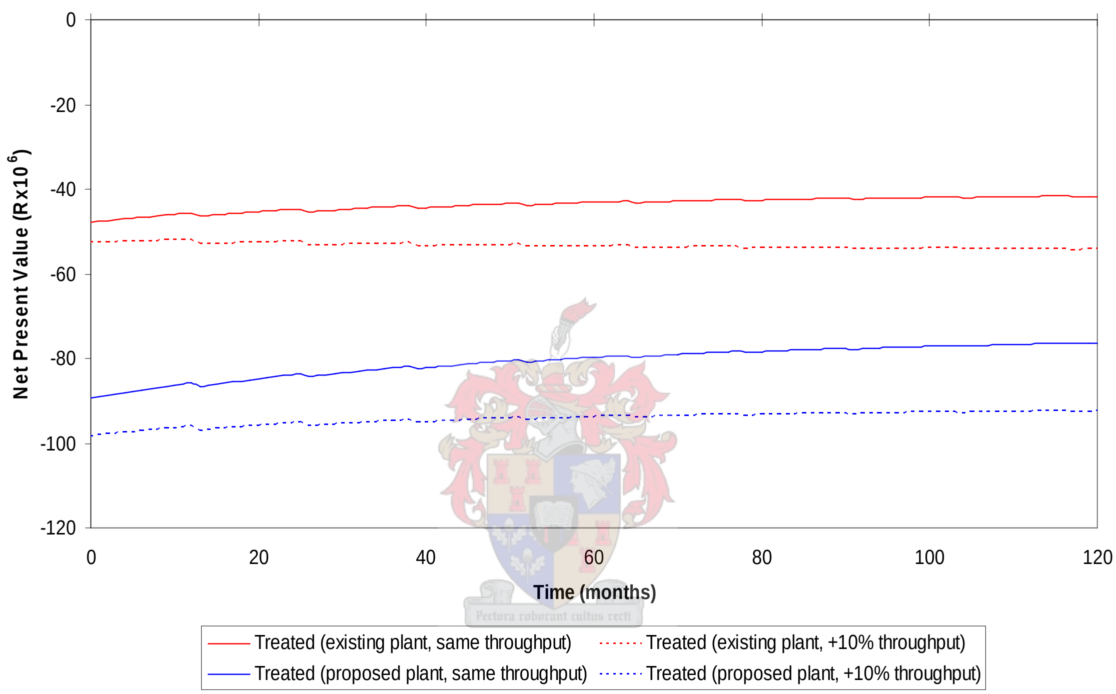

Figure 7.4 - NPV of the plant alterations based upon energy and media savings alone (2004)

Similar to what was shown for the projected plant operation based upon the 1989 data supplied by Palabora, Figure 7.4 compares the savings in grinding energy and media versus the capital expenditure required for each of the two plant alterations in an attempt to determine whether this technology has the ability to pay for itself in terms of savings alone given the current operating conditions at Palabora. It can be seen that only negligible savings are generated in all cases after the addition of microwave pretreatment. This is mostly due to the much lower throughputs associated with the current operation at Palabora, where savings in the grinding energy and grinding media cannot be amplified sufficiently for these to play a significant role in plant profitability. Therefore, any attempt to define a payback time based on these savings alone would be futile. Under these conditions, however, this technology can only recoup the capital expenditure within a reasonable time frame based upon increases in liberation and recovery. The same applies for the further addition of gravity separation with microwave treatment at both the same and increased throughput.

To further determine the effect of the implementation of microwave pretreatment on the operation at Palabora, an investigation of the plant profitability margins was performed. Since the two main factors controlling the plant income are the rand/dollar exchange rate and the price of copper, the break even point in each of the cases under investigation was determined.

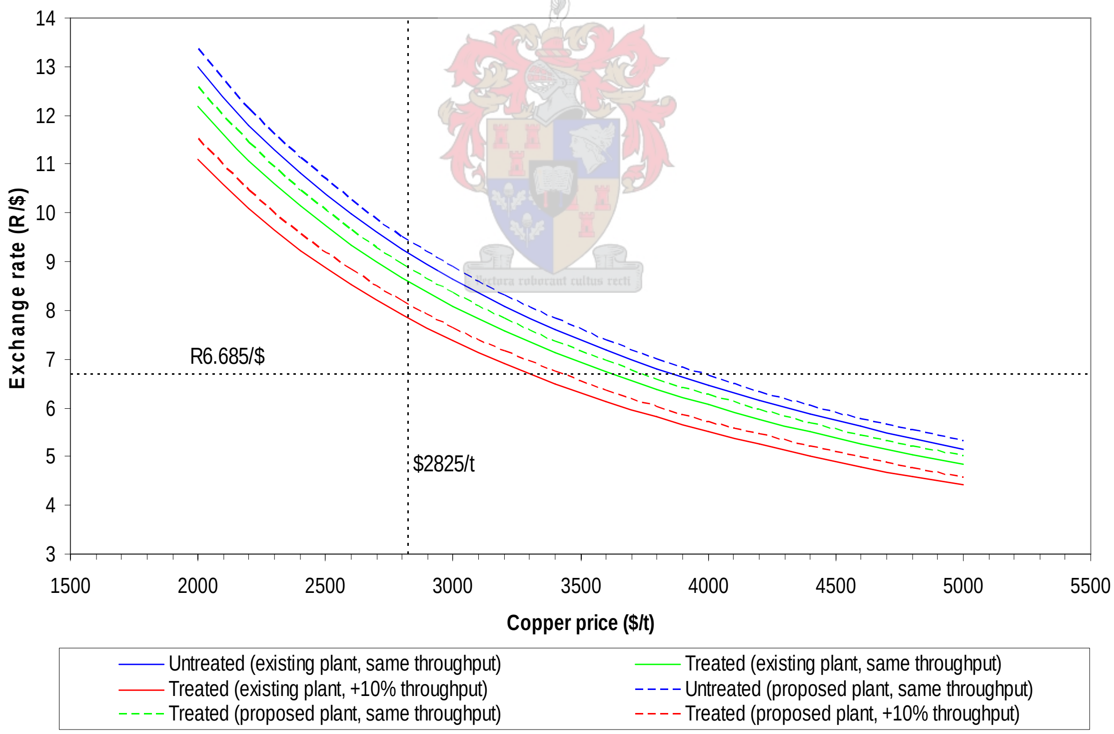

Figure 7.5 - Profitability of Palabora operation against exchange rate and copper price

Figure 7.5 shows the break even point for operation of Palabora during the first 6 months of 2004 in terms of requirements of copper price and exchange rate combinations. Any operating point above the respective curve for each case would lead to profitable operation under those conditions. It can be seen that the addition of microwave treatment increases the chance of the plant moving into the profitable region, however, the combinations of exchange rates and copper prices required in each case were unrealistic at the time.

It is therefore concluded that economic operation of the plant, under the conditions prevailing during the first half of 2004, could not be fully facilitated by the application of microwave technology alone, but that other cost saving schemes would need to be implemented as well. It also appears as if the combined introduction of microwave pretreatment with gravity separation (to remove gangue material at large particle sizes) would not help the plant to achieve the required operating conditions for profitability any better than the easier and cheaper application of just microwave technology, but would in fact hamper any attempt at a return to profitable operation at Palabora.

Depending on where the bottle neck occurs in the operation the additional throughput, which is facilitated by the introduction of microwave pretreatment of the ore before milling, would increase the chance of successful operation somewhat as well.

8. CONCLUSIONS

Experimental work in preparation for simulations

An important aspect of microwave treating ores is that, under the right conditions of ore mineralogy and power inputs, it is possible to cause significant macroscale damage to the ore particles, resulting in comminution during the thermal pretreatment of the ore (Kingman et al., IMPC XXII). Measurements of the size distribution of the Palabora ore before and after microwave treatment showed that microwave induced breakage had not occurred to the extent of the formation of new particles (see Figure 5.1). It thus appears that a treatment of 10.5 kW for 0.5 seconds in the applicator used was not sufficient to induce particle breakage in the Palabora ore during the thermal treatment itself.

The breakage rate experiments that were performed on the ore (see section 4.5), however, showed that at every grinding time tested, a finer size distribution was produced for treated ore than was the case for untreated ore (refer to Figure 4.4). This is indicative of the damage caused to the ore on a microscale, as a direct result of microwave treatment of the ore before milling.

It further appears that, after microwave treatment has been applied, an optimum grinding time exists where the most benefits in terms of size reduction of the larger particles occurs without an increase in the production of fines (see Figure 5.8). This grinding time is seen to be about 3 minutes, and after this time the amount of fine material produced increases drastically with microwave pretreatment of the material. This is most likely due to the greater surface area exposed (and thus available for abrasive wear) in the finer particle size distributions produced in microwave treated material at the same grinding times as for untreated material. The intergranular fracturing of particles (and subsequent liberation of mineral grains at larger particle sizes) caused by microwave treatment may lead to greater losses of valuable minerals to slimes, since more large, fully liberated valuable minerals are thus exposed to abrasive wear for longer periods of time, and thus the early removal of liberated valuable minerals before further comminution takes place is essential in ensuring that the advantages offered by microwave treatment are correctly exploited.

For grinding times longer than approximately 4 minutes, the developing size distributions in the batch mill are increasingly affected by the inability of the laboratory mill to break the larger particles, resulting in the uncommon cumulative size distributions which develop at long grinding times (see Figure 4.4). This is due to the dimensions of the mill and the media used, where not enough impact energy can be supplied to break the stronger large particles, resulting in a slowing down of the breakage rates of the larger particles with time once the more brittle large particles have been broken. Thus, when the back calculations were performed to obtain the breakage parameters of the ore (see section 3.3.5 and section 5.4), it was found that the best model fits were obtained when only those size distributions measured at times where the effect of rod size was not seen were used in the back calculation. As a result, the breakage parameters for the ore were calculated from data obtained up to 3 minutes of grinding.

Subsequent scale-up of these parameters, followed by modelling of the rod mill and comparison of these results with those from the plant data, showed that the unscaled parameters better described the breakage of the ores in the plant mill. It appears that scaling of the pseudo-parameters which are obtained from the back-calculations using the measured size distributions in the breakage rates tests is not suitable, since the purpose of scaling is lost when the values of the breakage parameters are not correct in themselves, but only act together in the functional forms to describe the breakage characteristics of an ore.

The grinding time of 16.4 minutes, chosen for use with the bulk of the ore sample provided by Palabora and which would be used in further tests, was such that 80% of the treated ore would be finer than 800 μm after milling. After grinding each of 14 batches of treated material, and 10 batches of untreated material, for this time, the following were noted:

- A finer grind size is achieved for the treated ore after milling than is the case for the untreated ore (see Figure 4.6).
- Slightly more copper reports to the larger size classes in the microwave treated ore (see Figure 5.3), most likely indicating the liberation of copper at larger particle sizes during grinding. Since more attrition and less impact breakage of large particles takes place in the untreated material, it is also more likely that the liberated copper produced will be much finer in the untreated ore.
- Results showed that more iron reported to the smaller size classes in the treated ore (see Figure 5.4). As the iron exists predominantly in the form of magnetite, it would appear that this mineral is weakened through the treatment and subsequently grinds faster than is the case in untreated ore.
- Of the major gangue elements, only calcium showed a large response to the application of microwave treatment, with more of this element reporting to the finer size classes (see Figure 5.5). This element occurs predominantly in the form of calcite and apatite and it is reasonable to assume that the mineralogy of the ore (i.e. the associations of calcite and apatite with other minerals) must make these minerals particularly susceptible to weakening during the microwave treatment.

From the fully liberated density distributions of the minerals present in the ore (see Figure 5.12), as well as the gravity concentration criterion associated with the splitting of each mineral from every other mineral in the ore (see Table 5.4), it appears that of the valuable minerals, only valeriite has a density low enough that it would not be able to be split from the gangue material easily. QEMSCAN results, obtained from the products of the grinding of the microwave treated and untreated Palabora ore samples, later showed that of the gangue minerals present, only calcite and dolomite demonstrated the possibility for almost fully reporting to the light fraction in a gravity concentration process, and that it is likely that slightly more calcite and dolomite will report to the light fraction after microwave treatment due to the enhanced liberation of these gangue minerals (see Figure 5.13).

Comparison of the mineral data from the QEMSCAN analysis of the -850+212 μm size class with the XRF data for the floats and sinks obtained from the gravity separation tests performed on the same size class, allowed the gravity separation to be quantified in terms of particle densities being misplaced from their correct classification when reporting to the light and heavy fractions (see Figure 5.16). This then allowed for the modelling of the gravity separation plant in the flowsheet simulations.

QEMSCAN analysis of the size fractions suitable for flotation showed that the amount of fully liberated copper minerals increased by 13.6% after microwave pretreatment and subsequent milling of the ore, against that obtained from just milling the untreated ore. The amount of fully liberated copper minerals not including valeriite, which is difficult to float, increased by 8.4% after microwave treatment. Due to the small quantities of copper present in the low grade ore, the micro-flotation testing performed on the ore for this thesis did not produce any meaningful results, however, the QEMSCAN results show good agreement with the results of flotation tests performed previously on Palabora ore by other workers (Sahyoun et al., 2004), who showed an increase in final recovery of copper from flotation of 8% after microwave treatment.

Flowsheet simulations

Based on an efficiency of 90% in the conversion of power from plug to microwave applicator, a treatment of 10 kW with a residence time of 0.5 seconds equates to an energy consumption of 1.62 kWh/t of ore. Calculations showed that this microwave treatment resulted in a 61% reduction in the work index of the ore in the rod mill (see APPENDIX B).

Simulations of the existing process flowsheet at Palabora showed that significant increases in throughput were possible in the milling circuit after the introduction of microwave pretreatment of the ore. Based upon the minimum 20% passing size which can be produced at a certain throughput, there is a possibility of increasing the throughput in the existing plant by 46%, while still retaining the same grind size as is required for flotation in the existing operation (see Figure 6.10).

It was found that a reduction of 19% in energy usage was possible with the addition of a microwave unit to pretreat the ore before each rod mill (see Table 6.5). This energy reduction takes into account the energy cost of the microwave applicator as well. A comparison of the hold-ups occurring in the flowsheet simulations and the actual plant rod mills and ball mills, showed that the energy consumption of these items would be under predicted by between 14% and 18% in the simulations. The energy savings predicted by the simulations would thus be conservative estimates for the savings on the actual plant. These energy reductions are in line with the results obtained by other workers such as Wills et al., 1987, who, even when using conventional heating methods, showed that thermal treatment lead to a reduction of 55% in grinding energy requirements in an ore mined at South Crofty, and Kingman et al., 2004, who, using much smaller energy inputs (i.e. < 1 kWh/t) than was the case for the work performed in this thesis, showed reductions of up to 30% in grinding energy could be achieved in ore mined at Palabora. At the same time a small reduction of just less than 1% in the use of grinding media is predicted (see Table 6.6).

It was further seen that, after microwave pretreatment, where the throughput is increased by 10%, it is still possible to reduce the total energy consumption associated with comminution by 18% per ton of ore milled, over the energy use in the existing plant (see Table 6.5). Once again a small reduction of just less than 1% in the use of grinding media is predicted (see Table 6.6).

While there is a small possible increase in maximum throughput for the untreated material after the addition of the gravity separation circuit, this is limited to about 400 t/h in each milling circuit (see Figure 6.10), which translates to an increase of just 3.2% in throughput over that seen in the existing plant operation. With the addition of microwave pretreatment of the ore as well, however, the process shows the same potential for an increase in throughput of 46% as is seen for microwave treated ore in the existing plant. At the same time, the 80% passing size of the material reporting to flotation after gravity concentration is much lower, even though the 20% passing sizes do not differ.

With the addition of a gravity separation plant to remove gangue from the process early on, it can be seen that reductions in energy and grinding media usage, over those of the existing process, can be achieved for both treated and untreated ore (see Table 6.5 and Table 6.6). A reduction of 12% in total energy use and 3% savings in grinding media consumption for the untreated ore, and 28% savings in energy use and 7% saving in grinding media consumption for microwave treated ore, are possible (when using a separation density of 2.967 s.g. in the gravity separation plant). Given a 10% increase in throughput which is only made possible by the microwave pretreatment of the ore, it is possible to produce the desired feed size for the flotation circuit while still reducing the energy usage per ton of ore fed to the milling circuit by 28% and the media consumption by 6%, over the base case of processing untreated ore in the existing plant.

When the split density of the gravity separation section is varied between 2.817 s.g. and 3.117 s.g., it is seen that this had no effect on the total comminution energy required, however, the grinding media consumption decreases very slightly as the split density is increased (see Table 6.3). The greatest effect of an increase in the separation density, in the gravity separation plant, is to bring about a greater amount of material reporting to the light fraction. It is seen that by increasing the separation density to 3.117 s.g., up to 15% of the total gangue in the rod mill product can be removed before further grinding in the ball milling circuit (see Figure 6.9).

Since the copper is present in such small quantities, any amount of misplaced material during gravity concentration can be detrimental to the final copper recovery after flotation. It is seen that for the treated material, the maximum increase in grade reporting to flotation of about 5% is accompanied by a loss of around 2.3% of the total copper in the process feed to the gravity concentration tails (see Figure 6.7), while for the untreated material the maximum grade increase of 4.6% comes with an associated loss of 2% of the total copper. Since the gravity concentration process removes around 77% of the gangue from the material reporting to it for both treated and untreated material, the main reason for these difference in the results between microwave treated and untreated ore would be the slightly larger amount of material reporting to the gravity concentration process after microwave treatment (see Figure 6.16).

It is seen that on average the total amount of material reporting to the flotation plant decreases by 5.5% for the case of processing untreated material in the gravity separation plant, and by 6.8% when the ore is first microwave treated before gravity separation, over that noted for the existing operation.

The addition of a gravity separation plant to the process flowsheet also changes the shape of the product size distributions of the treated and untreated material sent to flotation (see Figure 6.15). This is as a result of the removal of large gangue particles in the gravity pre-concentration step and will impact positively on the copper recovery during flotation, since the flotation circuits at Palabora also employ mills to grind unrecovered large particles for better liberation and subsequent recovery after being recycled back to the floatation cells.

Economic analysis of flowsheet simulations

Since the only plant data available was based on the 1989 operation of Palabora, this data was used in the flowsheet and economic modelling of the plant. Based on exchange rates, copper prices and materials and energy costs as at January 2005, the net present value of the plant (discounted at 20%) was determined for each of the cases investigated (see Figure 7.1). It was seen that the most profitable operation for the plant is that of the addition of microwave processing without gravity separation, where it is possible to raise the NPV of the plant by 23% (or R259 million) over a ten year period, and by 72% (or R795 million) given the 10% increase in throughput made possible by microwave pretreatment (see Table 7.6). In all cases, the addition of gravity separation to remove gangue leads to a decrease in the NPV of the plant when compared against the corresponding cases of not including gravity concentration, due to the unrecovered copper in the gravity separation tailings.

When compared against the monthly profits associated with a minerals processing plant, the capital costs associated with the implementation of the microwave technology are reasonable, and are recouped within about 4 months of operation, and after 16 months of operation, the net present value of the plant operation with microwave pretreatment of the ore surpasses that of the conventional processing operation (see Figure 7.1). A study of the payback time of microwave technology supposing only the case of savings in energy and grinding media (and thus no downstream benefits such as improved liberation and valuable mineral recovery were included in the calculations), showed that the savings generated will not in themselves be able to recoup the associated capital investments within any reasonable time frame, but over 10 years will lead to increases of R29 million in NPV for the addition of microwave pretreatment, and R16 million if this technology is implemented with a 10% increase in throughput (Figure 7.2), with the lower NPV in the latter case being due to the higher energy and media consumptions incurred when operating at higher versus lower throughputs over the same time period.

The best case scenario for gravity separation comes with the introduction of an ideal recycle stream over the rod mill, to ensure that the entire rod mill product is sent to gravity separation. Under ideal conditions, this potentially leads to the removal of 77% of the gangue material from the flotation feed, however, at the same time this is accompanied by a loss of 9.7% and 9.5% of the copper, and 18% and 18.5% of the magnetite, to the gravity concentration tails for the treated and untreated material respectively. The failure here of gravity separation to preconcentrate the Palabora ore without substantial losses of copper to the gravity separation tails, has led the author to believe that when dealing with low grade ores, only the combination of microwave treatment with more selective technologies could lead to further exploitation of the benefits offered by microwave treatment of low grade ores with respect to early gangue removal.

Due to the large changes that must be made to an existing plant to implement the use of microwave treatment with another suitable technology (as with the investigated case of the dual introduction of microwave treatment and gravity concentration), only purpose-built plants would implement the idea with ease. It is recommended that for existing plants, the benefits and process options afforded by microwave treatment are put to their best use in the existing process flowsheet without the implementation of costly changes and additions which may, or may not, further improve plant performance and profitability. Under these conditions, microwave treatment is seen to be a low-risk project with substantial returns.

The current operation of Palabora is vastly different from that reported in the 1989 plant description. The need to exploit higher grades of ore have moved the mining operation underground, and due to this the production rate has dropped from 80 000 tons per day in 1989, to around 20 800 tons per day during the first half of 2004 (see APPENDIX D). As at this time, the plant was making a severe loss, much of which was attributable to the strong rand and lower throughputs. It was seen that the introduction of microwave treatment to the Palabora process flowsheet during this time period would not on it’s own be able to return the plant to profitable operation (see Figure 7.3), but would none the less have decreased the losses suffered over the first half of 2004 from R158 million to R138 million (a reduction of 12.5%) given an additional 10% increase in throughput made possible by the weakened ore after pretreatment. The ability to increase the throughput will, however, depend on where the bottle neck now occurs in the present plant operation. Even for the case of implementing microwave pretreatment at the existing plant throughput, more than half of the capital cost of R48 million for the addition of the microwave processing facilities would have been recovered after the 6 month period investigated, setting the company up for reduced losses in the last 6 months of the same year.

The investigations into the economics of the new operating conditions prevailing at Palabora (2004), showed that the region for favourable operation, in terms of exchange rates and copper prices, is increased when microwave technology is added to the existing plant (Figure 7.5), but as of January 2005 these conditions were still outside the realm of possibility.

From the work performed in this thesis, it has been shown that the microwave pretreatment of ores before milling is a viable option for the minerals processing industry, and one which facilitates significant increases in plant profitability. At the same time, the moderate capital investments involved in implementing microwave pretreatment should provide a reasonably risk-free integration of this technology into conventional processing flowsheets.

9. REFERENCES

Al-Harahsheh, M., Kingman, S., Hankins, N., Somerfield, C., Bradshaw, S., Louw, W., The Influence of Microwaves on the Leaching Kinetics of Chalcopyrite, Minerals Engineering, 2005.

Amankwah, R.K., Khan, A.U., Pickles, C.A., Yen, W.T., Improved Grindability and Gold Liberation by Microwave Pretreatment of a Free-milling Gold Ore, Trans. Inst. Min. Metall. C., Vol. 114, March, 2005, pp. C30-C36.

Austin L.G., Weller K.R., Simulation and Scale-up of Wet Ball Milling, Proc 14th Int. Mineral Processing Congress, Ed. Maltby PDR, Can. Inst. Mining Metall. Montreal, 1982, pp I.8.1-I.8.13.

Bradshaw, S.M., Private communication, 2004.

Brown, J.H., Gaudin, A.H., Loeb, C.M., Intergranular Comminution by Heating, Mining Eng, 10, 1958, pp. 490.

Burt, R.O., Gravity Concentration Technology, Developments in Mineral Processing (ed. Fuerstenau, D.W.), volume 5, Elsevier Science Publishers B.V., Amsterdam, 1984.

Charles, W.D., Gallagher, A.E.J., Comminution Energy Usage and Material Wear, In: Design and Installation of Comminution Circuits, Mular, A.L., Jergensen, G.V., eds., SME, New York, 1982, pp. 2248-2274.

Chen, T.T.; Dutrizac, J.E.; Haque, K.E.; Wyslouzil, W.; Kashyap, S., The Relative Transparency of Minerals to Microwave Radiation, Canadian Metallurgical Quarterly, vol 23, 3, 1984, pp 349-351.

Cowen, R., Exploiting the Earth (work in progress under contract with John Hopkins University Press), http://www.geology.ucdavis.edu/~cowen/~GEL11 (online draft copy), April, 1999.

Das, P.K., Use of Cumulative Size Distribution to Back-Calculate the Breakage Parameters in Batch Grinding, Computers and Chemical Engineering, vol 25, 2001, pp 1235-1239.

Das, P.K., Khan, A.A., Pitchumani, B., Solution of the Batch Grinding Equation, Powder Technology, 85, 1995, pp 189-192.

Fitzgibbon, K.E.; Veasey, T.J., Thermally Assisted Liberation - A Review, Minerals Engineering, vol 3, 1/2, 1990, pp 181-185.

Ford, J.D., Pei, D.C.T., High Temperature Chemical Processing via Microwave Absorption, J. Microwave Power, Vol. 2, No. 2, pp. 61-64.

Gorbatsevich, F.F., Non-Linearity of Strain in Hard Crystalline Rocks, Int. J. Rock Mech. Min. Sci. & Geomech. Abstr., vol 33, no. 1, 1996, pp 83-91.

Haque, K.E., Microwave Energy for Mineral Treatment Processes – a Brief Review, Int. J. Miner. Process., 57, 1999, pp. 1-24.

Haque, K.E., Microwave Irradiation Pretreatment of a Refractory Gold Concentrate, In: Salter, R.S., Wysouzil, D.M., McDonald, G.W., eds., Proc. Int. Symp. On Gold Metallurgy, Winnipeg, Canada, 1987, pp. 327-339.

Hayes, P., Process Principles in Minerals & Materials Production, Hayes Publishing Co, Brisbane, 1993.

Herbst, J.A., Fuerstenau, D.W., Scale-up Procedure for Continuous Grinding Mill Design Using Population Balance Models, International Journal of Mineral Processing, 7, 1980, pp 1-31.

Hoffmann, N., Schönert, K., Bruchanteil von Glaskugeln in Packungen von Franktionen und Binären Mischungen, Aubereit. Tech., 12, 1971, pp 513-518.

Holderfield, S.P.; Salsman, J.B., Observed Trends in the Dielectric Properties of Minerals at Elevated Temperatures, Mat. Res. Soc. Symp. Proc., vol 269, 1992, pp 589-594.

Holman, B.W., Heat Treatment as an Agent in Rock Breaking, Trans IMM, 26, 1926-1927, pp. 219.

JKMRC, Mineral Comminution Circuits: Their Operation and Optimization, Napier-Munn, T.J. (Editor), Julius Kruttschnitt Mineral Research Centre, 1999.

Jones, D.A., Kingman, S.W., Whittles, D.N., Lowndes, I.S., Understanding Microwave Assisted Breakage, Minerals Engineering, 18, 2005, pp. 659-669.

Jones, M.P., Fullard, R.J., Mineral Liberation by Thermal Decomposition of a Carbonate Rock, Trans. IMM (Sec C), 75, 1966, pp. 127.

Kanellopoulos, A.; Ball, A., The Fracture and Thermal Weakening of Quartzite in Relation to Comminution, Journal of the South African Institute of Mining and Metallurgy, 1975, pp 45-52.

Kidybinski, A, Rheological Models of Upper Silesian Carboniferous Rocks, Int. J. Rock. Mech. Min. Sci. & Geomech. Abstr., 3, 1966, pp 279-306.

King, R.P., Modelling & Simulation of Mineral Processing Systems, Butterworth-Heinemann, 2001.

Kingman, S.W., The Effect of Microwave Radiation on the Comminution and Beneficiation of Minerals and Ores, Ph.D. Thesis, University of Birmingham, 1998.

Kingman, S.W., Rowson, N.A., Microwave Treatment of Minerals – a Review, Minerals Engineering, Vol 11, 1998, pp. 1081-1087.

Kingman, S.W.; Vorster, W.; Rowson, N.A., The Influence of Mineralogy on Microwave Assisted Grinding, Minerals Engineering, 2000.

Kingman, S., Whittles, D., Jackson, K., Miles, N., Bradshaw, S., Application of High Electric Field Strength Microwave Energy for Processing Ores and Minerals, XXII International Mineral Processing Congress (IMPC), Cape Town International Conference Centre, Cape Town, South Africa, The South African Institute of Mining and Metallurgy 2003, pp. 327-335.

Kingman, S.W., Jackson, K., Cumbane, A., Bradshaw, S.M., Rowson, N.A., Greenwood, R., Recent Developments in Microwave-Assisted Comminution, Int. J. Miner. Process, 74, 2004, pp. 71-83.

Klimpel, R.R., Austin, L.G., The Back-Calculation of Specific Rates of Breakage and Non-Normalized Breakage Distribution Parameters From Batch Grinding Data, International Journal of Mineral Processing, 4, 1977, pp. 7-32.

Manser, R.J., The Economics of Thermal Pretreatment, Internal Report, Camborne School of Mines, 1983.

Marland, S., Han, B., Merchant, A., Rowson, N., The Effect of Microwave Radiation on Coal Grindability, Fuel, 79, 2000, pp. 1283-1288.

McCarter, W.A., Placer Recovery, D.I.A.N.D. - K.P.M.A. Placer Mining Short Course, Whitehorse, Yukon, April 20-22, 1982.

Meredith, R., Engineer's Handbook of Industrial Microwave Heating, The Institution of Electrical Engineers, Exeter, 1998.

Metaxas, A.C, Foundations of Electroheat : A Unified Approach, John Wiley & Sons Ltd, Chichester, 1996.

Meyer, C., Bir Umm Fawakhir: Insights into Ancient Egyptian Mining, JOM, 49 (3), 1997, pp. 64-68.

Mintek, The Selection of Grinding Balls for Specific Ores, and the Development of a Suitable Theory of Ball Wear, Application Report No. 10, Mintek, 1991.

Mintek Techno Economics Department, Metallurgical Equipment Costs, Mintek, March 1991.

Myers, W.M., Calcining as an Aid to Grinding, J. Am. Ceram. Soc., 8, 1925, pp. 839.

Napier-Munn, T.J., Morell, S., Morrison, R.D., Kojovic, T., Mineral Comminution Circuits. Their Operation and Optimization, JKMRC Monograph Series in Mining and Mineral Processing 2, University of Queensland, Australia, 1996.

Oldfather, C.H., Diodorus of Sicily, Cambridge, MA: Harvard U. Press, 1967.

PMC (Palabora Mining Company), Plant Operations Description, private Palabora Mining Company report, 1990.

Pocock, J., Veasey, T.J., Tavares, L.M., King, R.P., The Effect of Heating and Quenching on the Grinding Characteristics of Quartzite, Powder Technology, vol 95, 1998, pp 137-142.

Prasher, C.L., Crushing and Grinding Process Handbook, John Wiley & Sons Limited, Chichester, 1987.

Radziszewski, P., Predictive Model for Ball Mill Wear, Canadian Metallurgical Quarterly, vol 36, 2, 1997, pp 87-93.

Rajagopal, V., Iwasaki, I., Grinding Media Selection Criteria for Wear Resistance and Flotation Performance, Comminution, UNKNOWN SOURCE.

Rao, S.R., Moon, K.S., Leja, J., Effect of Grinding Media on the Surface Reactions and Flotation of Heavy Metal Sulfides, In: Flotation, A.M. Gaudin Memorial Volume, (ed) M.C. Fuerstenau, 1976, pp 509-527.

Rogovin Zvi, Casali Aldo, Herbst JA, Tracer study of mass transport and grinding in a rod mill, Intl Jnl of Mineral Processing, 22, 1988, pp 149-167.

Roussy, G.; Thiebaut, J.-M., Evaluation of the Local Electrical Field Inside an Heterogeneous Material, Irradiated by Microwaves, Journal of Microwave Power and Electromagnetic Energy, vol 29, 2, 1994, pp 76-80.

Roussy, G.; Pearce, J.A., Foundations and Industrial Applications of Microwave and Radio Frequency Fields, John Wiley & Sons Ltd, Chichester, 1995.

Ruhmer, W.T., Handbook on the Estimation of Metallurgical Process Costs (2nd edition), Mintek Special Publication No. 14, August 1991.

Rutter, E.H., The Effect of Strain-Rate Changes on the Strength and Ductility of Soldenhofen Limestone at Low Temperatures and Confining Pressures, Int. J. Rock. Mech. Min. Sci., vol 9, 1972, pp 183-189.

Sahyoun, C., Kingman, S.W., Rowson, N.A., The Effect of High Powered Microwave treatment on Flotation of Carbonate Copper Ore, UNKNOWN SOURCE, 2004.

Salsman, J.B.; Williamson, R.L.; Tolley, W.K.; Rice, D.A., Short-Pulse Microwave Treatment of Disseminated Sulfide Ores, Minerals Engineering, vol 9, 1, 1996, pp 43-54.

Scheding, W.M., Sherring, A.J., Binns, D., Parker, R.H., Wills, B.A., The Effect of Thermal Pre-treatment on Grinding Characteristics, Camborne School of Mines Journal, vol 81, 1981, pp. 43-44.

Schönert, K., Role of Fracture Physics in Understanding Comminution Phenomena, Trans. Soc. Min. Eng., AIME 252, 1972, pp 21-26.

Sherring, A.J., 1981, The Effect of Thermal Pretreatment on Grinding Characteristics, Internal Report, Camborne School of Mines.

Standish, N.; Worner, H.K.; Obuchowski, D.Y., Particle Size Effect in Microwave Heating of Granular Materials, Powder Technology, vol 66, 1991, pp 225-230.

Tavares, L.M.; King, R.P., Application of Thermal Treatment to Improve Comminution, SME Annual Meeting, Denver, Colorado, 1995.

Tavares, L.M., King, R.P., Effect of Microwave-Induced Damage on Single-Particle Comminution of Ores, SME Annual Meeting, Phoenix, Arizona, March 11-14, 1996.

Tavares, L.M., King, R.P., Fracture Energies of Copper Ore Subject to Microwave Heating, Utah Comminution Center, University of Utah, August, 1996.

The Tech., Vol. V, Massachusetts Institute of Technology, Boston, April 1, 1886, No. 12., pp. 179-180.

Tinga, W.R., Fundamentals of Microwave-Material Interactions and Sintering, Mat. Res. Soc. Symp. Proc., vol 124, 1988, pp 33-43.

Vorster, W.; Rowson, N.A.; Kingman, S.W., The Effect of Microwave Radiation Upon the Processing of Neves Corvo Copper Ore, Int. J. Miner. Process., vol 63, 2001, pp 29-44.

Walkiewicz, J.W, Kazonich, G., McGill, S.L., Microwave Heating Characteristics of Selected Minerals and Compounds, Mineral and Metallurgical Processing, 5 (1), 1988, pp. 39-42.

Walkiewicz, J.W., Clark, A.E., McGill, S.L., Microwave Assisted Grinding, IEEE Transactions on Industry Applications, 27 (2), pp. 239.

Walkiewicz, J.W., Lindroth, D.P., Clarck, A.E., Grindability of Taconite Rod Mill Feed Enhanced by Microwave Induced Cracking, SME Annual Meeting, Reno, Nevada, Feb. 1993, pp 1-4.

Wang, Y., Forssberg, E., Microwave Assisted Comminution and Liberation of Minerals, Mineral Processing on the Verge of the 21st Century, Özbayoğlu et al. (eds), Balkema, Rotterdam, 2000.

Whiten, W.J., A Matrix Theory of Comminution Machines, Chemical Engineering Science, Vol. 29, 1974, pp. 589-599.

Whittles, D.N., Kingman, S.W., Reddish, D.J., Application of Numerical Modelling for Prediction of the Influence of Power Density on Microwave Assisted Grinding, Int. J. Min. Proc., 68, 2003, pp. 71-91.

Wills, B.A.; Parker, R.H.; Binns, D.G., Thermally Assisted Liberation of Cassiterite, Minerals and Metallurgical Processing, 1987, pp 94-96.

Wong, D., Microwave Dielectric Constants of Metal Oxides at High Temperature, MSc. Thesis, University of Alberta, Canada, 1975.

Xia, K., Pickles, C.A., Applications of Microwave Energy in Extractive Metallurgy, a Review, CIM Bulletin, Vol. 90, No. 1011, June, 1997.

Yates, A., Effect of Heating and Quenching Cornish Tin Ores Before Crushing, Trans IMM, 28, 1918-1919, pp. 41.

Yelloji Rao, M.K., Natarajan, K.A., Electrochemical Aspects of Ball Wear During Sulfide Grinding, Comminution, UNKNOWN SOURCE.

APPENDIX A MATLAB CODE (BREAKAGE AND SELECTION FUNCTIONS)

```
%REQUIRED FORMAT OF DATA FILE
% This program reads the data in from the file containing the breakage data in the form of discrete particle
% size distributions. The file must have the following form (with all the shown entries being pure numeric
% inputs)
%
%           time_0        time_1        time_2        ...    time_n
% size_1    mass_t0_s1    mass_t1_s1    mass_t2_s1    ...    mass_tn_s1
% size_2    mass_t0_s2    mass_t1_s2    mass_t2_s2    ...    mass_tn_s2
% size_3    mass_t0_s3    mass_t1_s3    mass_t2_s3    ...    mass_tn_s3
%   .            .             .             .         .         .
%   .            .             .             .         .         .
%   .            .             .             .         .         .
% size_m    mass_t0_sm    mass_t1_sm    mass_t2_sm    ...    mass_tn_sm
%
% Where:
% time_# - the time of grinding
%     time_0 should be 0 and be representative of the initial condition of the mill feed
%     time_n should be the last grinding time
% size_# - the on sieve size
%     size_0 should be the top size class (thus all masses on this sieve size should be 0)
%     size_m should be 0 (thus representing all material smaller than the smallest actual sieve used)
% mass_tn_sm - the mass on the sieve sm after grinding time tn
%==========================================================================
function brk
%DEFINE GLOBAL VARIABLES
global Fe Fp grinding_times A C x xl S1 alpha mu lambda phi5mm gamma beta delta
%--------------------------------------------------------------------------
%OBTAINING REQUIRED INFORMATION
% Read in data from excel file with same format as explained above
[NUM, ALP] = xlsread('Breakagedata.xls','untreated');
% Size of A
[NUM_m, NUM_n] = size(NUM);
```

```
% Assign individual mineral data to arrays
grinding_times = NUM(1,2:NUM_n)';
size_class = NUM(2:NUM_m,1);
size_class(length(size_class)) = (size_class(length(size_class))+size_class(length(size_class)-1))/2;
size_distributions = NUM(2:NUM_m,2:NUM_n);
% Determine cumulative size distributions
cum_size_distributions = cumsum(size_distributions);
cum_size_distributions = cum_size_distributions(NUM_m-1:-1:1,:);
for loop = 1:length(max(cum_size_distributions))
   cum_size_distributions(:,loop) = cum_size_distributions(:,loop)./max(cum_size_distributions(:,loop));
end
% Define sizes
x = flipud(size_class);
xl = length(x);
xm = max(size_class);
% Order experimental data into a single matrix
Fe = flipud(1-cum_size_distributions(2:xl,:));
Fe = 1-cum_size_distributions(2:xl,:);
%----------------------------------------------------------------------------------------------------------------------
%CHOOSE INITIAL CONDITIONS FOR SELECTION AND BREAKAGE FUNCTION VALUES
% Constants used in construction of selection function
% For selection function of the form
% S = (S1*dp^alpha)/(1+(dp/mu)^lambda)
S1 = 0.80667;
alpha = 2.3359;
mu = 15.1615;
lambda = 2.8050;
% Constants used in construction of breakage function
% For breakage function of the form
% B(x,y) = phi(x/y)^gamma + (1-phi)(x/y)^beta
phi5mm = 0.8054;% 0 <= phi <= 1, if necessary, set as a constant because optimization is unbounded
gamma = 0.8054;
beta = 0.6883;
% where phi = phi5mm(y5mm/y)^delta
delta = 0.6608;%set as a constant because optimization is unbounded
% Select which of the following parameters
% [S1 alpha mu lambda phi5mm gamma beta delta] will be considered as variables (all others are thus
```

```
% considered to be constants) - remember to change the associated variables in 'function SSQ'
v0 = [S1 alpha mu lambda];
%------------------------------------------------------------------------------------------------------------------------
%SOLVE OPTIMIZATION PROBLEM
% Find minimum of SSQ function
[optimum_values,SSQ,EXITFLAG] = fminsearch(@optimization,v0);
SSQ
parameter_names = '    S1       alpha     mu       lambda    phi5mm    gamma     beta      delta'
optimum_values = [S1 alpha mu lambda phi5mm gamma beta delta]
%------------------------------------------------------------------------------------------------------------------------
% Plot results of predicted size distributions with time
figure;
hold on
plot(x(1:end-1),Fe,'b-')
plot(x(1:end-1),Fp,'r-.')
title('Cumulative Size Distribution')
xlabel('Particle Size (micron)')
ylabel('Cumulative Fraction Passing')
legend('Experimental','Predicted',2)
axis tight
%------------------------------------------------------------------------------------------------------------------------
% Plot selection function
for loop = 1:length(x)-1
   sel_func(loop)                                                                                                    =
(optimum_values(1)*x(loop)^optimum_values(2))/(1+(x(loop)/optimum_values(3))^optimum_values(4));
end
figure;
hold on
plot(x(1:end-1),sel_func,'b-')
title('Plot of Selection Function versus Particle Size')
xlabel('Particle Size (micron)')
ylabel('Selection Function Value')
axis tight
%=================================================================================
function SSQ = optimization(v0);
global Fe Fp grinding_times A C x xl S1 alpha mu lambda phi5mm gamma beta delta
% Convert input v to values for use in calculation selection and breakage functions
```

```
S1 = v0(1);
alpha = v0(2);
mu = v0(3);
lambda = v0(4);
% phi5mm = v0(5);
% gamma = v0(5);
% beta = v0(6);
% delta = v0(7);
% Selection function values
% S = (S1*dp^alpha)/(1+(dp/mu)^lambda)
for j = 1:xl
    S(j) = (S1*x(j)^alpha)/(1+(x(j)/mu)^lambda);
end
% Cumulative breakage function values
% B(x,y) = phi(x/y)^gamma + (1-phi)(x/y)^beta
% where phi = phi5mm(y5mm/y)^delta
for j = 1:xl
    for i = 1:xl-1
        if i <= j
            phi = phi5mm*(5000/x(j))^delta;
            B(i,j) = phi*(x(i)/x(j))^gamma + (1-phi)*(x(i)/x(j))^beta;
        end
    end
end
%---------------------------------------------------------------------------------------------------------------------------
%CALCULATE ALL INFORMATION REQUIRED FOR SOLUTION OF BATCH GRINDING
%EQUATION
% dF/dt = A*F + C
% Form the A matrix
A = zeros(xl-1,xl-1);
for j = 1:xl-1
    for i = 1:xl-1
        if i == j
            A(i,j) = -S(j+1)*B(i,j+1);
        elseif i < j
            A(i,j) = S(j)*B(i,j)-S(j+1)*B(i,j+1);
        end
```

```
    end
end
% Form the C matrix
C = S(xl)*B(:,xl);
%-----------------------------------------------------------------------------------------------------------------------
%SOLVE BATCH GRINDING EQUATION
% Solve differential equation
[t,Fp]=ode45(@ODE_solver,grinding_times,Fe(:,1));
%-----------------------------------------------------------------------------------------------------------------------
%CALCULATE SSQ FUNCTION
nt = length(grinding_times);
temp = zeros(xl-1,nt);
Fp = Fp';
for k=1:nt
    for i = 1:xl-1
        temp(i,k) = ((Fp(i,k)-Fe(i,k))/Fe(i,k))^2;
end
end
SSQ = (1/(nt-1))*sqrt(sum(sum(temp)));
%=======================================================================================================================
%ORDINARY DIFFERENTIAL EQUATION SOLVER FOR PREDICTED SIZE DISTRIBUTIONS
function Fp = ODE_solver(t,y);
global A C
for i=1:length(C)
    Fprime(i)=A(i,:)*y+C(i);
end
Fp = Fprime';
```

APPENDIX B CALCULATION OF NEW WORK INDEX FOR TREATED MATERIAL

Mill conditions	Untreated	Treated
Tonnage through mill (t/h)	387.72	992.16
Hold up in mill (t)	22.32	22.32
80% passing size of feed (μm)	13500	13500
80% passing size of product (μm)	1160	1160
Power factor (power = BWI x factor)	80.6	205.8

If we assume that it requires the same amount of mill energy per hour to produce the same 80% passing size in both situations of processing treated and untreated material, given the same hold up of material in the mill in both situations and the different residence times required to achieve the same size distributions, we have

$$\begin{aligned}
\text{Energy consumed} &= \text{Energy consumed} \\
\text{Power factor x W.I.} &= \text{Power factor x W.I.} \\
80.6 \times 13.5 \text{ kWh/t} &= 205.8 \times \text{W.I.}
\end{aligned}$$

therefore W.I. = 5.29 kWh/t for treated material

APPENDIX C MODEL PARAMETERS USED FOR SIMULATION

C.1. MODEL PARAMETERS FOR EXISTING FLOWSHEET

ROD MILL

Parameter	Untr.	Tr.	Tr. (+10%)
Model	RODM	RODM	RODM
β	0.736	0.736	0.736
γ	0.996	0.996	0.996
δ	0.518	0.518	0.518
ϕ_{5mm}	0.392	0.392	0.392
S_{1mm}	0.289	1.088	1.088
α	0.525	1.004	1.004
μ	13.281	1.447	1.447
λ	0.69	1.149	1.149
Residence time of water	3.45	3	3.14
Exp. factor for variation of trans. vel. with size	0.24	0.24	0.24

BALL MILL 1

Parameter	Untr.	Tr.	Tr. (+10%)
Model	MILL	MILL	MILL
β	3.723	3.723	3.723
γ	0.748	0.748	0.748
δ	0	0	0
ϕ_{5mm}	0.72	0.72	0.72
S_{1mm}	0.35	0.35	0.35
α	1.52	1.52	1.52
μ	10	10	10
λ	2.8	2.8	2.8
Residence time	5.91	2	2.5

BALL MILL 2

Parameter	Untr.	Tr.	Tr. (+10%)
Model	MILL	MILL	MILL
β	3.723	3.723	3.723
γ	0.748	0.748	0.748
δ	0	0	0
ϕ_{5mm}	0.72	0.72	0.72
S_{1mm}	0.35	0.35	0.35
α	1.52	1.52	1.52
μ	10	10	10
λ	2.8	2.8	2.8
Residence time	4.48	2	1.8

HYDROCYCLONE 1

Parameter	Untr.	Tr.	Tr. (+10%)
Model	CYCA	CYCA	CYCA
Short circuit to overflow	0.35	0.35	0.35
Sharpness index	0.25	0.25	0.25
D_{50} (μm)	350	350	350
Exponent	0.5	0.5	0.5
Partition function	Logistic	Logistic	Logistic

HYDROCYCLONE 2

Parameter	Untr.	Tr.	Tr. (+10%)
Model	CYCA	CYCA	CYCA
Short circuit to overflow	0.45	0.45	0.45
Sharpness index	0.2	0.2	0.2
D_{50} (μm)	380	380	380
Exponent	0.5	0.5	0.5
Partition function	Logistic	Logistic	Logistic

C.2. MODEL PARAMETERS FOR PROPOSED FLOWSHEET

ROD MILL

Parameter	Untr.	Tr.	Tr. (+10%)
Model	RODM	RODM	RODM
β	0.736	0.736	0.736
γ	0.996	0.996	0.996
δ	0.518	0.518	0.518
ϕ_{5mm}	0.392	0.392	0.392
S_{1mm}	0.289	1.088	1.088
α	0.525	1.004	1.004
μ	13.281	1.447	1.447
λ	0.69	1.149	1.149
Residence time of water	3.45	3.45	3.14
Exp. factor for variation of trans. vel. with size	0.24	0.24	0.24

BALL MILL 1

Parameter	Untr.	Tr.	Tr. (+10%)
Model	MILL	MILL	MILL
β	3.723	3.723	3.723
γ	0.748	0.748	0.748
δ	0	0	0
ϕ_{5mm}	0.72	0.72	0.72
S_{1mm}	0.35	0.35	0.35
α	1.52	1.52	1.52
μ	10	10	10
λ	2.8	2.8	2.8
Residence time	4.5	0.5	0.95

BALL MILL 2

Parameter	Untr.	Tr.	Tr. (+10%)
Model	MILL	MILL	MILL
β	3.723	3.723	3.723
γ	0.748	0.748	0.748
δ	0	0	0
ϕ_{5mm}	0.72	0.72	0.72
S_{1mm}	0.35	0.35	0.35
α	1.52	1.52	1.52
μ	10	10	10
λ	2.8	2.8	2.8
Residence time	3.5	0.5	0.95

SIEVE BEND 1

Parameter	Untr.	Tr.	Tr. (+10%)
Model	SCR1	SCR1	SCR1
D_{50} (μm)	850	850	850
Water split to undersize	0.77	0.77	0.77
Sharpness parameter	0.94	0.94	0.94

SIEVE BEND 2

Parameter	Untr.	Tr.	Tr. (+10%)
Model	SCR1	SCR1	SCR1
D_{50} (μm)	212	212	212
Water split to undersize	0.95	0.95	0.95
Sharpness parameter	0.94	0.94	0.94

HYDROCYCLONE 1

Parameter	Untr.	Tr.	Tr. (+10%)
Model	CYCA	CYCA	CYCA
Short circuit to overflow	0.35	0.35	0.35
Sharpness index	0.25	0.25	0.25
D_{50} (μm)	350	350	350
Exponent	0.5	0.5	0.5
Partition function	Logistic	Logistic	Logistic

HYDROCYCLONE 2

Parameter	Untr.	Tr.	Tr. (+10%)
Model	CYCA	CYCA	CYCA
Short circuit to overflow	0.45	0.45	0.45
Sharpness index	0.2	0.2	0.2
D_{50} (μm)	380	380	380
Exponent	0.5	0.5	0.5
Partition function	Logistic	Logistic	Logistic

APPENDIX D PALABORA MINING COMPANY OVERVIEW (4TH QUARTER 2004)

D.1. PRODUCTION STATISTICS

	4Q 2003	1Q 2004	2Q 2004	3Q 2004	4Q 2004	FULL YEAR 2003	FULL YEAR 2004
Palabora mine							
Tonnes hoisted ('000 tonnes)	2,022	1,833	1,910	2,405	2,464	5,999	8,612
Ore treated ('000 tonnes)	2,838	2,101	1,897	2,345	2,314	11,415	8,657
Average ore copper grade (%)	0.63	0.76	0.74	0.75	0.73	0.59	0.74
Copper concentrates produced ('000 tonnes)	46.3	35.9	35.4	64.2	52.2	163.3	187.7
Average concentrate grade (copper%)	31.3	29.7	28.3	27.7	30.6	32.1	29
Copper in concentrates ('000 tonnes)	14.5	10.7	10	17.8	16	52.4	54.4
Palabora smelter/refinery							
New concentrate smelted on site ('000 tonnes)	72.5	59.4	68	59	67	267.6	253.4
New copper anodes produced ('000 tonnes)	21.3	15.8	19.7	14.4	17.3	76.7	67.2
Refined new copper produced ('000 tonnes)	20.9	17.9	17.2	16.2	16.2	73.4	67.5
By-products							
Magnetite concentrate ('000 tonnes)	68	105	160	144	165.2	215	574.3
Refined nickel sulfates ('000 tonnes)	38	53	37	36	40.8	152	167.1
Vermiculite plant							
Vermiculite produced ('000 tonnes)	35.6	38.4	51.5	52.7	50.8	173.2	193.4

D.2. OPERATIONS OVERVIEW FOR 2004

Mine

Daily production from the underground mine in the period continued to improve and averaged 26,778 tonnes, 18% higher than the fourth quarter of 2003. A daily production record of 35,191 tonnes was achieved.

Mill throughput was consistent with underground mine production. The total underground ore treated during the fourth quarter of 2.3 million tonnes was 33% higher than in the same quarter of 2003. In 2003 ore treated was supplemented by ore scavenged from the open pit ramps.

Copper

Copper in concentrate production was higher in the fourth quarter of 2004 compared with 2003 due to the higher grade and improved recovery. Recoveries from underground ore averaged 88% in the quarter and 87.1% for the year.

Smelter throughput was affected by unplanned maintenance on the Power Plant. Concentrate feed to the smelter continued to be supplemented by purchased concentrates, (15,000 tonnes in the quarter).

Refined copper output was in line with anode supply from the smelter.

Vermiculite

Production for the fourth quarter of 2004 was 42% higher than the corresponding quarter in 2003, due to the closure of operations in December 2003 to match prevailing market activities. Continued improvement in mining and plant operations has improved overall production for 2004 to 3% above plan.

Magnetite

Production of coal-washery medium grade magnetite for domestic use was supplemented by increasing volumes of coarse magnetite sales for export to the Chinese market.

APPENDIX E CAPITAL COST CALCULATIONS

E.1. EXISTING FLOWSHEET

MICROWAVE POWER SOURCES AND APPLICATORS (per circuit)

RELEVANT INFORMATION

Description	Value	Units
Installed cost	4000	$/kW
Energy consumption	1.622	kWh/t
Exchange rate (Jan 2005)	6.0225	R/$
Magnetron replacement	100	$/kW
Safety factor for power required	1.1	-

COST PER CIRCUIT

Operating conditions	Flowrate	Power required	Total cost	Total cost
	t/h	kW	$ x 10^3	R x 10^3
Untreated (same throughput)	387.7	0.0	0	0
Treated (same throughput)	387.7	691.9	2767	16667
Treated (+10% throughput)	426.6	761.2	3045	18338

MAGNETRON REPLACEMENT (10 000 HOURS, +/- 13 MONTHS)

Operating conditions	Magnetron replacement	Magnetron replacement
	$ x 10^3	R x 10^3
Untreated (same throughput)	0.0	0
Treated (same throughput)	69.2	417
Treated (+10% throughput)	76.1	458

E.2. PROPOSED FLOWSHEET

MICROWAVE POWER SOURCES AND APPLICATORS (per circuit)

RELEVANT INFORMATION

Description	Value	Units
Installed cost	4000	$/kW
Energy consumption	1.622	kWh/t
Exchange rate (Jan 2005)	6.0225	R/$
Magnetron replacement	100	$/kW
Safety factor for power required	1.1	-

COST PER CIRCUIT

Operating conditions	Flowrate	Power required	Total cost	Total cost
	t/h	kW	$ x 10^3	R x 10^3
Untreated (same throughput)	387.7	0.0	0	0
Treated (same throughput)	387.7	691.9	2767	16667
Treated (+10% throughput)	426.6	761.2	3045	18338

MAGNETRON REPLACEMENT (10 000 HOURS, +/- 13 MONTHS)

Operating conditions	Magnetron replacement	Magnetron replacement
	$ x 10^3	R x 10^3
Untreated (same throughput)	0.0	0
Treated (same throughput)	69.2	417
Treated (+10% throughput)	76.1	458

SIEVE BEND #1 (per circuit)

RELEVANT INFORMATION

Description	Value
Cost parameter - a	10.350
Cost parameter - b	5.362
Cost parameter - c	1.266
Cost index (March 1991 SSA PPI)	345.6
Cost index (November 2004 SSA PPI)	939.3
ME factor for DFC (x purchased cost)	3.89

COST PER CIRCUIT

Operating conditions	Flowrate	95% particle	Slot opening	Capacity per metre	Width required
	m^3/h	µm	mm	m^3/h	m
Untreated (same throughput)	593.9	1197	1.600	230	2.58
Treated (same throughput)	593.7	1196	1.6	230	2.58
Treated (+10% throughput)	653.0	1195	1.6	230	2.84

Operating conditions	No of units	Width (x) (max 0.5 - 3 m)	Unit cost (Mar 1999)	Unit cost (Nov 2005)	Total cost (Nov 2005)
	-	m	R x 10^3	R x 10^3	R x 10^3
Untreated (same throughput)	1	2.58	32.6	88.7	345
Treated (same throughput)	1	2.58	32.6	88.7	345
Treated (+10% throughput)	1	2.84	35.8	97.2	378

SIEVE BEND #2 (per circuit)

RELEVANT INFORMATION

Description	Value
Cost parameter - a	10.350
Cost parameter - b	5.362
Cost parameter - c	1.266
Cost index (March 1991 SSA PPI)	345.6
Cost index (November 2004 SSA PPI)	939.3
ME factor for DFC (x purchased cost)	3.89

COST PER CIRCUIT

Operating conditions	Flowrate	95% particle	Slot opening	Capacity per metre	Width required
	m^3/h	µm	mm	m^3/h	m
Untreated (same throughput)	425.7	309	0.310	43.5	9.79
Treated (same throughput)	445.7	309	0.31	43.5	10.25
Treated (+10% throughput)	488.5	309	0.31	43.5	11.23

Operating conditions	No of units	Width (x) (0.5-3 m)	Unit cost (Mar 1999)	Unit cost (Nov 2005)	Total cost (Nov 2005)
	-	m	$R \times 10^3$	$R \times 10^3$	$R \times 10^3$
Untreated (same throughput)	4	2.45	31.0	84.4	1313
Treated (same throughput)	4	2.56	32.4	88.0	1370
Treated (+10% throughput)	4	2.81	35.4	96.2	1496

SPIRAL CONCENTRATORS (per circuit)

RELEVANT INFORMATION

Description	Value
Cost parameter - a	41.33
Cost parameter - b	0.9821
Cost parameter - c	0.006308
Cost index (March 1991 SSA PPI)	345.6
Cost index (November 2004 SSA PPI)	939.3
ME factor for DFC (x purchased cost)	3.89

COST PER CIRCUIT

Operating conditions	Flowrate	Capacity	Number of starts	Cap. (x) (1.5-70 t/h)
	t/h	t/h/start	-	t/h
Untreated (same throughput)	299.1	5	3	15
Treated (same throughput)	303.9	5	3	15
Treated (+10% throughput)	343.7	5	3	15

Operating conditions	No of units	Unit cost (Mar 1999)	Unit cost (Nov 2005)	Total cost (Nov 2005)
	-	R x 10^3	R x 10^3	R x 10^3
Untreated (same throughput)	20	57.5	156.2	12154
Treated (same throughput)	21	57.5	156.2	12762
Treated (+10% throughput)	23	57.5	156.2	13978